TABLE OF CONTENTS

TABLE OF CONTENTS(Continued)

TABLE OF CONTENTS(Continued)

TABLE OF CONTENTS(Continued)

LIST OF FIGURES

LIST OF FIGURES(Continued)

LIST OF FIGURES(Continued)

LIST OF TABLES

1. INTRODUCTION

1.1 Subject

The subject of this report is the research performed to determine the feasibility of designing and constructing a prototype Autonomous Shadow Vehicle that follows a Lead Maintenance Vehicle for use in highway maintenance operations to protect highway maintenance personnel from injury by high-speed highway vehicles. An Autonomous Shadow Vehicle is driverless and follows the Lead Vehicle. Hence, personnel who would normally be driving a Shadow Vehicle are removed from potential danger and injury. Furthermore, highway maintenance productivity is increased and highway maintenance activities that presently cannot "cost justify" the use of a Shadow Vehicle with a driver may be able to "cost justify" using an Autonomous Shadow Vehicle.

Currently the Minnesota Department of Transportation(MNDOT) is using Radio Controlled Shadow Vehicles. The steering, throttle, and brake of a Radio Controlled Shadow Vehicle is controlled by a maintenance worker standing on the roadside using joy sticks on a control box that transmits the commands to the Radio Controlled Shadow Vehicle's actuators. This radio control approach is only usable for low speeds(walking speeds) and stop and go situations. The use of an Autonomous Shadow Vehicle proposed by this research project would eliminate the need for a maintenance worker to perform the radio control function. However, it is proposed that the Autonomous Shadow Vehicle has a back-up radio control mode in addition to its autonomous tracking systems.

1.2 Research Objectives

The main objective of this research is to research feasible technologies for autonomous tracking by the Shadow Vehicle, and to design and construct an Autonomous Shadow Vehicle that tracks a Lead Vehicle at a desired range. Track for this report is defined to mean that the Autonomous Shadow Vehicle follows a Lead Vehicle in the same manner Shadow Vehicles driven by maintenance workers presently follow Lead Vehicles. Hence, curves will be considered in the design process.

It is proposed that the research and experimentation consist of three phases, Phases I, II, and III. In Phase I, tracking technologies are to be researched and evaluated and feasibility of designing an Autonomous Shadow Vehicle is to be determined. In Phase II, feasibility of the tracking approach selected is demonstrated using pre-prototype hardware and software. In Phase III, a prototype Autonomous Shadow Vehicle and Lead Vehicle with the appropriate hardware are designed and constructed in partnership with the private sector. The description of the research and experimentation objectives of Phase I, the subject of this report, follows.

The principal objectives of Phase I are to:

1) Research the literature for technologies that potentially could be used for designing a tracking system(s) for an Autonomous Shadow Vehicle.

2) Research the feasibility of using a transmitting antenna on the Lead Vehicle and a receiving antenna array on the Autonomous Shadow Vehicle as a tracking system.

3) Research the feasibility of using Global Positioning Satellite(GPS) technology to design a tracking.

4) Research the feasibility of using a 3-D symbol mounted on the Lead Vehicle and a video camera mounted on the Autonomous Shadow Vehicle as a tracking system.

5) Research, design, and simulate control systems to control the steering, throttle, and brake actuators of the Autonomous Shadow Vehicle.

6) Evaluate and recommend a tracking system(s) for use in Phase II.

1.3 Research Findings Summary

1.3.1 Current Shadow Vehicle Operations

Shadow vehicles, used in highway maintenance operations to provide a safer operating environment for operating personnel, are usually heavy vehicles which have a flashing arrow board mounted in the rear. They are used for a variety of tasks including street sweeping, laying cones for lane closure, painting lines, placing thermoplastic lines, laying Bott Dots, and crack sealing. Street sweeping and painting or placing lines and dots are carried out in a moving lane closure mode while crack sealing takes place inside a lane closed by cones.

For all tasks the shadow vehicle travels to site at normal highway operating speeds often traversing minor roads and frequently traveling on ramps of freeway interchanges. This segment of the maintenance task will not be automated at this stage and the automated shadow vehicle should be driven to site by crew members needed at the site for other work or towed. If no such crew member is available, consideration should be given to towing the automated shadow vehicle to site, or towing one of the lighter maintenance vehicles to site.

Once at the site the maintenance vehicles and shadow vehicle may need to change lanes before or during the task. Changing lanes before work begins may be necessary in all tasks so that work can begin from the left shoulder. This part of the maintenance task must also be accomplished with a driver for the shadow vehicle or with one vehicle being towed.

Changing lanes during the task is necessary in setting cones for lane closure, and may be necessary in painting or placing lines and dots. For lane closure the shadow vehicle moves from the shoulder to the first lane as the crew begin to lay the taper. In painting or placing lines and dots it will be necessary to change lanes during the task if work is taking place in the center lanes of a freeway with three or more lanes in one direction. This aspect of the task poses problems for automation because while changing lanes the shadow vehicle is acting independently of the maintenance vehicle.

Two shadow vehicles are often used in street sweeping. Only the shadow vehicle closest to the street sweeper is being considered for automation.

Crack sealing is the only operation which involves having crew members on the road between the maintenance vehicle and the shadow vehicle. Sometimes the vehicles are stationary while this is happening but sometimes the vehicles are moving ahead slowly. For automation while moving it will be very important to ensure that crew members will not interfere with the Autonomous Shadow Vehicle's tracking system. Similarly objects being towed by the

maintenance vehicle (such as signs for lane closure or equipment for crack sealing) should be checked for interference with the tracking line-of-sight and redesigned if necessary. Section 2 discusses current shadow vehicle operations in more detail.

1.3.2 Shadow Vehicle Automation - Geometric and Safety Factors

The proposed separation between the shadow vehicle and the maintenance vehicle for operation in automated mode is a tracking line-of-sight of 10 to 200 feet. As the Lead Vehicle enters a horizontal curve, the Autonomous Shadow Vehicle will close the range to the Lead Vehicle to maintain a tracking line-of-sight with the Lead Vehicle until exiting from the curve when it will resume the desired tracking line-of-sight range. Tracking line-of-sight for the research project will be defined as the position of the centerline(a line from the front to the back down the center of the vehicle that approximately passes through its center of gravity) of the Autonomous Shadow Vehicle such that it approximately coincides with the center line of the Lead Vehicle and such that the wheels(left or right) are within ±2 feet. No obstruction of the tracking line-of-sight between the Lead Vehicle and Autonomous Shadow Vehicle will be caused by highway geometric features or by bridges over sag curves. When the shadow vehicle is operating on the shoulder crews should watch for overhanging objects which may interfere with the Autonomous Shadow Vehicle's tracking system.

Two advantages of keeping the shadow vehicle within tracking line-of-sight behind the maintenance vehicle occur on vertical and horizontal curves. Since the camera is set at a fixed angle to the shadow vehicle, there will be a slight offset of the location of the Lead and Autonomous Shadow as the vehicles travel over vertical curves. This displacement is less than one tenth of one foot, for curves with design speeds of 40 mph or more, when the separation is 40 feet. In contrast a separation of 100 feet causes vertical displacements up to 2 feet for similar curves.

On horizontal curves the shadow vehicle attempts to track the maintenance vehicle in a straight line. This introduces a lateral displacement of the shadow vehicle as it follows the maintenance vehicle around a curve. A separation of 40 feet limits this offset to 1.4 feet on curves with radius 500 feet, and to 0.8 feet on curves with radius 1000 feet. If the maintenance vehicle travels in the center of a twelve feet wide lane and if the shadow vehicle is 8 feet wide, an offset of 1.4 feet places one side of the shadow vehicle 0.6 feet from the lane line. A greater separation between the shadow vehicle and maintenance vehicle would result in unacceptably large lateral displacements.

The main disadvantage of maintaining small separations between the shadow vehicle and maintenance vehicle lies in safety for roll forward and for safe stopping of the shadow vehicle if the

maintenance vehicle stops. Forty feet separation provides adequate safety for sudden stops of the maintenance vehicle for operating speeds up to at least 13.6 mph for speeds up to 30 mph greater distances are required. Forty feet separation provides adequate safety for shadow vehicle roll forward after impact if a heavy shadow vehicle is used (25,000 pounds) and operating speed is fast (25 mph). At lower operating speeds 40 feet separation will not prevent the shadow vehicle from running into the maintenance vehicle if the impacting vehicle is larger. For example at 10 mph operating speed the 40 feet separation is only safe for impacting vehicles up to 20,000 pounds in weight. Lighter shadow vehicles provide less safety for roll forward. For example safe separation exceeds 40 feet if a 10,000 pound shadow vehicle traveling at 10 mph is impacted by a vehicle weighing 10,000 pounds. Section 3 discusses the geometric factors in more detail.

To take advantage of the greater safety provided by large shadow vehicles a heavy shadow vehicle should be used for automation. To take advantage of the greater safety provided by higher operating speeds (up to 13.6 mph for 40 feet separation) it would be best to introduce automation in operations such as street sweeping or lane closure. However, in the lane closure task the shadow vehicle needs to operate independently of the maintenance vehicle for a portion of the task. From the operations point of view street sweeping is a better candidate for automation. The only problem to overcome here is the need to have the shadow vehicle driven to site or towed to the site by the sweeper. Another possible first candidate is crack sealing which is done at slow speed but inside a closed lane. The major considerations for the tracking system here are the stop and go operation and the need for operators to work on the road between the Autonomous Shadow Vehicle and the Lead Maintenance Vehicle.

1.3.3 Comparison of Tracking Technologies

An extensive literature search was performed. A partial list of the material reviewed is given at the end of this report under References. Various technologies were discovered that might prove to be viable for the Shadow Project application. Table 1.1 contains a summary of the characteristics of the technologies considered for use in designing tracking systems based on the research findings. Table 1.1 shows the advantages and disadvantages of the different technologies. The characteristics important to the tracking task are identified in the left hand column of Table 1.1. The objective is to identify technologies which best satisfy all of the desired characteristics listed in Table 1.1.

Based on Table 1.1 and our research findings, it is evident that Antenna Array, Vision and Relative GPS tracking systems are the most appropriate technologies to use. It is anticipated that these three technologies will be cost effective and will compliment each other. To ensure safe operation of the Autonomous Shadow Vehicle, it is recommended that all three systems be used for redundancy purposes.

The major strength of an Antenna Tracking System is that weather conditions will not appreciably effect its operation. The major strength of a Vision Tracking System is that it can assure that the Autonomous Shadow Vehicle has acquired the appropriate target for tracking, i.e., a proposed 3-D symbol mounted on the back of the Lead Maintenance Vehicle. The Relative GPS Tracking System will provide an additional check on the Antenna and Vision Tracking Systems. Furthermore, each of these three systems has completely different operating characteristics such that something that might interfere with the operation of one of the tracking systems is not likely to effect the operation of the other two tracking systems. As the GPS technology matures it is expected that it will become more reliable. The technologies reviewed are discussed in more detail in Section 4.

Table 1.1 Tracking Sensor Technology Comparison

	ULTRA-SONIC 20-100KHz REF. 1	LED LASER INFRARED/ VISIBLE MOD. UP TO 200MHz REF. 2,19,38, 43	DIFF. GPS 1.2/1.5GHz REF. 4,7,8,9, 33,34,35, 36,37	RELATIVE GPS 1.2/1.5GHz REF. 4,7,9, 33,34, 35,36,37	ANTENNA ARRAY 10GHz REF. 10,18,20, 21,23,24, 25,26,27, 28,29,31, 32,40,44,45	MM SCANNING/ RADAR 30-100GHz REF. 3,5,6,15, 16,17,24	VISION REF. 11,12,13, 14,39,41, 42,46, 47, 48,49
RAIN (MODERATE)	POOR	FAIR	EXCELLENT	EXCELLENT	EXCELLENT	EXCELLENT	GOOD
FOG (MODERATE)	POOR	POOR	EXCELLENT	EXCELLENT	EXCELLENT	EXCELLENT	GOOD
SNOW (MODERATE)	POOR	POOR	EXCELLENT	EXCELLENT	EXCELLENT	EXCELLENT	GOOD
LATERAL ACCURACY ±6"	POOR	GOOD	POOR	EXCELLENT	GOOD	EXCELLENT	GOOD
RANGE ACCURACY 5-10%	FAIR	GOOD	POOR	EXCELLENT	GOOD	EXCELLENT	EXCELLENT
RELATIVE YAW ACCURACY ±1.0°	POOR	GOOD	N/A	GOOD	GOOD	GOOD	GOOD
CURVE TRACKING	PROBABLY POOR	TBD	N/A	GOOD	GOOD	GOOD	GOOD
INTERFERENCE REJECTION	FAIR	GOOD	GOOD	GOOD	GOOD	GOOD	GOOD
EFFECT OF REFLECTIONS	SMALL TO LARGE	SMALL TO LARGE	SMALL TO LARGE	SMALL	SMALL IF NARROW BEAM	SMALL IF NARROW BEAM	SMALL
EFFECT OF VARYING LIGHT CONDITIONS	N/A	GREAT	N/A	N/A	N/A	N/A	SMALL IF OBJECT IS LITE
OPERATIONAL RELIABILITY	GOOD	GOOD	GOOD TO POOR	GOOD TO POOR	GOOD	GOOD	GOOD
PUBLIC ACCEPTANCE	UN-CERTAIN	POOR	EXCELLENT	EXCELLENT	GOOD	POOR	EXCELLENT
SENSOR COST ESTIMATE	$5,000	$10,000	N/A	$10,000	$10,000	$50,000	$5,000
PHASE I ASSESSMENT	REJECT	REJECT	REJECT	3RD LEVEL CHECK	PRIMARY SYSTEM	REJECT	SECONDARY SYSTEM

1.3.4 Safety Redundancy Check & Shadow Vehicle Control

It is proposed that a safety redundancy checker software program compare the data generated by each sensor tracking system to ensure that the data presented is consistent before sending it on to the steering and range Shadow Vehicle controllers. The block diagram in Figure 1.1 illustrates this flow of data.

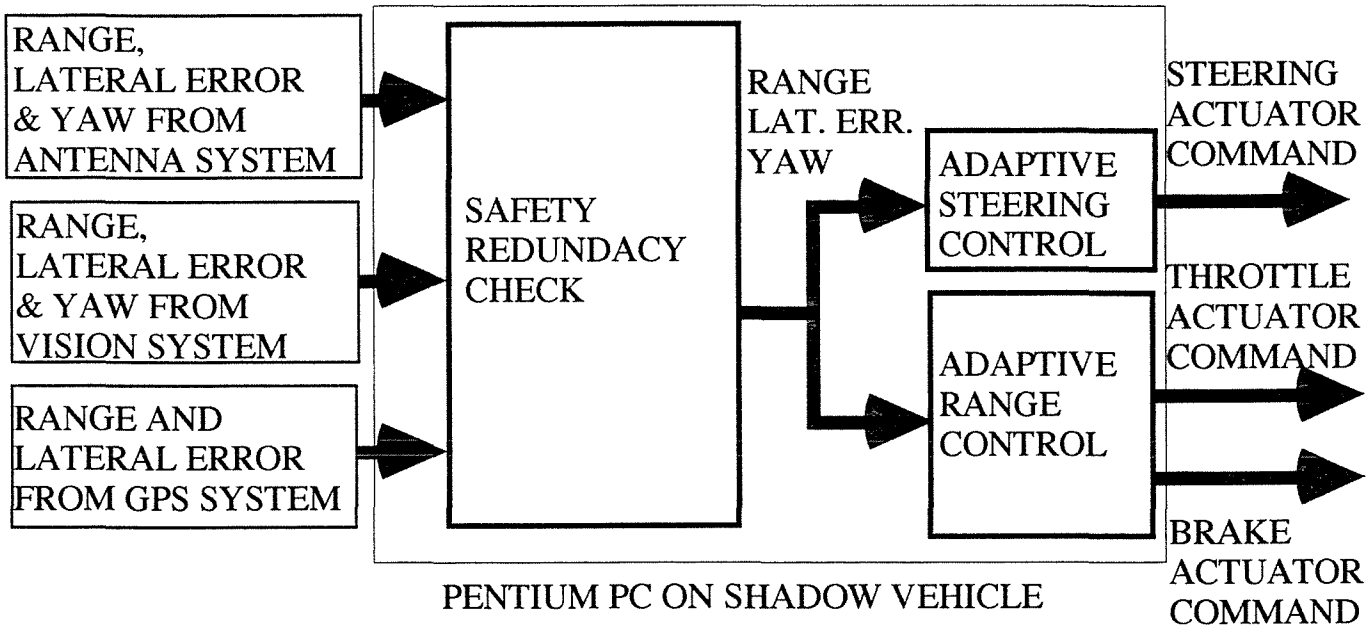

Figure 1.1. Safety Redundancy Check & Control

Range, lateral error and yaw angle of the shadow vehicle relative to the lead vehicle determined by the Antenna, Vision and Relative GPS Tracking Systems are inputs to the safety redundancy check program. The safety redundancy check program checks for agreement of the current data produced by all of the sensors and also compares the sensor data with predicted values based on past sensor data and the fed back steering angle. If two sensors do not agree within an allowable tolerance, data from the sensor that is most likely correct will be used and a warning will be sent to the lead vehicle driver. The Relative GPS Tracking System also has bi-directional data transmission capability that allows information to be sent to the Lead Vehicle driver. The range, lateral error, and yaw data that have been determined to be correct are sent to adaptive controllers that send commands to the steering, throttle and brake actuators. These control systems are discussed in more detail in Section 8.

1.3.5 Antenna Array Tracking System

In order for the Shadow vehicle to autonomously follow a Lead vehicle, it needs to know range(distance between the two vehicles), lateral displacement(the amount of shift left or right from bore-sight), and yaw angle(direction angle of Shadow vehicle with respect to Lead vehicle). The antenna design objective was to be able to determine range(±10%), lateral displacement(±6"), and yaw angle(±1.0^{o}). The general idea of the system is to mount a transmitting antenna on the Lead vehicle(with a very narrow beam) and a receiving antenna array(RAA) on the Shadow vehicle. Section 1.3.5.1 describes a design based on using a transmitting antenna array. Section 1.3.5.2 describes a design based on using a parabolic dish as the transmitting source. The parabolic dish approach is proposed for use as the Antenna Tracking System.

1.3.5.1 Transmitting Antenna Array Tracking System

The general idea of the system is to mount a 110 element transmitting antenna array(TAA) on the Lead vehicle(with a very narrow beam) and a set of 15 receiving antenna array(RAA) on the Shadow vehicle, as shown in Figure 5.1. The TAA emits a pencil beam pattern, as shown in Figure 5.2, which is directed at the RAA. At the RAA, magnitude and phase are read from each of the 15 elements. If the RAA is directly behind the TAA, i.e., no lateral shift or yaw, the magnitude and phase from the RAA will be symmetrical about the center element, as shown in Figure 5.4. If the RAA is laterally displaced, the magnitude and phase shift accordingly, as shown in Figure 5.5. If the RAA is laterally displaced and yawed, the magnitudes will indicate the lateral shift and the phases indicate that it is yawed, as shown in Figure 5.6. The magnitude and phase from the RAA are then pre-processed to obtain relative amplitude and phase measurements. The relative information is then fed into an A/D converter and then into a neural network. The neural network will then map magnitude and phase into the required range, lateral displacement, and yaw angle. This is the necessary information needed to control the shadow vehicle accordingly. A summary of the first antenna design is listed in Table 1.2.

Table 1.2. Summary of Antenna Design

	Antenna Type	No. of Elements	Element Spacing (m)	Antenna Height (m)	Antenna Width (m)	Antenna Placement
Transmitter	Array	110	0.015	0.5	1.65	Lead Vehicle
Receiver	Individual Elements	15	0.014	0.5	2.0	Shadow Vehicle

A model was developed in C language to test the antenna design. The model was developed based on far-field calculations. This means that all simulations were required to be performed with at least a 100m between transmitting antenna array and the receiving antennas. A range of 100-150m(steps of 1-5m), lateral displacement of ±0.6667m(in steps of 0.1667m), and yaw angle of $\pm 3^{o}$(in steps of 1^{o}) was used in simulations to show proof of concept.

1.3.5.2 Transmitting Parabolic Dish Tracking System

The original antenna array tracking system has been revised to reduce overall cost and manufacturing complexity. The original transmitting dipole array consisted of 110 dipole elements spaced 0.015m (one half wavelength for a 10GHz excitation source). It was discovered that reproduction of an antenna with this many elements and element spacing would prove to very difficult. This difficulty arises from the fact that each element would have to be hand tuned to account for the different line lengths between each element and the source, i.e., impedance matching of the elements to the source. The output pattern had a half power beam width of 0.2 degrees. This antenna has been replaced with a parabolic dish antenna with a diameter of 1.2192m (4ft). The output pattern has a half power beam width of 1.7 degrees and a gain of 40dB. The increased beam width size will still allow the receiving antenna to detect any change in orientation of the transmitting antenna relative to the receiving antenna.

The increased size of the transmitting antenna beam width has required that the receiving antenna design to be revised. The width of the receiving antenna is set at 2m. The number of elements of the receiving antenna has been reduced to seven dipole elements spaced 0.333m apart. This reduction in the number of receiving elements was acceptable due to the fact that the transmitted beam width was larger and the spacing on the receiving antenna could be increased and still maintain phase and amplitude resolution.

The general idea of the system is as before. The transmitting antenna emits a pencil beam pattern which is directed at the receiving antenna. At the receiving antenna, the phase and amplitude from each of the elements is measured. Based on the phase and amplitude distribution on the receiving elements range, lateral displacement and yaw angle are attainable. These are the three necessary parameters needed to computer control the Shadow vehicle relative to the Lead vehicle. Table 1.3 summarizes the revised antenna design.

Table 1.3. Summary of Antenna Design Revision

	Antenna type	No. of Antennas/ Elements	Element Spacing (m)	Antenna Height (m)	Antenna Width	Antenna Placement
Transmitter	Parabolic Dish	1	N/A	1.2192	1.2192	Lead Vehicle
Receiver	Individual Elements	7	0.333	0.5	2.0	Shadow Vehicle

1.3.6 Vision Tracking System

Figure 1.2 illustrates the proposed Vision Tracking System.

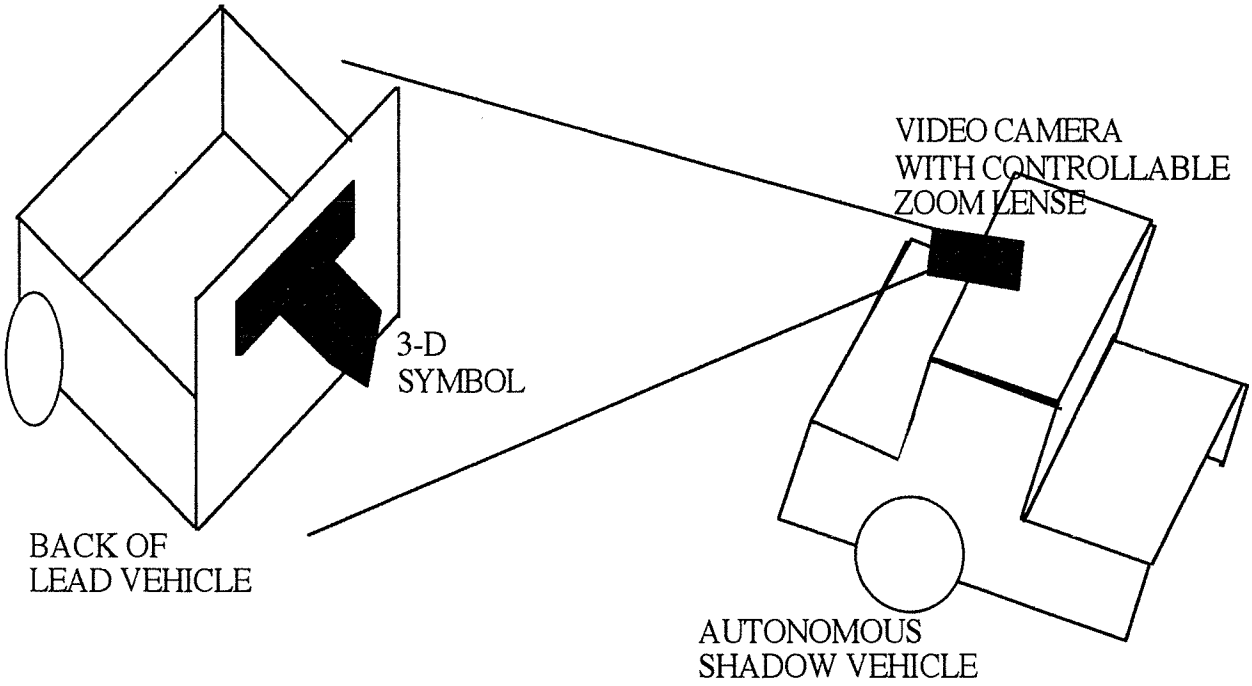

Figure 1.2. Vision Tracking System

An extensive literature search was performed. Research was not found that replicated this research. The image processing techniques used in this research are well known [54], [55], [56], [57], and [58]; but, this research has applied the techniques uniquely. One paper was located that uses stereo (two cameras) to track a light on a lead vehicle [11]. However, the possibility of tracking light or lights other than that of the lead vehicle or daylight effects of the sun were not addressed. The primary focus of this research was to ascertain if one camera can be used. The research objective in this reqard was met. Demonstrations using a single video camera and a symbol were performed. The data from the experiment verified that for ranges up to 45 feet, using vision to track a lead vehicle is clearly viable for moderate weather conditions. That is, if a human can see the target symbol on the back of the Lead Vehicle, then so can the vision system. The results also indicate that tracking for ranges up to 200 feet can also be performed using vision techniques.

It is proposed that a 3-D symbol such shown in Figure 1.3 be mounted on the back of lead maintenance vehicles. Lights are mounted inside of the symbol to eliminate shadows on the symbol and for night operation.

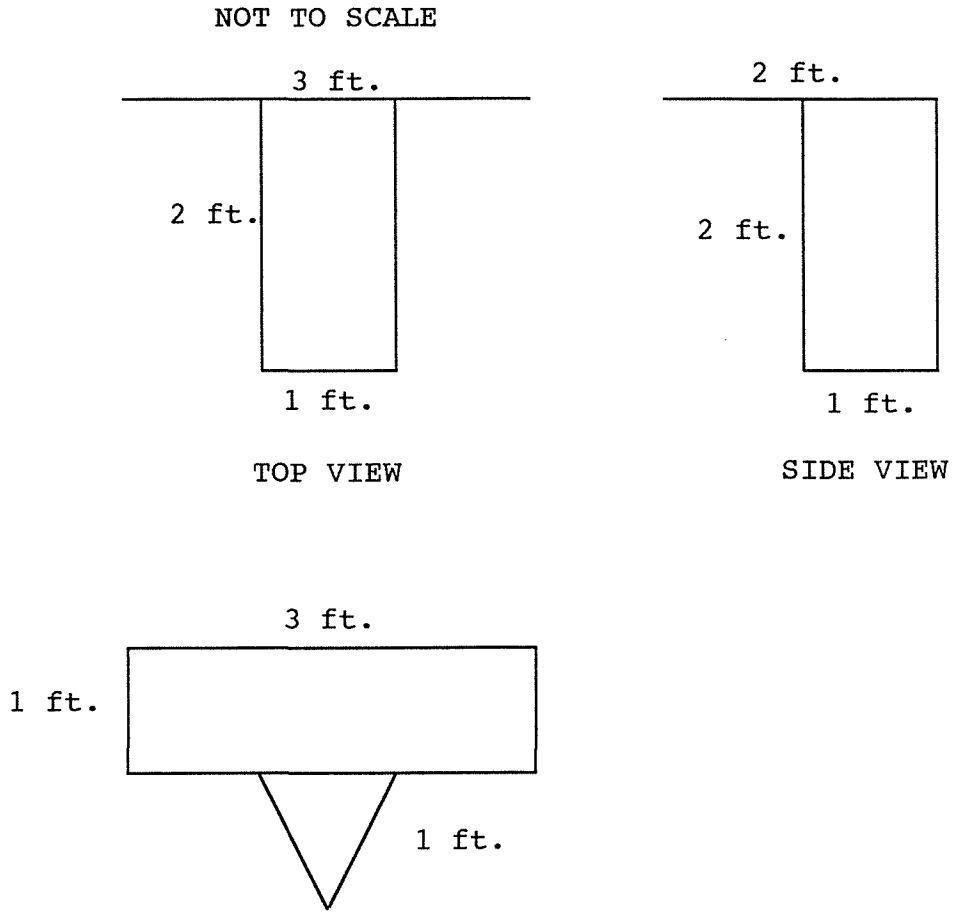

Figure 1.3. Proposed Symbol for Lead Vehicle

A video camera with a controllable zoom lens is mounted on top of the shadow vehicle and points down at the symbol on the lead vehicle. Whether a fixed iris or computer controlled iris to control the amount of light entering the lens should be used will be determined in Phase II. A machine vision algorithm executed by a Pentium PC on the shadow vehicle determines that in fact the symbol and no other object has been acquired by the camera. Points on the symbol found by the machine algorithm are then fed to a neural network executed by the Pentium PC that determines range, lateral error and yaw angle of the Autonomous Shadow Vehicle relative to the Lead Vehicle. Range, lateral error and yaw angle are sent to a safety redundancy checker software program. If the safety redundancy checker software program determines that valid data has been received, it sends the determined range, lateral error, and yaw angle on to the Autonomous Shadow Vehicle control system software program executed by the Pentium PC.

1.3.7 Relative GPS Tracking System

Figure 1.4 illustrates the basic concept of the proposed Relative GPS Tracking System.

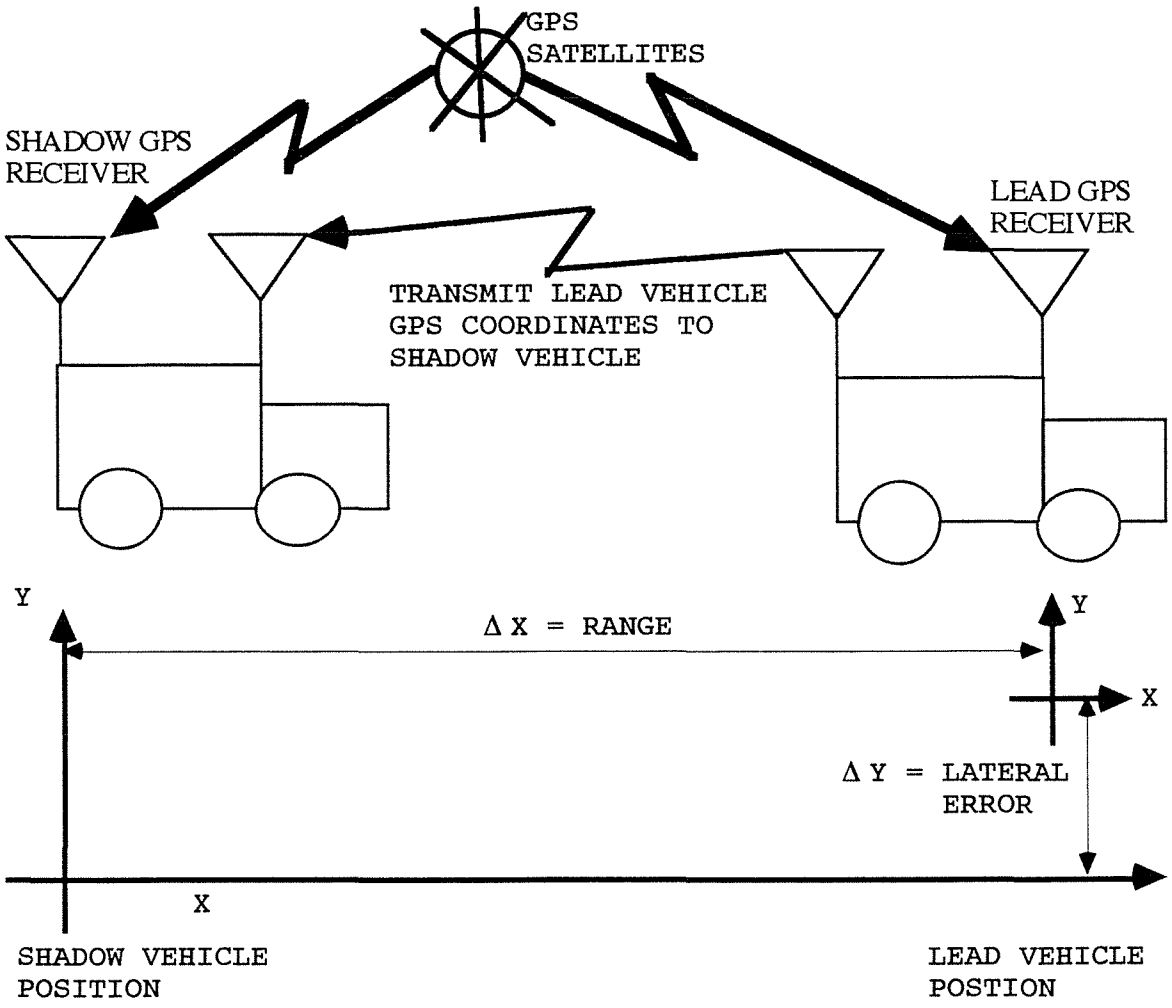

Figure 1.4 Relative GPS Tracking System

GPS XYZ coordinates of the Lead Vehicle are received by Lead Vehicle and transmitted back to Autonomous Shadow Vehicle. GPS XYZ coordinates are also received simultaneously by the Autonomous Shadow Vehicle. Autonomous Shadow Vehicle coordinates are subtracted from the Lead Vehicle's coordinates to find range and lateral error of the Autonomous Shadow Vehicle relative to the

Lead Vehicle. Curves can be detected by mapping(plotting) the GPS coordinates of the Lead Vehicle.

GPS coordinates are updated every second. Therefore, if the only tracking system used is the proposed Relative GPS Tracking Systems, then, a rate gyro or position gyro would be required to obtain control information at least every 0.1 seconds.

GPS satellites can be occluded by hills and buildings. Differential stations(repeater stations broadcasting local corrections) will increase reliability. Even though GPS may drop-out from time to time, the Relative GPS Tracking System will add a third level check. Range, lateral error and approximated yaw angle are sent to the safety redundancy checker and shadow vehicle control system which are also executed on the Pentium PC.

1.3.8 Throttle, Brake and Steering Controllers

An extensive literature search and review of the literature related to longitudinal and lateral control of vehicles was performed. Based on this review, digital controllers for control of throttle, brake, and steering actuators were designed, and simulated. Section 8 describes the throttle and brake controllers and Section 9 describes the Steering controller. The simulations indicate that the designed controller using a 0.1 second sampling interval meet the requirements for this research project.

1.4 Organization of the Report

Section 2 discusses current shadow vehicle operations. Section 3 continues discussing shadow operations in terms of the impact of freeway geometry and safety factors that need to be considered. Section 4 discusses the technologies researched for use in designing tracking systems for this project. Section 5 describes the antenna research and design performed in Phase I and that is proposed for Phase II, experimentation and feasibility demonstration. Section 6 describes the vision research and design performed in Phase I and that is proposed for Phase II, experimentation and feasibility demonstration. Section 7 describes the GPS research and design performed in Phase I and that is proposed for Phase II, experimentation and feasibility demonstration. Section 8 describes the longitudinal control research and design performed in Phase I and that is proposed for Phase II, experimentation and feasibility demonstration. Section 9 describes the lateral control research and design performed in Phase I and that is proposed for Phase II, experimentation and feasibility demonstration. Section 10 contains the references referred to in the body of this report.

2. CURRENT SHADOW VEHICLE OPERATIONS

2.1 Tasks

Shadow vehicles are used in highway maintenance operations to provide a safer operating environment for maintenance personnel. The minimum weight of a vehicle that may be used as a shadow vehicle is 4000 pounds [50]. A more typical weight is 25,000 pounds. The speed at which shadow vehicles operate when in service as a shadow vehicle varies depending on the type of maintenance task. Typical tasks and the associated operating speed are shown in Table 2.1 and each of the tasks are described below.

TABLE 2.1 Shadow Vehicle Tasks and Operating Speeds

TASK	SPEED
Sweeping	6 to 12 mph
Setting Cones for Lane Closure	15 mph
Painting Lines	25 mph
Placing Thermoplastic Lines	2 to 3 mph
Laying Bott Dots	Stop and Go
Crack Sealing	Stop and Go

2.2 Work Vehicles and Operating Modes

2.2.1 Street Sweeping

Street sweeping is one of the most common highway maintenance tasks in which shadow vehicles are utilized. Sweeping operations are carried out on curbed sections of highway where trash and debris is retained by the curb. On freeways these sections are typically found on bridges and other elevated segments. The task may involve one or two shadow vehicles. Two shadow vehicles are

used where sight distances for oncoming traffic are restricted. The driver of the second shadow vehicle positions the vehicle far enough back from the operation to provide advance warning to traffic. In order to indicate lane closure between the first and second shadow vehicle, the driver of the first shadow vehicle drops flares at regular intervals along the highway.

In street sweeping the vehicles are operating on the shoulder and, depending on the available width of the shoulder, they may or may not occupy part of the adjacent lane. The work crew includes the driver of the sweeper truck and a driver for a pick-up truck which travels in front of the sweeper truck. The driver of the pick-up truck, or an additional crew member riding as a passenger in the pick-up, removes any large objects along the curb. On multi-lane highways it is necessary to sweep both the right and left sides of the road. The pick-up truck, street sweeper vehicle, and shadow vehicle(s) are positioned on the appropriate shoulder at the beginning of the task. For operations on the left side of the road this necessitates crossing other lanes of traffic before the work begins. The shadow vehicle stays directly behind the sweeper truck during the sweeping, but not while changing lanes for positioning on the left side of the road.

2.2.2 Lane Closure

Lane closure is another task in which shadow vehicles are commonly used. In this task the vehicles begin from the shoulder and move out into the lane(s) to be closed. The shadow vehicle follows a single maintenance vehicle with a crew of two maintenance workers. The maintenance vehicle carries lane closure cones and roadwork ahead signs, and tows a lane closed sign. The crew member assigned to placing the cones generally sits in a special seat on the left side of the maintenance vehicle but could alternatively be on the right side.

In the early stages of the lane closure task stops are made while the work crew leaves the maintenance vehicle and sets up the required road work ahead and lane closure signs. When the vehicles are stopped, the driver of the shadow vehicle turns the vehicle's wheels in toward the side of the road to provide additional safety if the shadow vehicle is hit from behind. The driver of the shadow vehicle also keeps an eye on traffic so that she/he can give a warning to the crew on the road if they are in any danger. Cones are first placed along the edge of the shoulder then, after the lane closed sign has been placed (this is the one towed by the maintenance vehicle), the crew begins to taper out the cones into the lane(s) to be closed.

During placement of the taper the maintenance vehicle remains on the inside of the cones but the shadow vehicle moves out into the adjacent lane to "take the lane" and give warning that the lane is closed. At this time the shadow vehicle is not behind the maintenance vehicle. After the taper is about half way across the

lane to be closed, the shadow vehicle moves back behind the maintenance vehicle for the remainder of the task. This procedure is used for closing lanes on the right side of the road with the crew member sitting on the left side of the maintenance vehicle and for closing lanes on the left side of the road with the crew member sitting on the right side of the vehicle.

To release a closed lane back to traffic, cone pick up is performed by the crew on a maintenance vehicle and the vehicle is protected by a shadow vehicle. There are two alternative procedures for cone pick up. In the preferred method the maintenance and shadow vehicles travel in the same direction as traffic. The shadow vehicle travels outside the cones, in the closed lane, while the cone pick up crew travel inside the cones to pick up the taper. Then the shadow vehicle travels directly behind the maintenance vehicle, essentially creating a moving lane closure, while the pick up crew remove the cones for the remaining length of the lane closure. Again the shadow vehicle is not directly behind the maintenance vehicle for the first part of this task.

In the other, and less preferred, method of cone pick up the maintenance and shadow vehicles travel in the opposing direction to traffic. To provide protection for the maintenance crew the vehicles travel backwards with the shadow vehicle preceding the maintenance vehicle in their direction of motion. Cones are picked up in reverse order of their placement. This method could not be automated.

2.2.3 Painting or Placing Lines and Placing Bott Dots

Placing of lines, either paint or thermoplastic, and bott dots is a moving operation. The maintenance vehicle is a special truck with a cage on one side for the maintenance worker. The cage is generally on the left side of the vehicle. Lane painting can be done at relatively high speeds (25 mph) but laying thermoplastic is done very slowly and placing bott dots is a stop and go operation. The work crew do not leave their vehicles except on minor mountain roads. In this task the shadow vehicle provides a moving lane closure. Stationary advance warning signs on the shoulder are moved along the highway as work progresses but the lane is not closed with cones. Lane changing, before execution of the task, will be necessary to place the maintenance and shadow vehicles in the appropriate location for the task.

For this task the maintenance vehicle and the shadow vehicle may be in any of the available lanes on the highway. On multi-lane highways with three lanes in each direction the work can be done from the right lane and from the left lane (if a vehicle is available with the cage on the right side.) But, if there are 4 or more lanes each way, or if the cage is on the left side of the vehicle the work must be done from a lane which is not adjacent to

the shoulder. This requires lane changing during execution of the task.

2.2.4 Crack Sealing

In contrast to placing line and bott dots, crack sealing is done inside a closed lane. Vehicles may be moving very slowly or stopped completely while sealant is placed. Crew members work outside the vehicles between the maintenance vehicle and the shadow vehicle. The maintenance vehicle tows a trailer containing the sealant.

2.3 Traveling to Site

For all shadow vehicle operations the maintenance vehicles and the shadow vehicle(s) begin the task from the shoulder, or inside a closed lane at the site. The vehicles are driven to site at normal operating speeds restricted only by applicable speed limits, other safety considerations and vehicle capabilities on grades. Generally, but not necessarily, the shadow vehicle will be driven to the site in convoy with other maintenance vehicles.

Automation of the shadow vehicle during this phase of the work is not feasible at this stage because the high speeds impose greater safety constraints. At 55 mph the separation between vehicles should be two seconds or 162 feet. Another obstacle to automation of the shadow vehicle while traveling to site are the sharp horizontal curves which may be encountered on ramps and minor roads. Shadow vehicle tracking of the maintenance vehicle on sharp curves, at relatively high speeds, poses a problem beyond the scope of work at this first stage.

For most maintenance tasks it will be feasible for the shadow vehicle to be driven to site by maintenance personnel needed at site for other work such as placing cones in lane closure. Another alternative would be to tow the shadow vehicle to the site, or tow one of the smaller maintenance vehicles to site so that the shadow vehicle driver becomes the driver of the towed maintenance vehicle for the maintenance task.

2.4 Positioning in Lane

As indicated earlier tasks involving shadow vehicles begin on the shoulder. If the work is on the left side of a multi-lane highway this means that the vehicles must change lanes to get to the left shoulder. Changing lanes may also be necessary during execution of the task for the line painting/bott dot placement. Current practice for lane changing requires the shadow vehicle to change lanes first. The shadow vehicle then provides space for the vehicles in front to change lanes. This is similar to the operation referred to as "taking the lane" during cone placement.

When the shadow vehicle changes lanes before or without the maintenance vehicle it cannot operate in automated mode. For street sweeping the shadow vehicle could be driven to the left side of the road or one of the vehicles could be towed there. However, for line painting/bott dot placement in some lanes of a multi lane highway, and for lane closure, lane changing is an integral part of the task presenting a more difficult problem to overcome before automation becomes practical in these tasks. For crack sealing lane changing is not an integral part of the task. The shadow vehicle can be driven, or towed, to the staging area inside the closed lane(s) and automated operation can then begin.

2.5 Site Distance & Dual Shadow Vehicle Considerations

Aspects of site distance must be considered. Sight restrictions due to highway geometry are discussed in the next chapter of this report. Other things which might interfere with the line of sight are objects or personnel between the shadow vehicle and the maintenance vehicle. In lane closure, the maintenance vehicle tows a sign board on a trailer. This must be checked and redesigned if necessary to allow a clear line of sight. In crack sealing, personnel may be working on the ground between the two vehicles. Consideration of personnel between the Autonomous Shadow Vehicle and the Lead Vehicle must be taken into account by the tracking systems if an Autonomous Shadow Vehicle is used for crack sealing operations. It may be necessary to restrict this type of work to stationary operation only. The possibility of other vehicles coming between the shadow vehicle and the maintenance vehicle must also be considered when designing the tracking systems.

Another sight distance concern occurs during moving lane closures for street sweeping or line painting and bott dot placement. When sight distances are restricted, oncoming traffic may not be able to see the shadow vehicle far enough in advance. Under these circumstances a second shadow vehicle is used, traveling as far back as necessary to be seen by oncoming traffic. The driver of this vehicle must vary his position to suit the needs of the situation. It may not be possible to automate this second shadow vehicle.

3. GEOMETRIC AND SAFETY FACTORS

3.1 Line-of-sight of Shadow Vehicle to Working Vehicle

The line of sight between two vehicles may be obstructed by horizontal curves, vertical curves, or overhead bridges and signs. The proposed mounting height of the camera (H1) on the shadow vehicle is eight feet and the proposed mounting height of the target (H2) on the maintenance vehicle is four feet. As shown in Tables 3.1 and 3.2, with these mounting heights camera sight distances on crest and sag vertical curves will be far in excess of a 40 feet separation between the shadow vehicle and the maintenance vehicle.

Table 3.1. Available Sight Distance Between Camera and Target for Selected Crest Curves

Design Speed (mph)	Sum of Grades (percent)	Curve Length (feet)	Camera Sight Distance (feet)
20	12	110	250
25	12	200	295
30	12	350	370

Notes: Sum of grades = 12%, and low speed curves provide the worst case scenarios.
Curve length taken from CALTRANS' Highway Design Manual[51].
Sight Distance based on equations from ref. 3 with H1 = 8 feet and H2 = 4 feet.

Table 3.2. Available Sight Distance Between Camera and Target for Selected Sag Curves

Design Speed (mph)	Sum of Grades (percent)	Curve Length (feet)	Camera Sight Distance (feet)
20	12	240	154
25	12	280	174
30	12	440	254

Notes: Sum of grades = 12%, and low speed curves provide the worst case scenarios.
Curve length taken from CALTRANS' Highway Design Manual[51].
Sight Distance based on equations from ref. 3 with H1 = 8 feet and H2 = 4 feet.

Since the camera, antenna array and transmitting dish are mounted high on the vehicles, another sight distance concern occurs when passing under bridges and other overhanging objects. Table 3.3 shows sight distance available when passing under a 15 foot high bridge. Again these distances are far in excess of a 40 feet separation.

Table 3.3. Available Sight Distance Between Camera and Target for Selected Sag Curves Under Bridges

Design Speed (mph)	Sum of Grades (percent)	Curve Length (feet)	Camera Sight Distance (feet)
20	12	240	420
25	12	280	440
30	12	440	520

Notes: Sum of grades = 12%, and low speed curves provide the worst case scenarios.
Curve length taken from CALTRANS' Highway Design Manual[51].
Sight Distance based on equations from ref. 4 with H1 = 8 feet and H2 = 4 feet.

As seen above no camera sight distance problem is anticipated on vertical curves for the 40 feet separation between shadow vehicle and maintenance vehicle. Since the camera and antenna array line of sight is far above the line of sight assumed in computation of safe stopping sight distance (H1 = 3.25, H2 = 0.5 feet), no problem is anticipated on horizontal curves. Safe stopping sight distances provide by design [51] are:

Speed(mph)	20	30	40	50	60
Safe stopping distance(feet)	125	200	325	550	1525

On any curve designed to provide these safe stopping distances the camera sight distance will be greater than these distances except in situations where overhanging objects interfere with the higher line of sight. On horizontal curves it will be important for maintenance workers to watch for overhanging obstacles which might interfere with the tracking system's line of sight.

3.2 Tracking on Vertical Curves

The line of sight of the camera will be fixed relative to the plane of the shadow vehicle. On vertical curves this will result in a vertical displacement of the camera's view of the target. Tables 3.4a and b show this vertical displacement for tracking distances of 40 feet and 200 feet. As seen from these tables a

tracking distance of 40 feet results in very small displacement while a 200 feet tracking distance would pose a significant problem in vertical displacement.

Table 3.4a. Vertical Offset of Camera Line of Sight on Target for Vertical Curves with Design Speeds 75, 60, and 45 mph for 40 Feet Separation of Vehicles

75mph			60mph			45mph		
A	L	DY	A	L	DY	A	L	DY
2%	11	0.01	2%	6	0.03	2%	2	0.08
4%	21	0.02	4%	11	0.03	4%	5	0.06
6%	31	0.02	6%	19	0.03	6%	7	0.07
8%	43	0.01	8%	26	0.02	8%	8	0.08
10%	53	0.02	10%	33	0.02	10%	10	0.08
12%	64	0.02	12%	39	0.02	12%	12	0.08

Notes: A = Total change of grade; L = curve length in stations; DY = vertical offset

Table 3.4b. Vertical Offset of Camera Line of Sight on Target for Vertical Curves with Design Speeds 75, 60, and 45 mph for 100 Feet separation of Vehicles

75mph			60mph			45mph		
A	L	DY	A	L	DY	A	L	DY
2%	11	0.36	2%	6	0.67	2%	2	2.00
4%	21	0.38	4%	11	0.73	4%	5	1.60
6%	31	0.39	6%	19	0.63	6%	7	1.71
8%	43	0.37	8%	26	0.62	8%	8	2.00
10%	53	0.38	10%	33	0.61	10%	10	2.00
12%	64	0.38	12%	39	0.62	12%	12	2.00

Notes: A = Total change of grade; L = curve length in stations; DY = vertical offset

3.3 Tracking on Horizontal Curves

On horizontal curves the shadow vehicle will attempt to remain in a straight line behind the work vehicle. The path of the shadow vehicle will therefore be displaced laterally. A small displacement is not a problem because all vehicles tend to move laterally in their lanes to some degree. However a large displacement could cause the shadow vehicle to move too close to the lane limits, or even out of the lane, and this would be hazardous.

Table 3.5 shows the horizontal displacement of the shadow vehicle for various curve radii and various separation distances between the shadow vehicle and the maintenance vehicle being tracked. As seen in this table lateral movements in excess of 1.7 feet, and up to 41.7 feet, could occur if the separation distance between the shadow vehicle and the vehicle being tracked was 100 to 200 feet. This is obviously not acceptable. Lateral offsets of 0.3 feet to

0.8 feet would occur for a separation distance of 40 feet on curves of 3000 to 1000 feet. This amount of lateral movement is tolerable. However on curves with a radius of less than 1000 feet the displacement increases rapidly with decrease in curve radius. Operation of the automated shadow vehicle should, therefore, be restricted to the larger radius curves.

Table 3.5. Displacement of Shadow Vehicle on Horizontal Curves

RADIUS (feet)	SEPARATION (feet)	DISPLACEMENT (feet)
500	40	1.4
	100	9.9
	200	38.5
1000	40	0.8
	100	5.0
	200	19.8
2000	40	0.4
	100	2.5
	200	10.1
3000	40	0.3
	100	1.7
	200	6.7

3.4 Safe Separation of Shadow and Working Vehicles

When asked about the separation distance between the shadow vehicle and the working vehicle, operators indicated that they try to maintain about 200 feet separation, varying the distance with the gradient along the road. This distance is based on the roll forward distance of a 25,000 pound shadow vehicle if the vehicle was hit from behind by a 60,000 pound truck traveling at 65 mph. As seen in Table 3.6 the roll forward distance is 133 to 238 feet for these circumstances if the shadow vehicle and the maintenance vehicle are traveling at 10 to 25 mph and the available friction ranges between 0.4 and 0.6.

Table 3.6. Roll Forward Distance for a 25,000 pound Shadow Vehicle on Level Road Impacting Vehicle Speed 65 mph

Shadow vehicle speed	Impacting vehicle weight	Roll forward distance (feet) for: Friction Factor (f) f=0.2	f=0.4	f=0.6	f=0.8
10 mph	4,000 lbs	52	26	18	13
	10,000 lbs	62	31	21	16
	60,000 lbs	400	200	133	100
25 mph	4,000 lbs	156	88	52	44
	10,000 lbs	223	112	75	56
	60,000 lbs	475	238	158	119

Notes: For design f is assumed to be between 0.3 and 0.4. This is based on the assumption of a poor road surface, poor tires, and wet road.
On downgrades the stopping force is counteracted by gravity and the "effective friction" is reduced (for example by about 0.06 on a 6% downgrade).

It is possible to reduce the separation distance below the roll forward distance while still maintaining safety. The separation distance does not need to be as large as the roll forward distance because the maintenance vehicle continues in motion while the shadow vehicle comes to a stop after being impacted (See Figure 3.1). Separation should be equal to the roll forward distance minus the distance through which the maintenance vehicle moves while the shadow vehicle comes to a stop. Table 3.7 shows these distances for a 25,000 pound shadow vehicle and, as can be seen the required separation is very low except when the shadow and maintenance vehicle are moving at a slow speed and the impacting vehicle is very large. These results are based on the assumption that the driver of the maintenance vehicle continues at the same speed, if the driver increases his speed when the shadow vehicle is struck the safety margin is increased. These results are also based on a heavy shadow vehicle (25,000 pounds). The required separation is larger for a lighter shadow vehicle (see Table 3.8)

Table 3.7. Required Separation Allowing for Continued Motion of Maintenance Vehicle for Shadow Vehicle Weighing 25000 pounds

Shadow vehicle speed	Impacting vehicle weight	Roll forward (feet)	Time to stop (sec)	Distance traveled (feet)	Safe Separation (feet)
10 mph	4,000 lbs	26	2.0	30	**
	10,000 lbs	55	2.9	43	12
	20,000 lbs	100	3.9	58	42
	60,000 lbs	199	5.6	82	118
25 mph	4,000 lbs	78	3.5	128	**
	10,000 lbs	111	4.2	153	**
	20,000 lbs	154	4.9	179	**
	60,000 lbs	238	6.1	223	14

*Notes: ** Indicates that the theoretical safe separation is zero for the condition considered here.*
Assumption: friction factor = 0.4 providing deceleration of 12.88 ft/sec/sec for shadow vehicle

Table 3.8. Required Separation Allowing for Continued Motion of Maintenance Vehicle for Shadow Vehicle Weighing 10000 pounds

Shadow vehicle speed	Impacting vehicle weight	Roll forward (feet)	Time to stop (sec)	Distance traveled (feet)	Safe Separation (feet)
10 mph	4,000 lbs	55	2.9	43	12
	10,000 lbs	118	4.3	63	55
	20,000 lbs	183	5.3	78	104
	60,000 lbs	274	6.5	96	178
25 mph	4,000 lbs	111	4.2	153	**
	10,000 lbs	170	5.1	189	**
	20,000 lbs	224	5.9	217	7
	60,000 lbs	295	6.8	249	46

*Notes: ** Indicates that the theoretical safe separation is zero for the condition considered here.*
Assumption: friction factor = 0.4 providing deceleration of 12.88 ft/sec/sec for shadow vehicle

The condition covered by Tables 3.7 and 3.8 is safety for the maintenance vehicle if the shadow vehicle is impacted from behind. With the separation shown in these Tables, and under the assumptions used, the shadow vehicle will not run into the maintenance vehicle.

The assumed friction factor was 0.4 producing a deceleration of 12.88 ft/sec/sec. The theoretically safe separation is less if the shadow vehicle decelerates more rapidly than this which is possible on a good road surface in dry weather. On downgrades the "effective friction factor" is reduced by the pull of gravity and in wet weather this may fall below the value of 0.4 assumed for the above tables.

Safe separation should also be provided for the condition in which the lead vehicle stops suddenly and space is needed for safe deceleration of the following vehicle. For manual operation of shadow vehicles CALTRANS now recommends 3 seconds separation [50] which is 45 feet at 10 mph and 90 feet at 25 mph. For normal driving a 2 second separation is recommended. This would be 29 feet at 10 mph and 73 feet at 25 mph. Since almost instantaneous reaction can be designed into an automated system two seconds separation is more than adequate for this safety condition.

An automated shadow vehicle separation distance of 40 feet is proposed when on 850 feet radius horizontal curves. If 2 seconds separation is required 40 feet is safe for speeds up to 13.6 mph. With one second separation, probably adequate in automated mode, 40 feet is safe for speeds up to 30 mph. As seen in Tables 3.7 and 3.8 the 40 feet separation is also safe for roll forward after impact except when the impacting vehicle is very heavy. Clearly additional safety is provided by the heavier shadow vehicle for which 40 feet separation is adequate for all impacting vehicle weights at 25 mph and for impacting vehicle weights of up to 20,000 pounds at a working speed of 10 mph.

4. TRACKING TECHNOLOGIES RESEARCHED

4.1 Ultrasound

Ultrasonics is unreliability in moderate weather conditions. Signals in the 20-100 kHz frequency range display signal degradation in moderated weather conditions. Furthermore, signal reflections generally pose major problems. Hence, this technology was ruled out for use as a reliable tracking technology. Ultrasonics was found to be of moderate cost. See reference [1].

4.2 Laser(Infrared & Visible)

Qualimatrix(a company in the San Francisco Bay Area) is researching using nonvisible infrared laser LED's(Light Emitting Diodes) as a tracking technology for range tracking. Qualimatrix is researching the use of this technology to determine range between vehicles for the PATH program. Their approach does not readily yield lateral displacement and they continue to have problems with the laser sensors regarding varying light conditions.

Another company, MacLeod Technologies, Inc., has employed nonvisible infrared laser technology as a tracking approach for Shadow Vehicles under a Strategic Highway Research Program grant SHRP-N-676 entitled "Automated Vehicle for Enhanced Work Crew Safety" [43]. Their approach uses a 5 milliwatt nonvisible infrared laser mounted at the rear of a Lead Vehicle that rotates at 3000 rpm and three laser beam detector arrays mounted on the front of an Autonomous Shadow Vehicle. Using the rotation rate of the laser, the time at which the laser strikes each of the three sensors on the Shadow Vehicle and the distance between the sensors, range, lateral displacement, and yaw angle can be calculated by the Shadow Vehicle computer. Test runs with actual vehicles were made; however, the researchers noted that tuning of the laser detector arrays was required under varying light conditions. They postulate that they will solve this problem in the next phase of the project. This approach is innovative, but, there are concerns as follows:

1) Problems with Varying Light Conditions: May be solvable, but, has not be proven so as of yet.

2) Lateral Displacement Accuracy: Claims were made in their report that a lateral displacement accuracy of ±1.2 feet was attained. This conclusion was based on angles measured by their detectors. An independent method to measure the lateral displacement must be used to validate the claim. Furthermore, based on the sparse technical information given in the report, another timing signal is

needed to signal the Shadow Vehicle that the rotating laser has just passed some fixed degree marker.

3) Possible Failure Modes: Failure of the electronics could cause a false timing measure. Tracking information relies on just three sensor readings. Possibly another redundant bank of detectors could be used to validate the sensor readings. If the rotation speed of the laser varies, false measurements would occur.

This type of technology currently does not perform well under varying light conditions. Furthermore, signs may be required declaring "Hazard - Laser in Operation" may create public concern. However, this technology has great potential. However, this technology was ruled out at this time as a reliable tracking technology. LED laser infrared/visible modulation up to 200MHz was found to be of moderate cost. See references [2], [19], [38] and [43].

4.3 Relative and Differential GPS

A GPS(Global Positioned Satellites) receiver determines the XYZ location of the receiver relative to a fixed global XYZ location to within approximately 100 m. If objects such as buildings and terrain occlude the GPS satellites from the receiver, the receiver may provide highly inaccurate data even though the receiver attempts to estimate what the coordinates are based on past coordinates. Differential GPS technology increases the accuracy by using fixed local stations to broadcast coordinate corrections. The accuracy of Differential GPS is approximately 1 to 3 m.

To overcome the accuracy problem whether using GPS or differential GPS technology, it is necessary to use two GPS receivers. One GPS receiver in the Lead Vehicle and one GPS receiver in the Autonomous Shadow Vehicle. Then by transmitting the GPS coordinates of the Lead Vehicle to the Autonomous Shadow Vehicle and subtracting the GPS coordinates of the Autonomous Shadow Vehicle from those of the Lead Vehicle highly accurate relative coordinates can be obtained. The accuracy of the relative position of one receiver with respect to the other is expected to be within ±10%. The current best update rate of the GPS coordinates that can be obtained is in the order of one second. For vehicles speeds up to 30 mph, a digital control system sampling rate of 0.1 seconds or smaller is desired. Estimates of angle, lateral displacement, and yaw angle every 0.1 seconds can be made using measured speeds and steering angles of both vehicles and using past data.

If a sufficient number of differential stations become operational, The Relative GPS strategy may used as a primary system. However, because of the current state of GPS technology,

it is suggested this technology be used as a redundant system to check the integrity of the other tracking systems. Relative GPS was found to be of moderate cost. A proposed system in described in Section 7.0. See references [4], [7], [8], [9], [33], [34], [35], [36] and [37].

4.4 Antenna Array(10-20GHz)

Use of antenna technology for direction finding is well known. However, the objective of this research was to determine if range, lateral displacement, and yaw angle could be found using antenna array approach. An antenna system that provided these needed parameters was not found via a literature search. On the other hand it was clear that the technology indicated that an antenna system can be designed to achieve the desired results. The primary concerns were size of the antennas and cost of the system. As the transmitting frequency is increased, the size of the antenna system decreases and the costs increase. The costs dramatically increase when the frequency crosses over the 1 to 2 GHz. Antenna arrays at the 20 to 200 foot range are expected to be reliable systems in moderate weather conditions.

Several conceptual designs have been researched by performing simulations. The results have reinforced the expectation that this technology will be reliable in obtaining range, lateral displacement, and yaw angle.

The antenna array tracking approach was chosen as the primary tracking technology for this application. Nevertheless, the vision tracking approach proposed to be the secondary tracking system is complementary to an antenna array system. That is, if only one tracking system is to be used, it would be proposed that the vision system be selected because we can be certain to a probability of 0.999999 that we have acquired the lead vehicle. Furthermore, range using vision can be accurately obtained using vision techniques.

An antenna array system is expected to be of moderate cost. Actual costs can not be determined until the proposed system is constructed and tested. A proposed system is described in Section 5.0. See references [10], [18], [20], [21], [23], [24], [25], [26], [27], [28], [29], [31], [32], [40], [44] and [45].

4.5 Millimeter Scanning Radar(30-100GHz)

Two scanning radar systems were considered in this research:

1) A system consisting of a rotating transmitting dish on the Autonomous Shadow Vehicle and a symbol mounted on the back of the Lead Vehicle that optimally reflects the transmitted signal back to the Autonomous Shadow Vehicle.

2) A system consisting of a rotating transmitting dish on the Lead Vehicle and an antenna array on the Autonomous Shadow Vehicle.

Millimeter scanning radar tracking systems were found to be very high cost systems. There is also a concern regarding negative public opinion of using these very high frequencies. It is expected that millimeter scanning radar tracking systems will be reliable systems in moderate weather conditions. This technology was found to be reliable for obtaining range, lateral displacement, and yaw angle. Although it was found to be a very robust system for tracking, for the reasons mentioned, this technology was rejected as a tracking technology for this application. See references [3], [5], [6], [15], [16], [17], and [24].

4.6 Vision

Vision technology has been widely used for target identification and tracking applications. Vision tracking systems are robust systems if the lighting can be controlled in some manner, a desired minimum spatial resolution(size of the object in the video frame is large enough) can be maintained, and computation can be performed within an acceptable time. Under the conditions mentioned, it is expected that a vision tracking system will perform very well in moderate weather conditions. It is expected that range, lateral displacement, and yaw angle can be determined within an acceptable accuracy. One of the main advantages of vision is that it can be determined to a probability of 0.999999 that the appropriate target has been acquired.

Vision was found to be of moderate cost. For the reasons mentioned, this technology is proposed as a secondary tracking system for the Autonomous Shadow Vehicle. A proposed system is described in Section 6.0. See references [11], [12], [13], [14], [39], [41], [42], [46], [47], [48], [49], [60], [102], [105], [107], [108], and [111].

5. ANTENNA TRACKING SYSTEM

The Initial design consisted of a Lead Vehicle transmitting antenna array of 110 elements. However, this approach proved to be too costly and a great deal of work would be required to tune each of these elements. As a result, it was decided to use a parabolic dish on the Lead Vehicle even though the beam width is wider. The approach whether using an 110 element array or dish is basically the same.

5.1 System Geometry

The initial transmitting antenna array(TAA) consisted of a 110 elements, 0.015m spacing, 1.64m wide and 0.5m tall. The TAA is excited by a 10GHz source. This will be mounted on the Lead vehicle, as shown in Figure 5.1.

The initial Receiving Antenna Array(RAA) consisted of 15 individual elements, 0.014m spacing, 2m wide, and 0.5m tall. The RAA will be mounted on the Shadow vehicle, as shown in Figure 5.1.

The transmitting antenna is now a parabolic dish antenna. The diameter is 1.2192m (4ft). The dish antenna is excited by a 10GHz source. This will be mounted on the Lead vehicle in the same location as the TAA, Figure 5.1.

The RAA has been modified to 7 individual elements, 0.333m spacing, 2m wide, and 0.5m in height. This will be mounted on the Shadow vehicle in the same location as the originally stated, Figure 5.1.

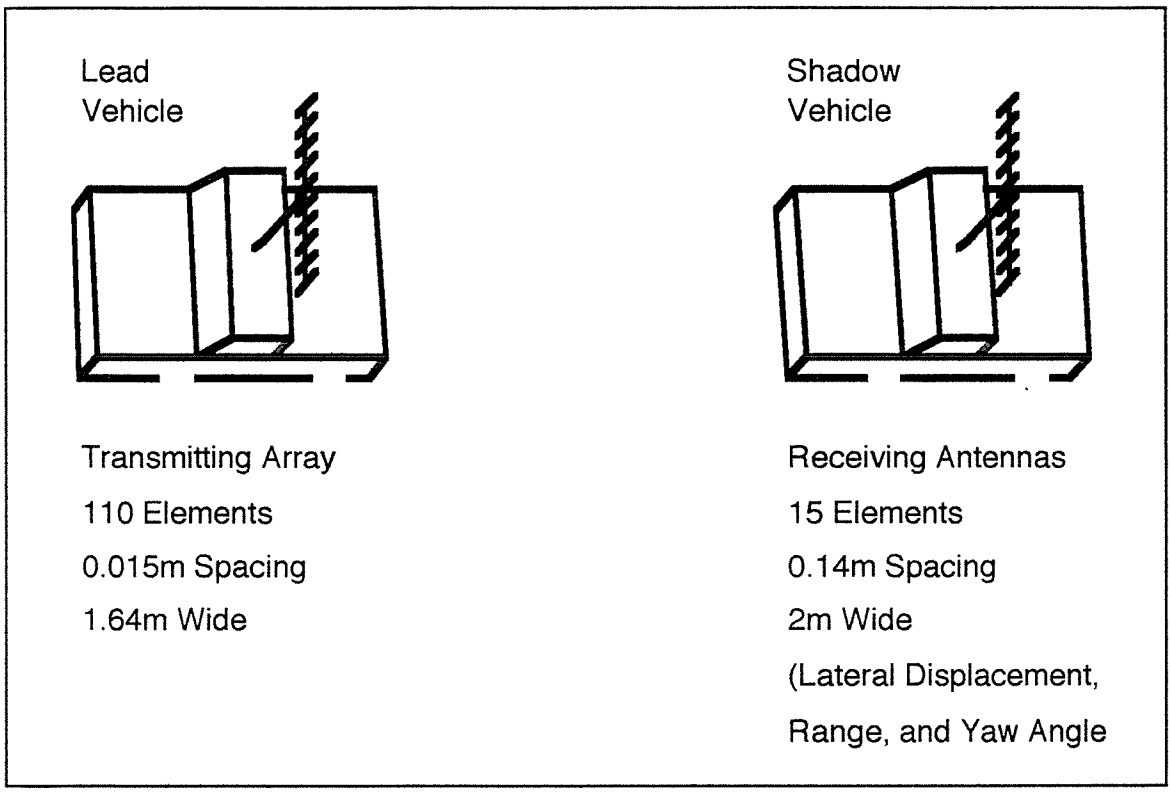

Figure 5.1. Shadow and Lead Vehicle Initial Antenna Array Design

5.2 Range and Lateral Displacement

The TAA was designed to have a pencil beam output pattern. The 10GHz excitation source was required due to the small wave length in relation to the short distances between the Lead vehicle and Shadow vehicle. This excitation source, along with a 110 elements spaced a half of a wave length apart produced the pencil beam pattern, as shown in Figure 5.2. The RAA was designed to pick up any variation in orientation of the TAA. The 15 elements and spacing between elements on the RAA was required to obtain ±5-10% accuracy's in range, lateral displacement and yaw angle.

In the simulations the TAA and the RAA were set to ranges from 100-150m(in steps of 1-5m). At each specified range, the RAA was the laterally displaced ±0.6667m(in steps of ±0.1667m). This was done to observe the changes in the magnitude and phase of the RAA. Based on the simulated results, the amplitude and phase distributions on the receiving elements showed that the magnitude and phase measured at the RAA could be used to obtain range and lateral displacement. For example, when the TAA and the RAA were set a 105m apart with no lateral displacement, the amplitudes and phases were perfectly symmetrical with the center elements showing the largest magnitudes and the least phase, as shown in Figure 5.3. When the TAA and the RAA were set a 120m apart and the RAA was laterally displaced +0.6667m, the magnitudes on each element decreased and shifted accordingly as did the phasing on each element, as shown in Figure 5.4.

5.3 Relative Magnitudes and Phases

Relative magnitudes and phases are used to calculate range, lateral displacement and yaw angle as opposed to using the magnitude and phase of each receiving array element to calculate these values. That is, the difference between receiving array element magnitudes and phases are used for training the neural networks described further on in this section.

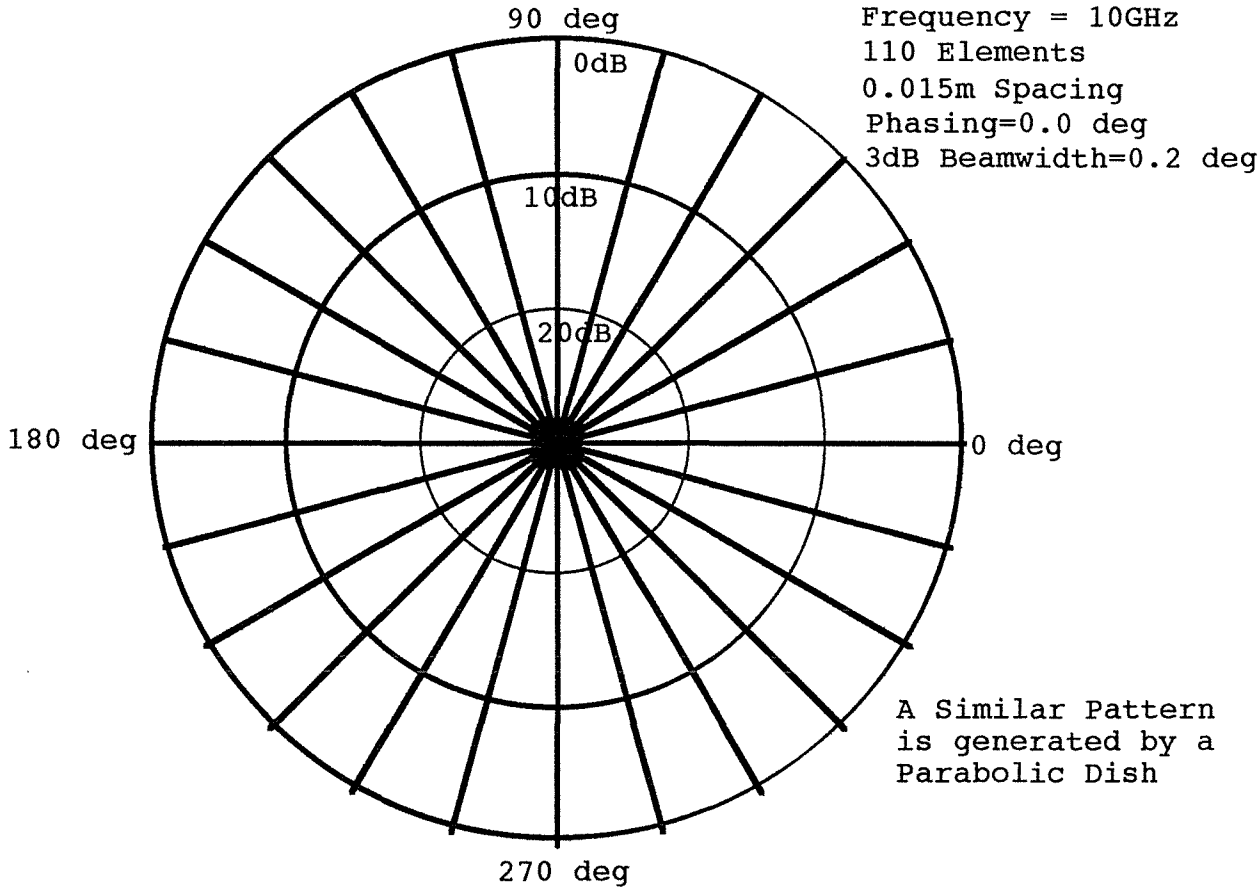

Figure 5.2. Transmitted Pattern by Lead Vehicle Antenna

5.4 Yaw Angle

When the TAA and the RAA were set 120m apart, yawed, and laterally displaced with respect to one another, showed little change in the magnitude and a drastic change in the phase. It is not apparent from the phase data how to develop a relationship to map the phase information into yaw angle. Hence, it was decided to use a neural network to map the magnitude and phase of the received signals into yaw.

5.5 Transmitting Array Output Pattern

As indicated in Figure 5.2, the Lead vehicle antenna array pattern is a pencil beam with negligible side-lobe levels. The array was designed this way so that any change in the orientation was detectable at the receiver.

5.6 Receiving Array Patterns

Figures 5.3, 5.4, and 5.5 contain graphs of the data generated from the system model developed in C language. MATLAB was used to graph the generated data. The following describes the notation used in the figures which is not clear from the graphs:

mar5srxx: The first four characters represent the date on which the data was generated, i.e., mar5 means march fifth. The fifth character, s, means the receiving antenna was shifted, i.e., left or right. The sixth character, r, means the receiving antenna was rotated about the center element. The xx is used to keep each file name unique. If the s/r are not present, the receiving antenna has not been shifted or rotated.

lateral shift: This is the amount that the receiving antenna has been shifted from the bore-sight relative to the transmitting array.

thetaL and thetaR: This is the phase difference of the right and left most elements with respect to the center elements phase.

TX#: number of elements in the transmitting array.

RX#: number of elements in the receiving antenna.

fr: source frequency used.

rot: amount of rotation of the receiving antenna.

spTX: spacing between elements of the transmitting array.

spRX: spacing between the elements of the receiving antenna.

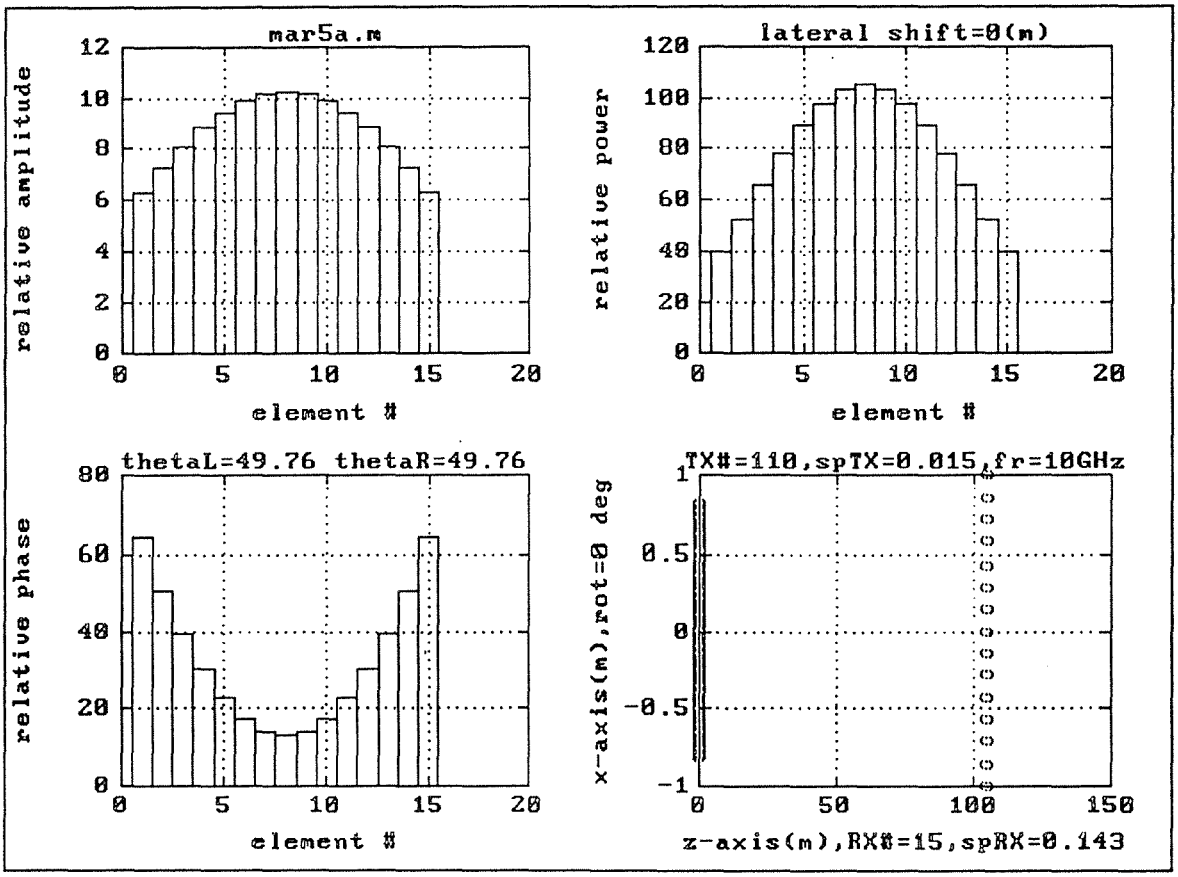

Fig. 5.3. Receiver output (range=105m, lateral displacement=0.0m, yaw=0.0 degrees).

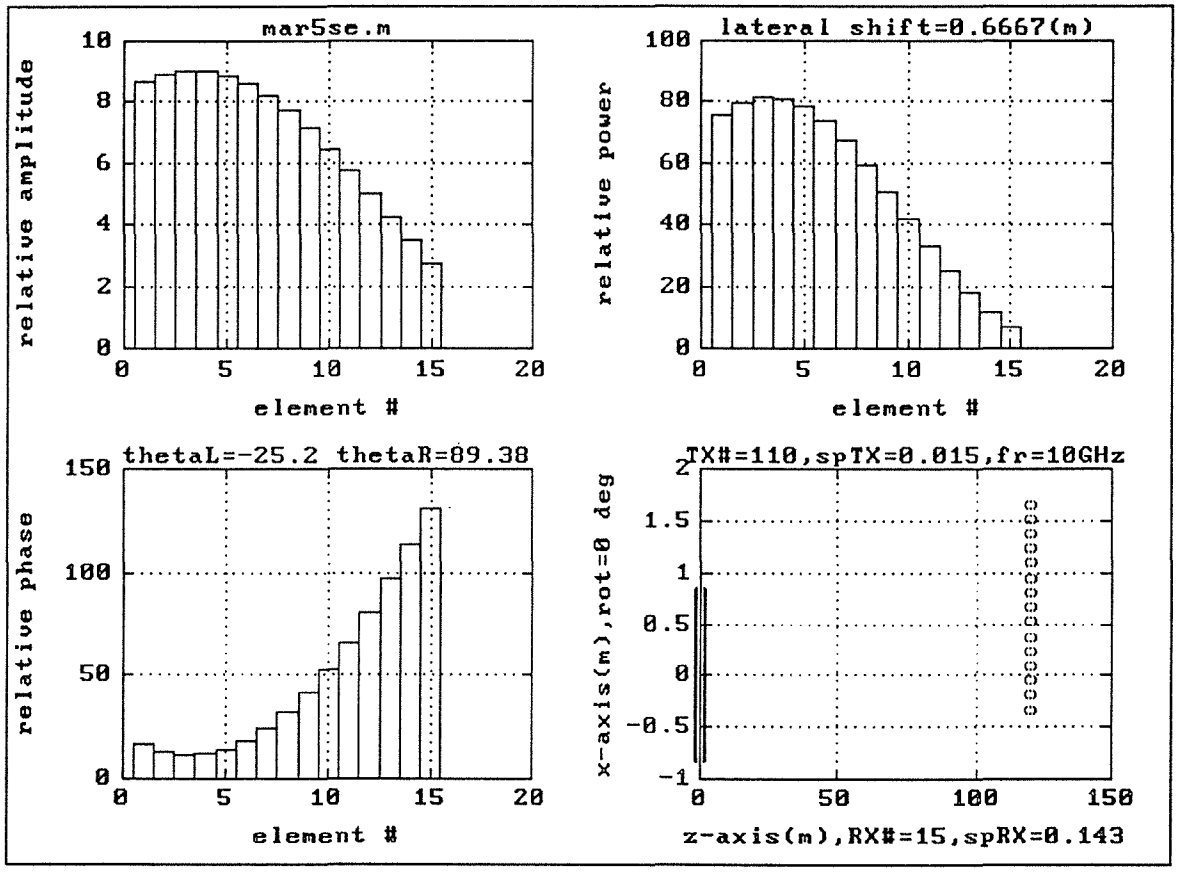

Fig. 5.4. Receiver output (range=120m, lateral displacement=0.6667m, yaw=0.0 degrees).

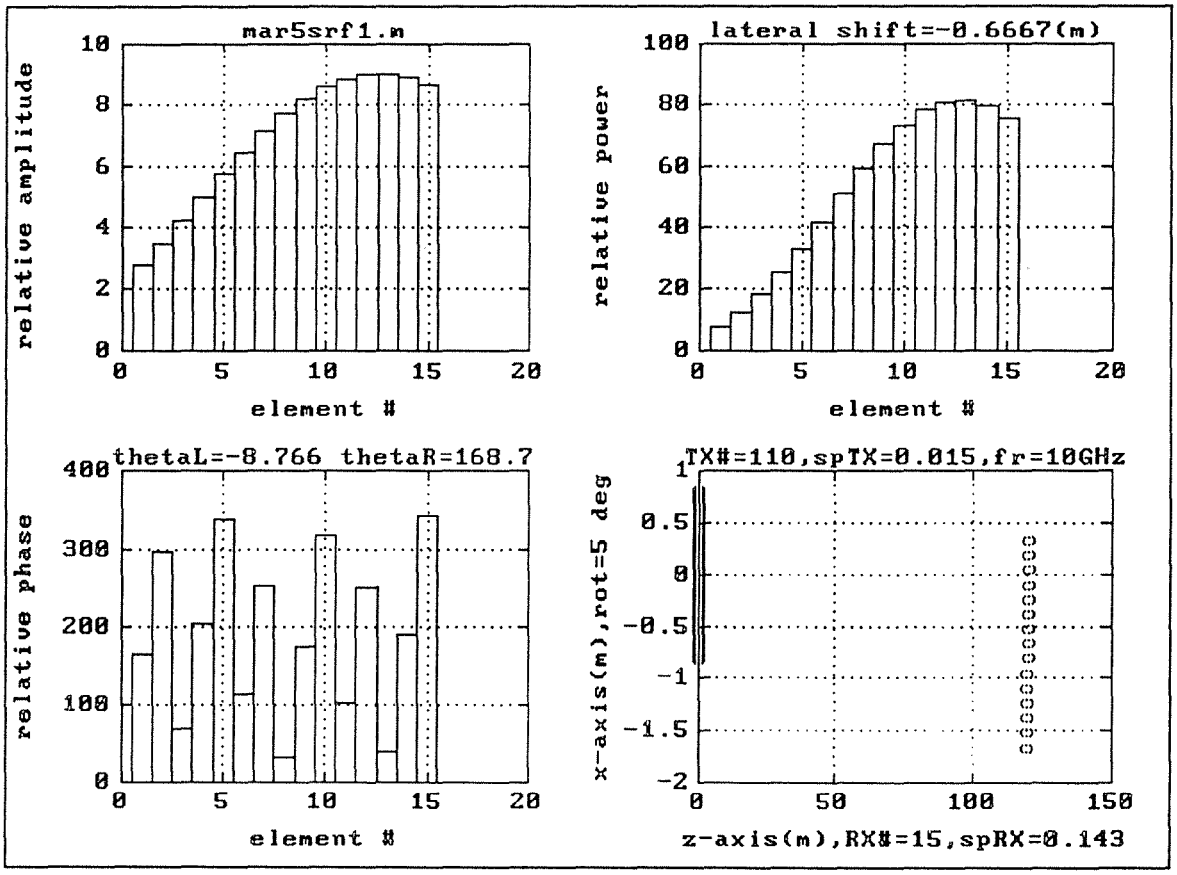

Fig. 5.5. Receiver output (range=120m, lateral displacement=-0.6667m, yaw=5.0 degrees).

5.7 Neural Network Implementation

A neural network was trained using NeuralWorks Professional II/PLUS developed by NeuralWare Inc. Two networks were trained using a back-propagation model with the Extended Delta-Bar-Delta learning algorithm. One network was trained to produce range and lateral displacement (using relative amplitude information), and the other was trained to produce yaw (using range, lateral displacement, and relative phase information).

The neural network used to produce range and lateral displacement consisted of one input layer(14 neurons), hidden layer 1(50 neurons), hidden layer 2(10 neurons), and an output layer(2 neurons),as show in Figure 5.6. The neural network used to produce yaw consisted of one input layer(16 neurons), hidden layer 1(50 neurons), hidden layer 2(10 neurons), and an output layer(1 neuron),as shown in Figure 5.7. The fifteen receiving elements provide the magnitude and phase information which were used as inputs to the neural networks which produced range, lateral displacement, and yaw angle.

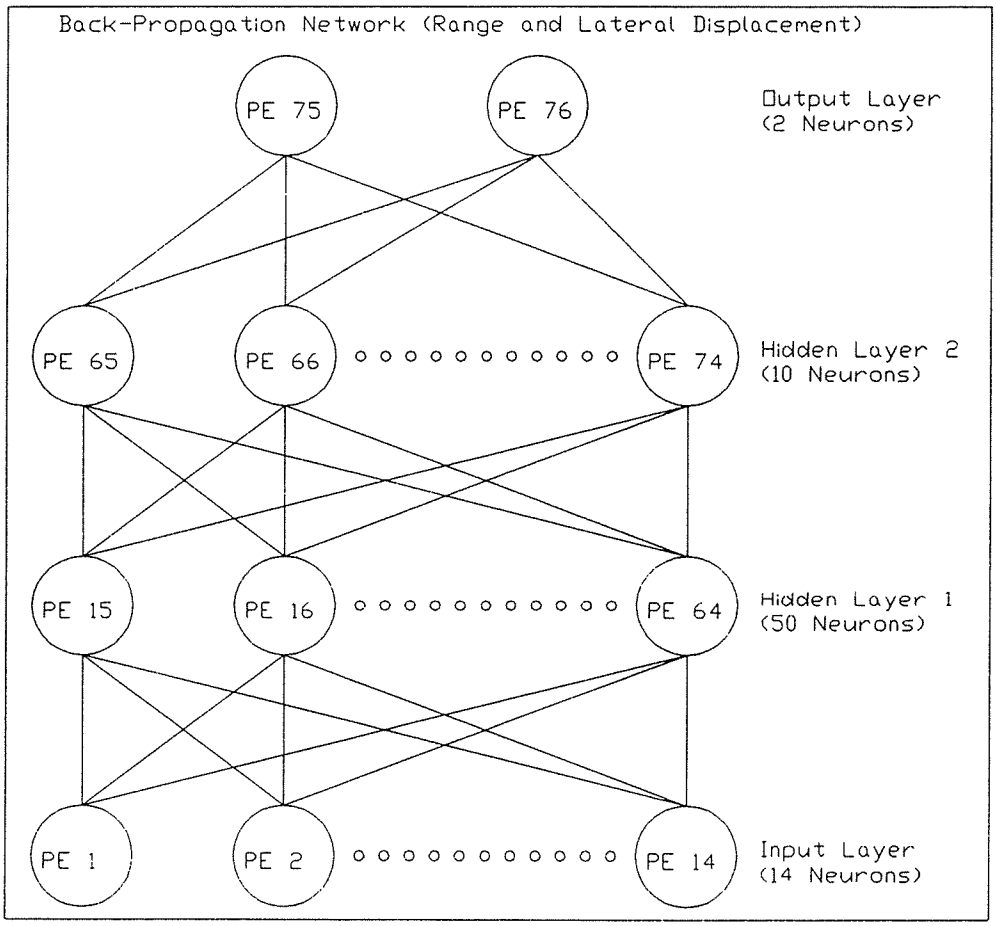

Fig. 5.6. Neural network design used to determine range and lateral displacement.

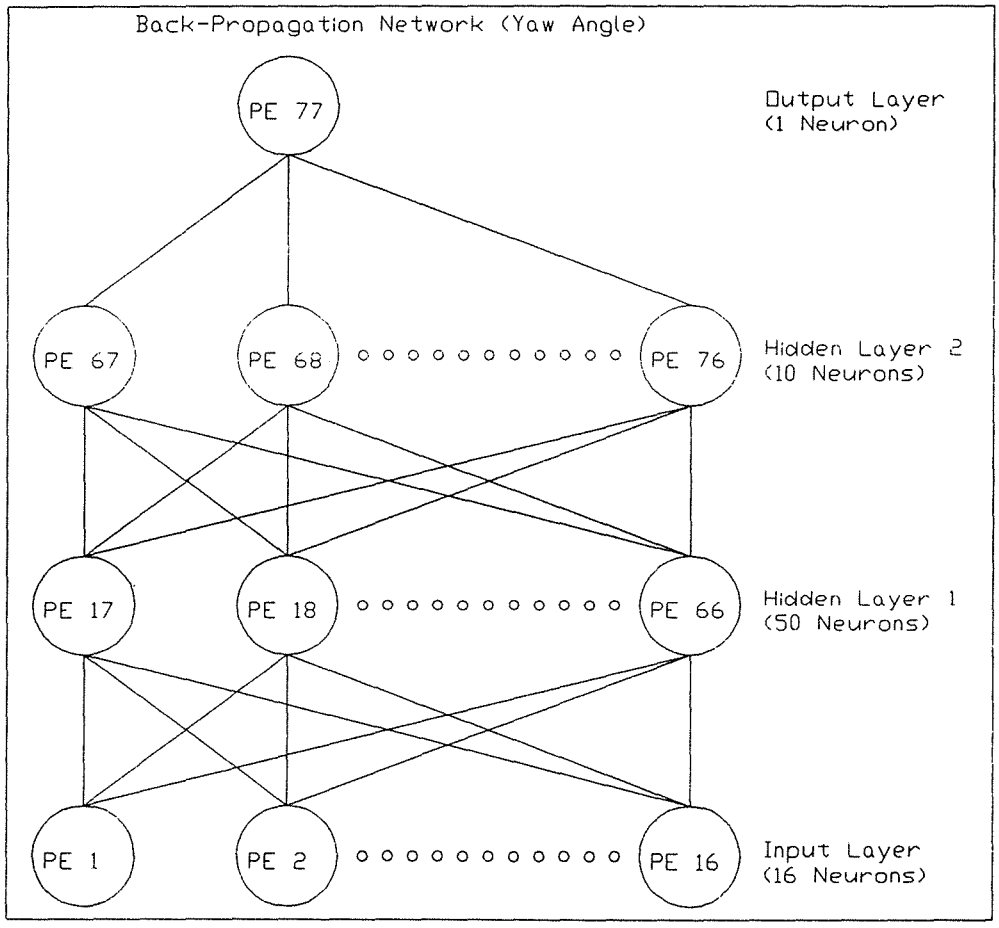

Fig. 5.7. Neural network design used to determine yaw angle.

The data used for training was obtained from the model developed in C language. The model was developed based on far-field approximations for the antenna system. Far-field calculations are used, as they are in most antenna research, due to the complexity of the calculations and unexplained phenomena of antenna systems at near-field. Using far-field calculations is an acceptable approximation to show the behavior patterns of antenna systems. Hence, all simulations were done with at least a 100m distance between the TAA and the RAA. The program performs an analysis of the antenna system and computes the amplitude and phase that each receiving element would receive for various ranges, lateral displacements, and yaw angles.

5.7.1 Range and Lateral Displacement

From the RAA, the measurements obtained are 15 magnitudes and phases. The received magnitude and phase of each RAA element is subtracted from the magnitude and phase of the center element to obtain relative magnitude and phase information. This gives 14 relative magnitudes and phases.

Fourteen relative amplitudes were used to train for range and lateral displacement. The starting distance was 100m and the ending distance was 150m. Range was incremented using 5m steps. For each range, the maximum lateral displacement was ±0.67m moving from left to right in 0.167m increments. Refer to Table 5.1 for a summary of results.

Table 5.1. Neural Network Training Results

	Error
Range	2%
Lateral Displacement	5%
Yaw	3%

5.7.2 Yaw Angle

Sixteen inputs were used to train for yaw, fourteen relative phases(the phase of each element minus the phase of the center element), the range, and the lateral displacement. The range and lateral displacement used are simulated here. For the application they will be the outputs of the neural network that produces range and later displacement. The starting distance was 100m and the ending distance was 150m. Range was incremented using 5m steps. For each range, the maximum lateral displacement was ±0.67m moving from left to right in 0.167m increments. Refer to Table 5.1 for a summary of results.

5.7.3 Neural Network Training Data

The training data required for training the two networks, shown in Figure 5.6 and Figure 5.7, for range, lateral displacement, and yaw will be obtained by physically measuring the true values(the desired range, lateral displacement, and yaw angle output from the neural network) and saving the raw data(obtained from the antenna system) in a file. The raw data and the true data will be saved in the file in a format so that it can then be fed to the neural network for training. After the neural network is trained, NeuralWare allows the trained network to be converted into a C function. This function will then be integrated into the existing control code for the Shadow vehicle.

5.8 Electronic System Design

5.8.1 Transmitting Antenna Design Revision

The original theoretical design of the transmitting antenna consisted of 110 elements with 0.015m spacing. This design would be very costly to manufacture due to the number of elements, spacing, and impedance matching of each element with respect to the source. Each of the antenna elements would have to be tuned such that each received equal power and 0 degree phasing from the source. This antenna design was based on the premise that the vehicles would be operating in close proximity of each other, a maximum size of 2m in width for the transmitting antenna was allowed, and a half power beam width of 0.2 degrees was required to show relative amplitude and phase changes across the 15 elements of the receiving antenna. Due to the complexity and cost of constructing the transmitting antenna array, it was decided to use a different type of transmitting antenna. One which could be easily ordered and mounted on the lead vehicle at a moderate cost. The new design is a parabolic dish antenna (40dB gain) with a 1.7 degree half power beam width, 4ft in diameter, and weighing 20lbs.

5.8.2 Receiving Antenna Design Revision

The design of the receiving antenna was changed from 15 elements spaced 0.14m apart to 7 dipole elements spaced 0.333m apart. This change was due to the fact that the transmitting antenna will now have a larger half power beam width. The increased beam width requires the spacing between the receiving elements be increased such that the changing phase and amplitude distribution is still discernible. The increased spacing of the receiving elements means a decrease in the number of receiving elements. Hence, a reduction in the overall cost of the receiving antenna.

5.8.3 Lead Vehicle Electronics Design

The cost associated with using spread spectrum technology in the microwave band grossly exceeded the budget . To combat this cost, a new design was completed to transmit the 10GHz signal. The new design consists of a GUNN oscillator and a power amplifier. The amplified source signal is fed directly to the transmitting dish antenna, see Figure 5.8.

5.8.4 Shadow Vehicle Electronics Design Revision

The change in the design of the Lead vehicle electronics constituted a change in the receiver electronics to decrease cost. See Figure 5.9 for the following discussion. The output from each of the seven elements is fed into a downconverter. This will step down the frequency into the MHz range. The local oscillator which feeds each mixer is first passed through a amplifier driver and then fed into an 8-way power divider. This drastically reduces cost since only one local oscillator, amplifier driver, and 8-way power divider is needed to feed seven mixers in the microwave band. Once the frequency has been downconverted, the cost of the components to process the received pattern becomes relatively inexpensive. The output from the mixers is then fed into 2-way power dividers. This gives two signals to process to obtain phase and amplitude per receiver element. One signal from a 2-way is fed into a phase detector and the other is fed into a peak detector. The output from these two devices is then passed into an A/D converter. The output from the A/D converter is then fed to a neural network function which maps the phase and amplitude values into range, lateral displacement, and yaw angle. These three values are then software manipulated in C code to computer control the Shadow vehicle.

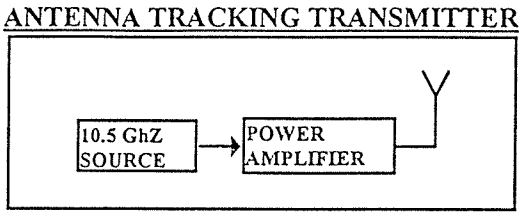

Figure 5.8. Lead Vehicle Transmission Electronics

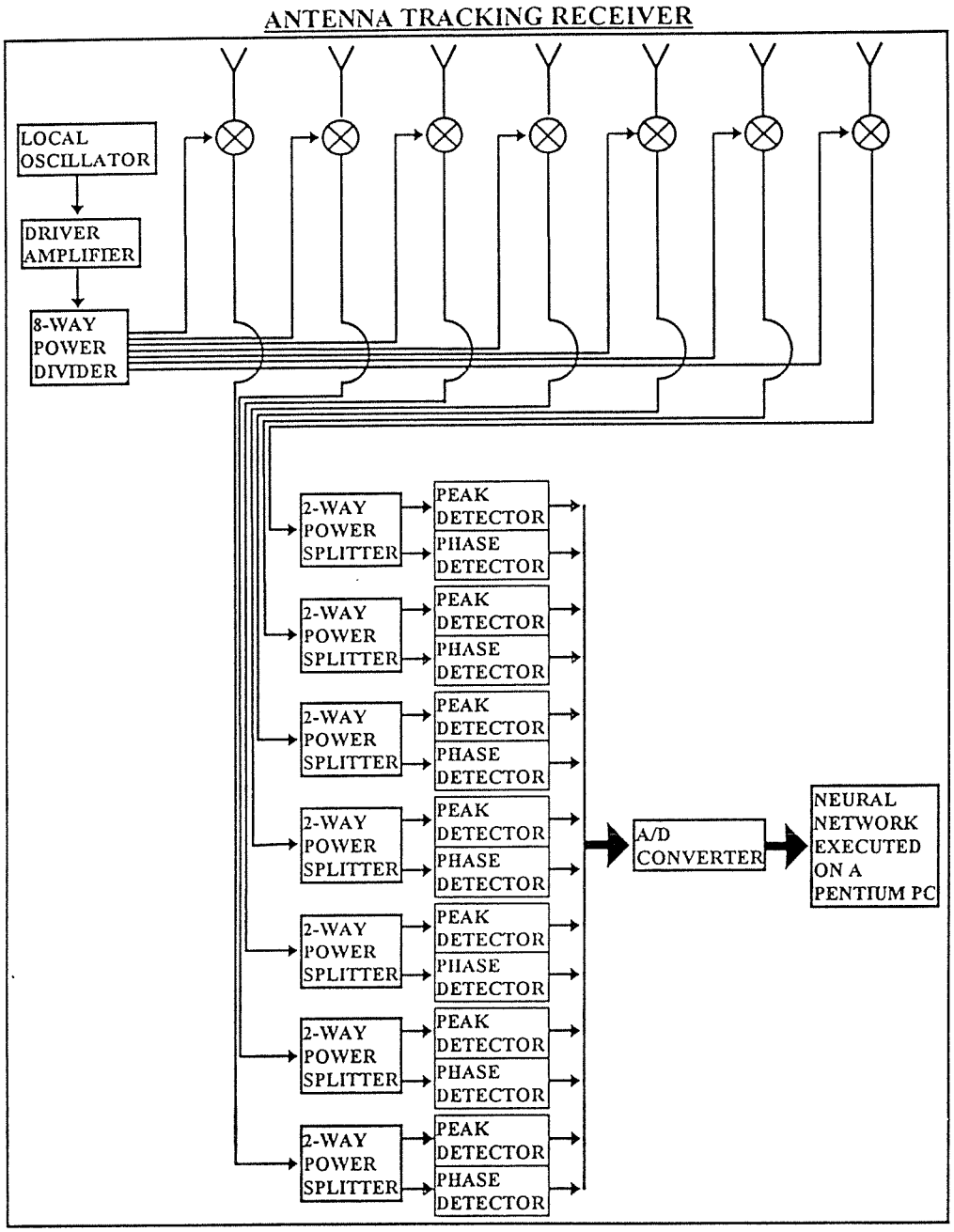

Figure 5.9 Shadow Vehicle Receiving Electronics

5.8.5 Antenna Tracking System Cost Estimate

An cost estimate for the major hardware components follows:

TRANSMITTER PARTS LIST

1. X BAND GUNN OSCILLATOR-PRICE: $460.00/Each
   Microwave Development Co., INC.
   Model: 88090-XXX
2. POWER AMPLIFIER-PRICE: $2,000.00/Each
   MITEQ
   Model: AMF-5B-1001100-30P
3. PARABOLIC DISH ANTENNA-PRICE: $1,400.00/Each
   Antenna Research Associates, INC.
   Model: PRA-11-11/A4
4. ESTIMATED LINE COST-PRICE: $20.00 @ $10.00/Section

RECEIVER PARTS LIST

1. 7 DIPOLE ANTENNA ELEMENTS-PRICE: $700.00 @ $100.00/Each
   Antenna Research Associates, INC.
   Model: mwh-1015A
2. X BAND GUNN OSILATOR-PRICE: $460.00/Each
   Microwave Development Co., INC.
   Model: 88090-XXX
3. LO DRIVER AMP-PRICE: $500.00/Each
   MITEQ
   Model AMF-1B-100110-20P
4. 8-WAY POWER DIVIDER-PRICE: $640.00/Each
   MITEQ
   Model: D0858
5. 7 DOUBLE BALANCED MIXERS-PRICE: $1,365 @ $195.00/Each
   MITEQ
   Model: DB0218LW2
6. 7 2-WAY POWER SPLITTERS-PRICE: $118.65 @ $16.95/Each
   Mini-Circuits
   Model: PSC-2-1W
7. 7 PHASE DETECTORS-PRICE: $132.65 @ $18.95/Each
   Mini-Circuits
   Model: RPD-1
8. 7 WAVE DETECTPRS-PRICE: $2,499.00 @ $357.00/Each
   Loral Narda Microwave Corp.
   Model: 4507
9. ESTIMATED LINE COST-PRICE: $440.00/Each

ESTIMATED SYSTEM COST FOR MAJOR COMPONENTS

TRANSMITTER	$3,880.00
RECEIVER	$6,855.30
TOTAL	$10,735.30

6.0 VISION TRACKING SYSTEM DESIGN

Various 3-D symbols were computer generated and the image of the symbol as seen by a video camera mounted on an Autonomous Shadow Vehicle was computed and displayed using MATLAB, a matrix oriented programming language. A candidate symbol was constructed out of light weight materials. Machine vision algorithms were coded in the "C" programming language for a 486 PC to locate the symbol in the image and to information about the symbol. Information about the symbol was then fed to a Neural Network. The trained Neural Network produced Ranges within ±1 foot, Lateral Displacements within ±6 inches, and Yaw Angles of ±1 degree. The following sections describe process in more detail.

6.1 Symbol & Simulation

Figure 6.1 illustrates the geometry used to obtain the homogeneous matrices that relate the camera location and orientation to the symbol location.

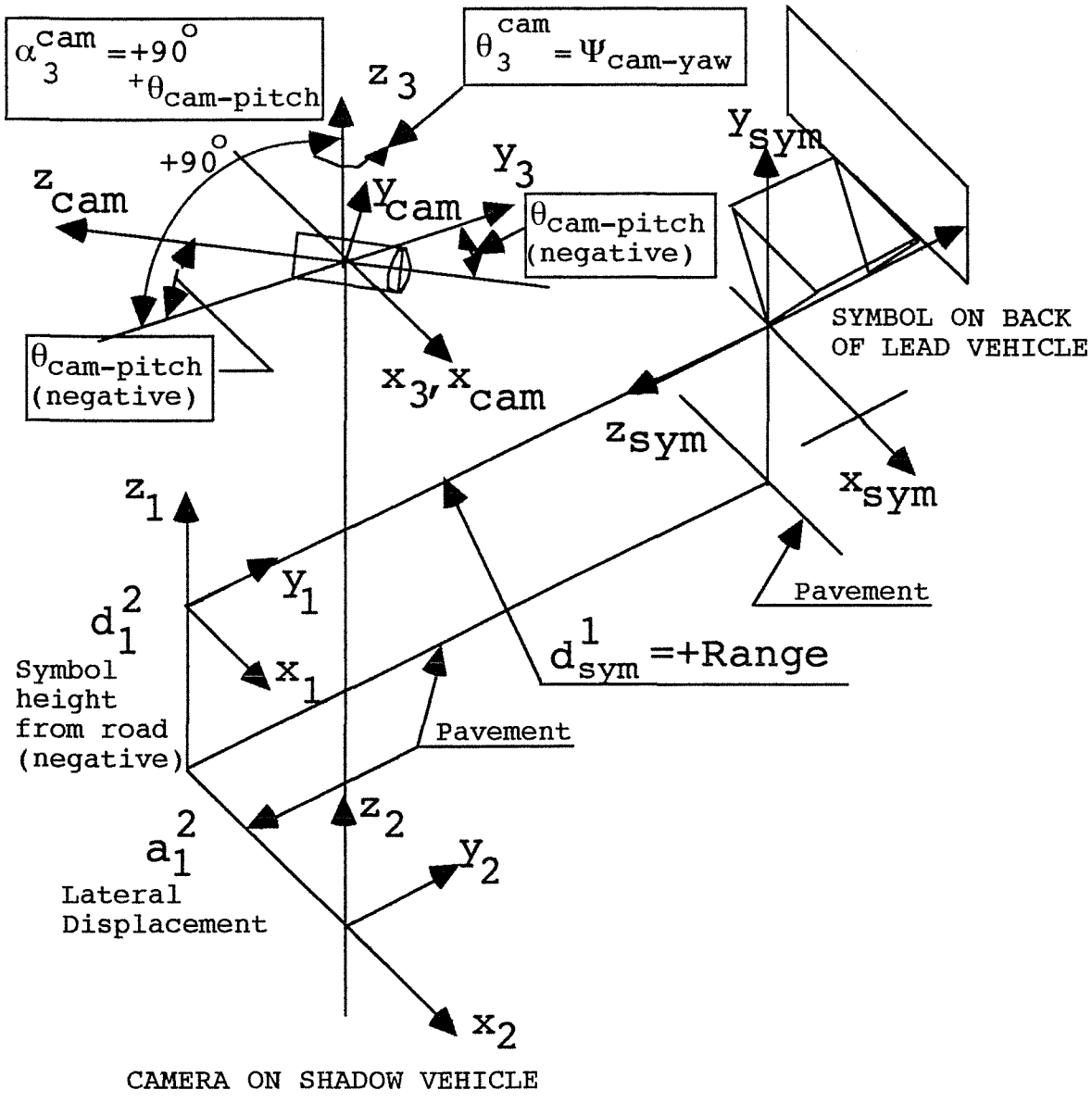

Figure 6.1. Camera To Symbol Geometry And Coordinate Frame Assignments

Homogeneous matrices are 4x4 matrices used in robotics that contain both position and orientation information [109]. Also, by using the Denavit-Hartenburg(D-H) convention, a parameter table can be constructed that represents the orientation and position of one frame to another. We will assume that the reader has some knowledge of coordinate frame transformations, homogeneous 4x4 matrices, and the D-H convention. The objective is to represent mathematically the location and shape of the Lead Vehicles symbol as seen in the video frame of the camera located on the Shadow Vehicle. Table 1 contains the D-H parameters that describe the transformations between frames.

Table 6.1. D-H Parameters For Figure 6.1

FRAME i TO i+1 TRANSFOR -MATION	α	**a**	**d**	θ	**VARIABLE**
T^1_{sym}	$\alpha^1_{sym}=-90^\circ$	0	d^1_{sym}=Range	0	d^1_{sym}=Range
T^2_1	0	a^2_1=Lat. Disp. (Right + Left -)	d^2_1=-(symbol to road)	0	a^2_1 = Lat. Disp.
T^3_2	0	0	d^3_2=+(Road to Camera)	0	NONE
T^{cam}_3	$\alpha^{cam}_3=+90^\circ$ $+\theta_{cam-pitch}$	0	0	$\theta^{cam}_3=$ $\psi_{cam-yam}$ (Left = + Right = -)	$\theta^{cam}_3=$ $\psi_{cam-yam}$.

We need T^{sym}_{cam} so that we can find the coordinates in the camera frame of a point in the symbol frame. T^{sym}_{cam} can be found by concatenating transformations as follows:

$$T^{sym}_{cam} = T^1_{sym} T^2_1 T^3_2 T^{cam}_3 . \qquad (6.1)$$

Hence,

$$P_{cam} = (T^{sym}_{cam})^{-1} P_{sym} \qquad (6.2)$$

where P_{cam} and P_{sym} are 4x1(row by column) column vectors containing the three-dimensional coordinates of a single point relative to the camera frame or symbol frame. For this report, the fourth element is a "1".

Next we can insert all points that describe a symbol in symbol frame coordinates as columns of a matrix we shall call $SYMBOL_{sym}$. We now can find the coordinates of all of the symbol points in terms of the camera frame and write

$$SYMBOL_{cam} = T_{cam}^{sym} SYMBOL_{sym}. \qquad (6.3)$$

Now we must take into account the effect of a camera lens. Depending on the focal length, the distance of the lens from the image plane of the camera, the symbol will appear larger or smaller in the camera image frame for a given range to the symbol. We shall identify this two-dimensional frame as the "image" frame. The coordinates of point on the symbol as it appears in the image frame can be computed as

$$Px_{image} = \frac{Px_{cam}}{\frac{-Pz_{cam}}{f} - 1} = \frac{Px_{cam}}{Magnitude} \qquad (6.4)$$

$$Py_{image} = \frac{Py_{cam}}{\frac{-Pz_{cam}}{f} - 1} = \frac{Py_{cam}}{Magnitude} \qquad (6.5)$$

where

$$Magnitude = \frac{-Pz_{cam}}{f} - 1. \qquad (6.6)$$

Pz_{cam} is the range of the camera to the symbol point and f is the focal length of the lens. Since the distance from the camera to points on the symbol is very large with respect to camera focal lengths, in general, (6.6) can be approximated as

$$Magnitude = \frac{-Pz_{cam}}{f}. \qquad (6.7)$$

We now rewrite (6.5) and (6.6) using (6.7) as

$$Px_{image} = \frac{Px_{cam} * f}{-Pz_{cam}} \qquad (6.8)$$

$$Py_{image} = \frac{Py_{cam} * f}{-Pz_{cam}} \qquad (6.9)$$

We, also want to express the x and y coordinates of the symbol point in the image frame in "pixels" instead of inches or mm. Since we have a digitized image, we are interested in resolution of the symbol, i.e., how many pixels represent the symbol. If the resolution becomes to small, it will be difficult to impossible to differentiate the symbol from noise or other objects in the image frame.

A scale factor, $K_{pixels\_per\_inch}$, was derived experimentally for two lenses that had 8.5 mm and 4.8 mm focal lengths. A wall area of 8' 5" wide by 4' high was marked at the corners and a triangular symbol with a base width of 48" and a height of 48" was drawn in the center of this area. The camera was then moved forward until the marked wall area filled the image frame. Experimentally, these distances were measured in the image frame in pixels. It was found that

$$K_{pixels\_per\_inch} = (f \text{ in mm}) * 98.5528 \qquad (6.10)$$

Equations (6.8) and (6.9) become

$$Px_{image} = \frac{Px_{cam} * K_{pixels\_per\_inch}}{-Pz_{cam}} \qquad (6.11)$$

$$Py_{image} = \frac{Py_{cam} * K_{pixels\_per\_inch}}{-Pz_{cam}} \qquad (6.12)$$

where the coordinates Px_{image} and Py_{image} are now in pixels.

Since the 8.5 mm lens gives a larger field-of-view, it was selected for this experiment.

Programs were written in MATLAB that implement the above equations and are available upon request. An overview flow-chart of the main program, CAMSIM.M, is shown in Figure 6.2.

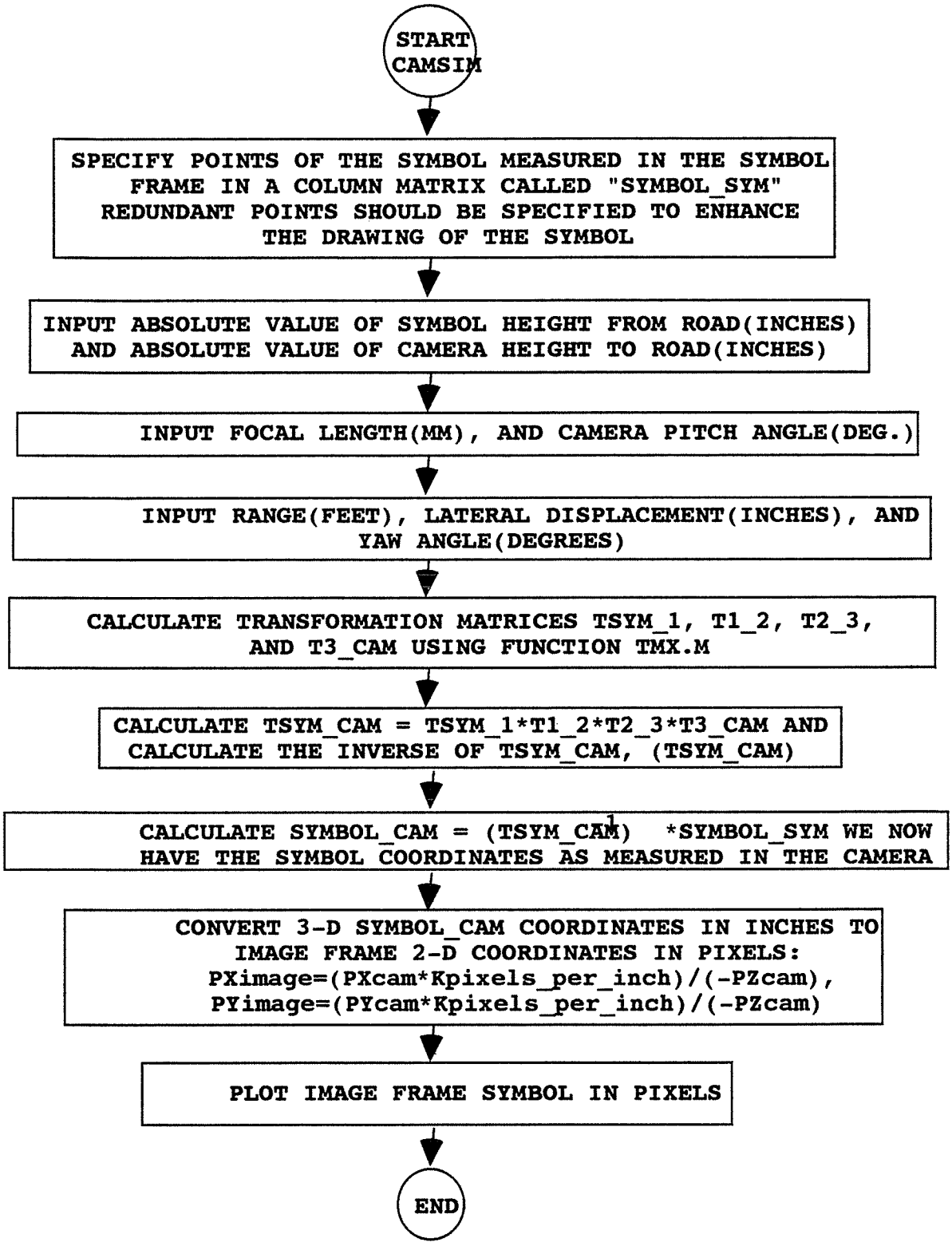

Figure 6.2. Flow-Chart of MATLAB Program CAMSIM.M

6.2 Yaw Angle Cone Experiments

If the Autonomous Shadow Vehicle is lateral displaced by 1 foot and yawed so that the symbol is in the center of the image frame the yaw angle of the Autonomous Shadow Vehicle relative to the Lead Vehicle is small and decreases as the range increases. For a range of 40 feet depicted in Figure 6.2, it can be seen that the yaw angle is 1.4 degrees.

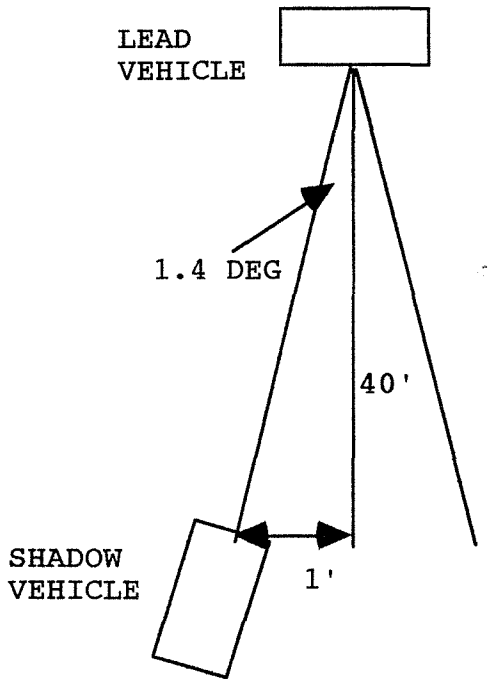

Figure 6.3. Yaw Angle for a Lateral Displacement of 1 ft. and symbol centered

Experiments were conducted to determine if yaw angle could be more accurately obtained with slits and a wedge object shown in Figure 6.4 and Figure 6.5 respectively. The motivation for experimenting with this approach is based on billboards whose image changed as one travels past it. The objects would be placed in the center of the symbol that is mounted on the back of the Lead Vehicle.

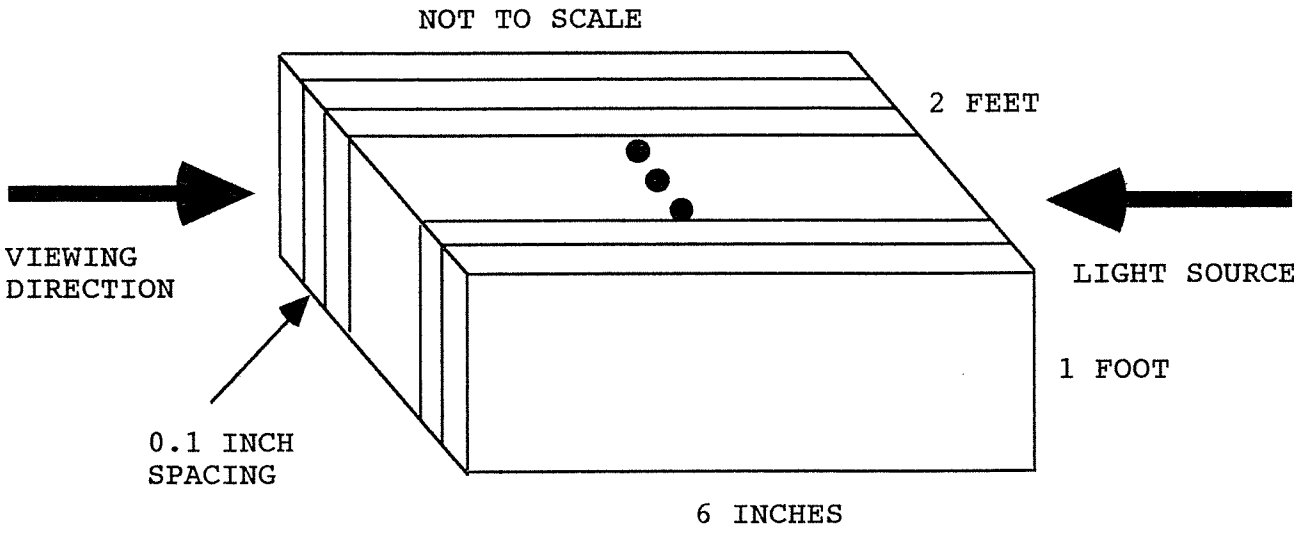

Figure 6.4. Slit Experiment

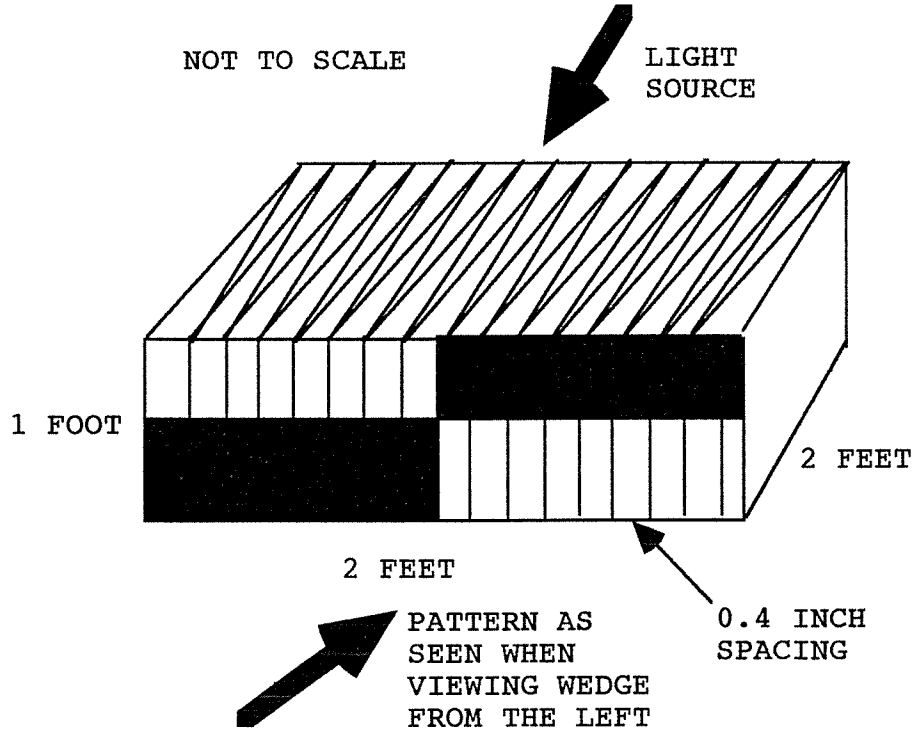

Figure 6.5. Wedge Experiment

In theory, if the light from the slit in Figure 6.4 can be seen by the camera, the Autonomous Shadow Vehicle is in a

$$\text{Cone Angle} = (0.1/24)*(180/\pi) = 0.955 \text{ deg.} \qquad (6.13)$$

behind the Lead Vehicle. However, reflections were encountered due to light reflecting inside of the slits even though the partitions were painted flat black and exiting at different angles. Highly light absorbing material most likely will reduce this problem. Based on this limited experiment, this approach has potential. However, it will not be pursued further unless required as determined by Phase II experimentation.

The wedge was partitioned into four quadrants as illustrated in Figure 6.5. The sides of each quadrant of the wedge were painted flat black so that when viewing the wedge from a left viewing angle a black and white checkerboard as shown in Figure 6.5 is seen by the camera. When viewing the wedge from the left to straight on, the checkerboard pattern changes until a solid gray is seen. As one moves from viewing the wedge straight on to the right a black and white checkerboard pattern emerges that is the inverse of the pattern shown in Figure 6.5. Again lighting was a problem. Reflections inside of the wedge and the challenge of uniformly lighting the wedge walls were problems. However, as with the slit experiment, based on limited experimentation, this approach has potential. However, the wedge approach will not be pursued further unless required as determined by Phase II experimentation.

6.3 Vision Based Neural Network Design

Following is a general outline of the steps using a video frame, machine vision processing and neural network implementation to obtain range, lateral displacement, and yaw angle:

1) Control the zoom lens on the camera based on the desired tracking range. This ensures that the symbol has sufficient resolution in the image frame.

2) Every 0.1 seconds a video frame is digitized(256x240 8 bit pixels) and thresholded and stored into a frame grabbers memory as a binary image(1's and 0's).

3) Based on the last location of the symbol and an estimate of the vehicle dynamics, the location of the symbol in the current frame is predicted. A search algorithm finds the edge of the symbol and "walks" around(chain codes) the edge of the symbol. As a result only a few pixels of the image need to be processed.

4) Various object descriptors will be computed and correlations performed to ascertain to a probability of 0.999999 or greater that the object is the symbol mounted on the back of the Lead Vehicle. Eight points on the Image points and other image information are then set to Neural Networks.

5) The Range Neural Network produces range. Area and perimeter are inputs to the Range Neural Network. The Range Neural Network consists of 8 neurons in the 1st layer, 2 neurons in the 2nd layer, and 1 neuron in the output layer whose output is range. The output of each neuron is an input to all neurons in the next layer. A radial-basis architecture was used.

6) The Lateral Displacement/Yaw Angle Neural Network produces lateral displacement and yaw angle of the Autonomous Shadow Vehicle relative to the Lead Vehicle. There are 10 inputs to this Neural Network. This Neural Network consists of 30 neurons in the 1st layer, 15 neurons in the 2nd layer, and 7 neurons in the 3rd layer and 2 neurons in the output layer whose outputs are lateral displacement and yaw angle. The output of each neuron is an input to all neurons in the next layer. A radial-basis architecture was used.

6.4 Cost Estimate for Major Vision Tracking System Components

Following is a cost estimate for the major hardware components for the proposed Vision Tracking System Components:

Video Camera	$ 895
Zoom Lens with controllable zoom, and iris.	$ 1500
Control Zoom Lens control box	$ 500
Pentium 90 MHz (Also performs computations for antenna, GPS, & control functions)	$ 1500
Frame Grabber	$ 1500
DSP Board	$ 1500
Total Major Components =	$ 7395

The above cost estimate does not include cables, camera housing, or cost to construct symbol on the Lead Vehicle. A more complete cost estimate will be made at the end of Phase II.

7. RELATIVE GPS TRACKING SYSTEM

7.1 Satellite System

GPS (Global Positioning system) is a satellite-based radio navigation system. It consists of 24 satellites arranged in six 55 degree orbit planes 10,898 nautical miles above the earth (Figure 7.1). A GPS receiver obtains signals from four or more satellites and uses these signals, or timing pulses, to establish a three dimensional position: longitude, latitude, and altitude. The signal consists of a string of binary pulses, and takes about one eleventh of a second to reach the receiver. The time of travel of the signal is estimated by the receiver by subtracting the time from its internal clock from the time the signal says it was broadcast. This estimate is multiplied by the speed of light to obtain a distance estimate, R1, to the first satellite. The same procedure is followed to obtain estimates to other satellites.

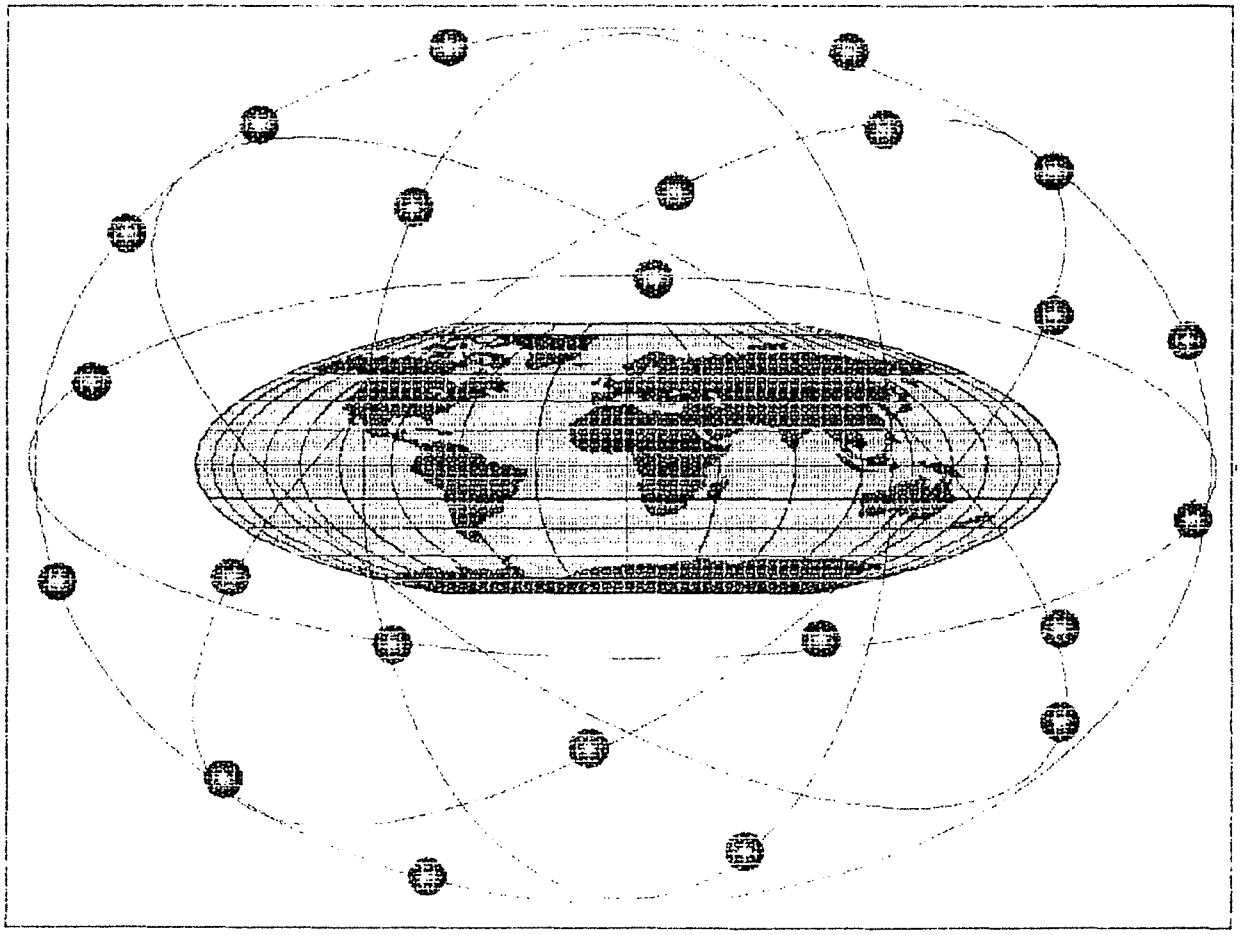

Figure 7.1 GPS Constellation

The inexpensive quartz clocks on the receivers are not perfectly synchronized to the more accurate atomic clocks on board the satellites. As a consequence, the receiver estimates a pseudo range to each of the satellites. The error in the pseudo range measurement is usually called the clock bias CB. Fortunately, all of the measurements to all of the satellites are corrupted with the same CB due to the good synchronization of the satellites to each other. This means that the CB can be algebraically eliminated by making four measurements instead of three to solve for the position coordinates. The system of equations used to make the calculations is as follows:

$$(X_1 - U_x)^2 + (Y_1 - U_y)^2 + (Z_1 - U_z)^2 = (R_1 - C_B)^2 \qquad (7.1a)$$

$$(X_2 - U_x)^2 + (Y_2 - U_y)^2 + (Z_2 - U_z)^2 = (R_2 - C_B)^2 \qquad (7.1b)$$

$$(X_3 - U_x)^2 + (Y_3 - U_y)^2 + (Z_3 - U_z)^2 = (R_3 - C_B)^2 \qquad (7.1c)$$

$$(X_4 - U_x)^2 + (Y_4 - U_y)^2 + (Z_4 - U_z)^2 = (R_4 - C_B)^2 \qquad (7.1d)$$

The unknowns are U_x, U_y, U_z, and C_B. They correspond to the coordinates of the user or receiver and to the clock bias. The variables X_i, Y_i, and Z_i are the position coordinates of the satellite being tracked. The receiver can solve for X_i, Y_i, and Z_i using the ephemeris constants transmitted by the satellite along with the timing pulse. Once the receiver has the ephemeris constants, it can then solve for the coordinates U_x, U_y, and U_z. There is no explicit solution for these equations, but they can be solved by iteration using Taylor polynomial expansions.

It is necessary for the satellites to transmit very accurate synchronized time pulses and orbital elements (ephemeris constants) in order to obtain an accurate set of coordinates. Satellites, however, tend to lose track of the time and where they are. This problem is circumvented by having a control station on earth track the satellites and periodically let them know the corrections that must be made to their on board clock and to their orbital elements.

7.2 Satellite Transmission

Satellite signal transmission is accomplished using a Spread Spectrum Multiple Access Modulation technique: Code Division Multiple Access (CDMA). Each satellite is assigned its own Coarse Acquisition (C/A) code and its own Precision (P)

code. The C/A code is available to the public free of charge; the P code is encrypted to restrict access and accuracy to unauthorized users --its reserved for military purposes. The C/A code has a chipping rate of 1 million bits per second and a repetition interval of 1023 bits. The P code has a chipping rate of 10 million bits per second and a repetition interval of $6X10^{12}$ bits(Approximately seven days pass before this code repeats.). Both are pseudo random codes. When any of the signals reaches a receiver, within the receiver an identical pulse train is generated to match the incoming signal. When this is accomplished, an autocorrelation function jumps from 0 to 1 --this signals that lock-on has occurred. Once lock-on has been achieved, the pseudo range can be calculated as mentioned before.

A data stream of 50 bits per second is superimposed onto the pulse train. It is conformed in the following way: The data is divided into 30 second frames of 1,500 data bits. Each frame is subdivided into five 6-second subframes of 300 bits. Subframe 1 contains the clock corrections. Subframes 2 and 3 contain the ephemeris constants. Subframe 4 contains navigation messages and satellite health status information. Subframe 5 contains the constellation almanac. In the almanac the satellite tells the users where all the other satellites are located. This way, the almanac can be used to decide which four satellites provide the most accurate navigation solution.

The objective of the GPS receivers is to acquire a set of coordinates for each vehicle, communicate both sets of data to the computer on board the shadow vehicle, and require the computer to set a heading that guides the shadow vehicle towards the lead vehicle (see Figure 7.2). For this purpose, each vehicle will be equipped with a GPS receiver. In particular, the GPS receiver module that will be used can be placed directly on one of the computer slots for ease of communication between the computer and the GPS module. This module uses multiple channels to track 6 different satellites continuously. This feature conduces to a time to first fix of approximately 120 seconds, and an update rate of 1 per second. These are desired qualities which will lead to efficient tracking.

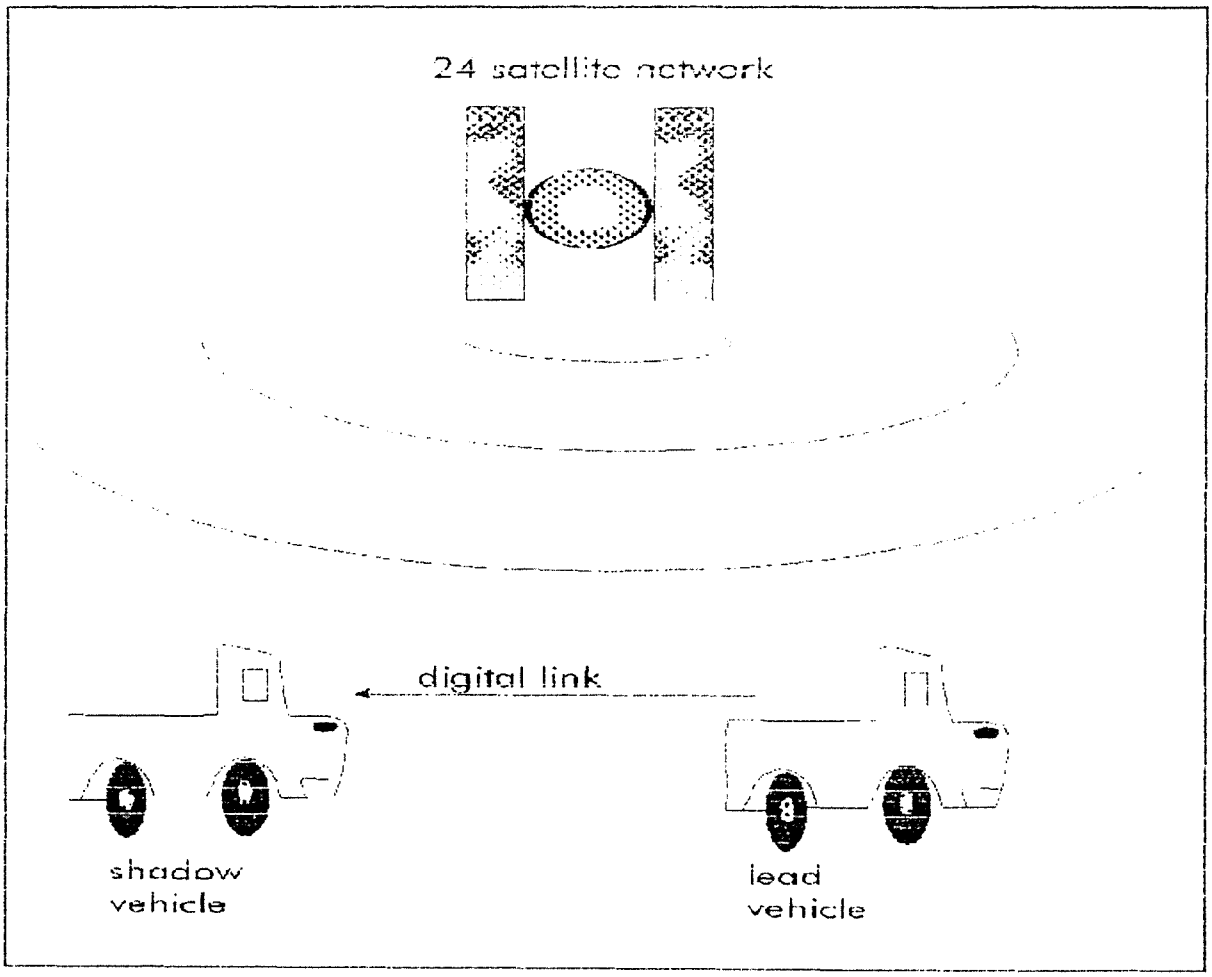

Figure 7.2 Relative GPS

7.3 Relative GPS

The position updates obtained with GPS are plagued with an unacceptable error which must be dealt with. This error is not the before mentioned clock bias --it was dealt with by using an extra satellite. The error that we are dealing with has to do simply with how good the receiver reports the position. Typically, this error is greater than 10ft. One method of reducing this error is known as differential GPS. Differential GPS consists of utilizing stationary GPS receivers to obtain and later broadcast a correction factor to the mobile receivers. This option limits the operation of the shadow vehicle to areas were the static stations are readily available. This creates a dependency which is counter intuitive in an autonomous vehicle. An alternative solution was developed: a radio spread spectrum digital link is added between the lead vehicle and the shadow vehicle (Figure 7.2). This link will be used to re-transmit the lead vehicle coordinates back to the shadow vehicle where the on-board computer will compare the data transmitted by the lead vehicle and its own GPS position. The idea is that both receivers (lead and shadow) will report the same inaccuracy. The computer then subtracts the shadow coordinates from the lead coordinates to obtain the position of the shadow vehicle relative to the lead vehicle -- effectively subtracting out the error or inaccuracy of the GPS coordinates. With this information, the computer can proceed to plot a course for the shadow vehicle to follow. Next is a description of how the digital link is implemented.

7.4 Relative GPS System Design

The lead vehicle must share pertinent information with the shadow vehicle. These data include speed, odometer reading, and steering angle in addition to the GPS coordinates. The speed, steering angle, and odometer reading will be taken directly from the lead vehicle's mechanical system and later compared, in a "checks and balances" sense, to the GPS information. As can be seen in Figure 7.3, the Lead Vehicle data gathering instrumentation consists of transducers that will read speed, steering angle, and displacement, a GPS receiver, and a microcontroller. Because of the different nature of the data sources, some processing is necessary prior to the transmission of the data. This preprocessing will be accomplished by the Motorola HC11 microcontroller. Once the data is correctly formatted, the microcontroller feeds the data to the digital transmitter, which sends the data to the shadow vehicle (Figure 7.4).

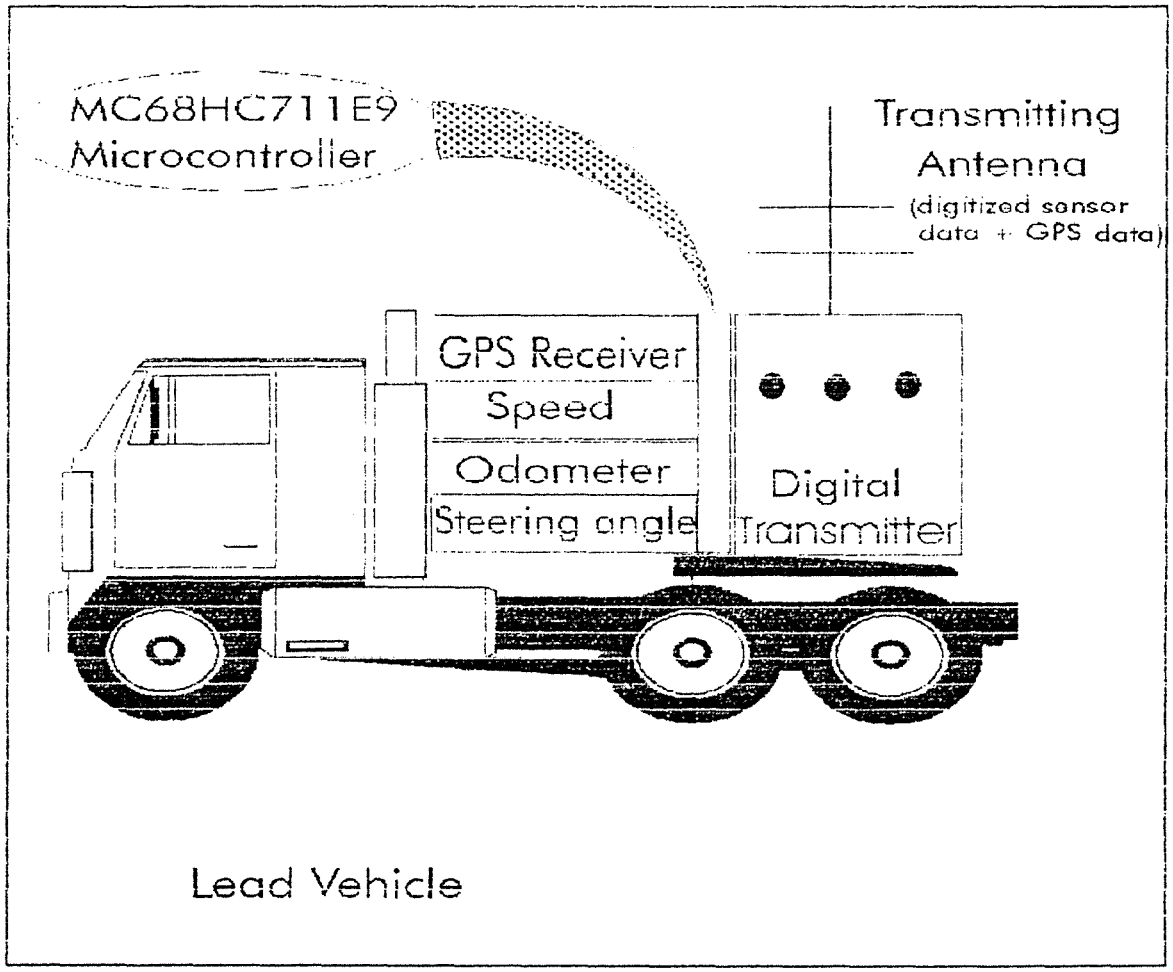

Figure 7.3. Lead Vehicle Instrumentation for Relative GPS

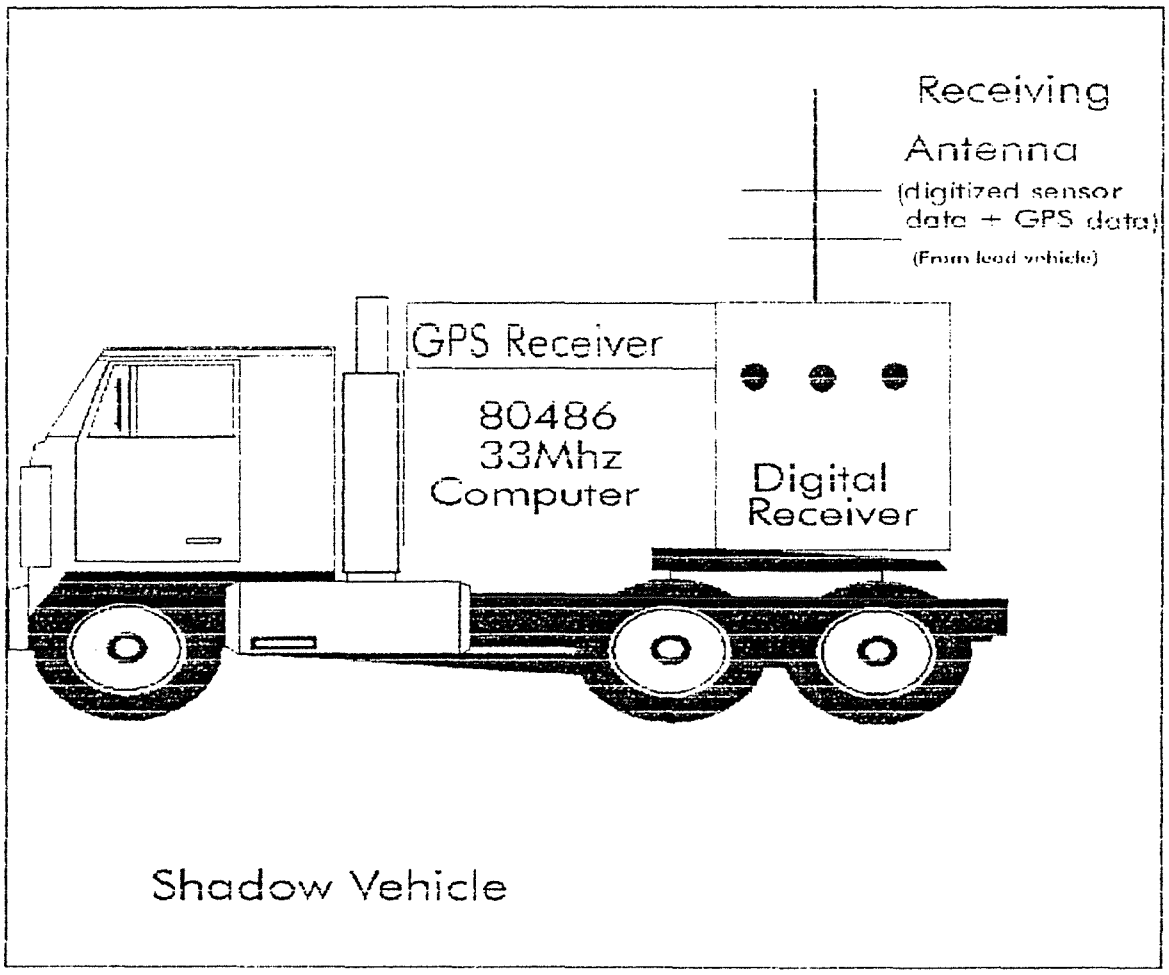

Figure 7.4. Shadow Vehicle Instrumentation for Relative GPS

The information of the lead vehicle will be transmitted using a spread spectrum modulation technique. This particular technique was sought because of its ability to escape friendly and unfriendly jamming signals. The fact that it operates in a none-regulated FCC frequency band is an added bonus. On the shadow vehicle, the receiver will capture the data sent by the lead vehicle and provide it as input to the computer (Figure 7.4). The computer is the cerebral of the shadow vehicle. Given the lead vehicle coordinates and the shadow vehicle's own coordinates, it will implement the algorithm to find the relative position to the lead vehicle. Once this is done, the computer will interface with the control system of the shadow vehicle to produce the signals that will allow the shadow vehicle to engage a course that will follow the desired path to the lead vehicle. All the interfacing of the system elements will be done via an RS232 standard interface. GPS is the third system added to the tracking shadow vehicle; GPS will introduce triple redundancy to the system to augment the robustness of the system and the safety of the users. In other words, the system as described above would be sufficient to guide the shadow vehicle; however, the GPS system is not sufficiently reliable as a sole solution because the signal tends to fade or disappear. Thus, the GPS system will work in conjunction with the other systems described in this document in such a way that there is always a reliable path for the shadow vehicle to follow.

7.5 The Microcontroller

A block diagram of the MC68306 (QUICC)is shown in Figure 7.5. Following is a brief description of the salient characteristics that make this chip a good choice. The QUICC(pronounced quick) processor is a specialized communications processor. The speed of the core processor is 4MIPS at 25Mhz. At this processing speed, the amount of data the shadow vehicle will need can be processed in 2.5 milliseconds or less. The microcontroller supports continuous mode transmission and reception on all serial channels. This will make possible the use of the full duplex capability of the spread spectrum transmitter/receiver. This means the computer on board the shadow vehicle can maintain constant communication with the lead vehicle, thus enabling the human inside the lead vehicle to oversee the entire process. Each serial channel can have its own pins; some channels can support totally transparent bit stream communication, binary synchronous communication, or synchronous communication. Priority and multiplexing of the channels is programmable. The QUICC also supports various protocols; this allows much liberty in the selection of peripheral devices.

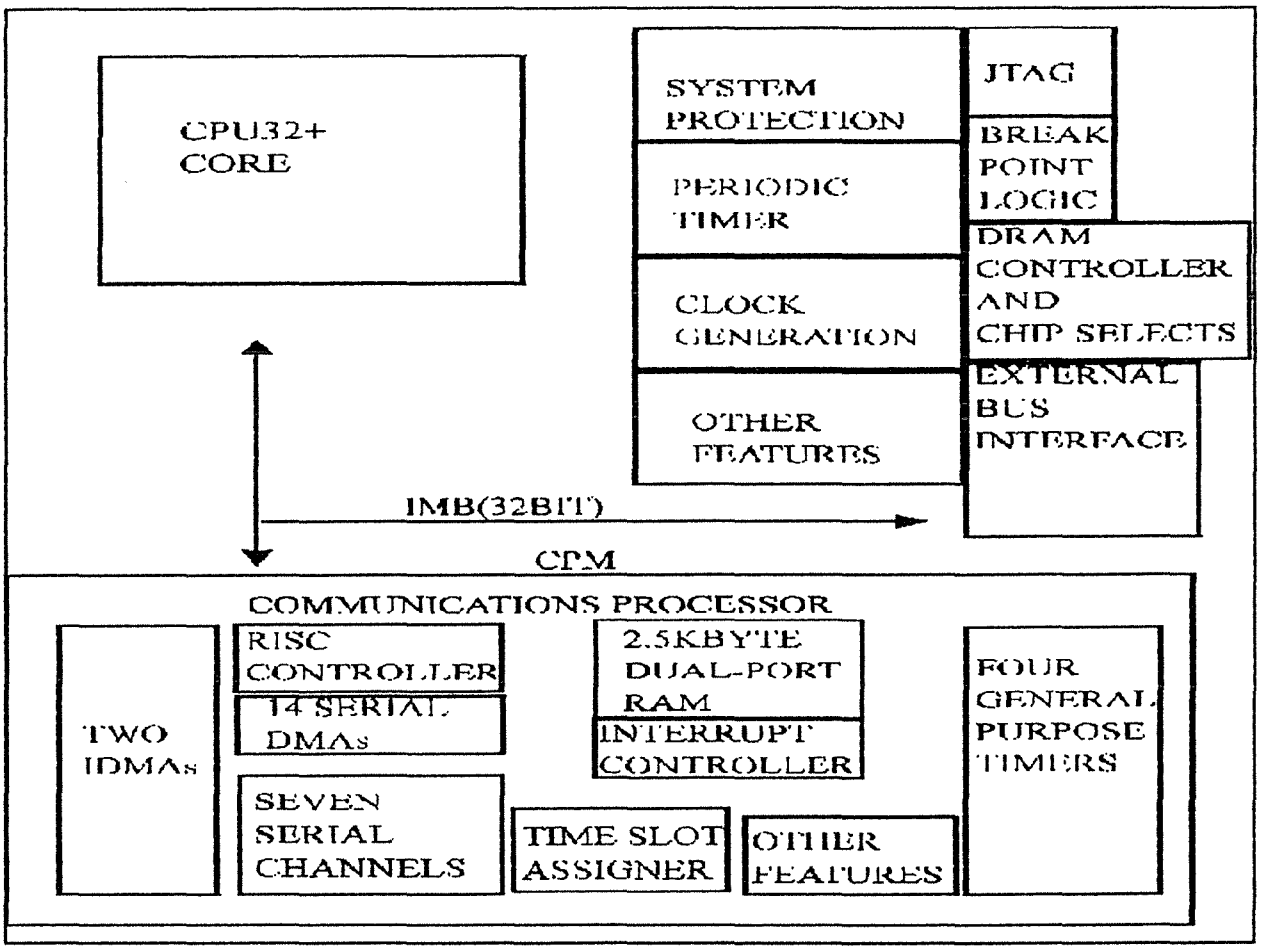

Figure 7.5. MC68306 Microprocessor Functional Block Diagram

Figure 7.6 shows the QUICC with pin connections. (Some pin connections have been omitted for clarity.) The external clock is a crystal oscillating at 25Mhz. The SPI, pin(cs7), (serial peripheral interface) can be used as a data acquisition port because it provides a plug-in interface to other MOTOROLA products such as the DAC that will be used to convert the sensor data. The GPS receiver is connected to SMC1, pin(cs5) (serial management controller) because of this channel's ability for totally transparent operation. The transmitter/receiver is connected to (cs3) because of this port's full duplex capabilities. Finally, one of the parallel ports will provide the output for the necessary control lines.

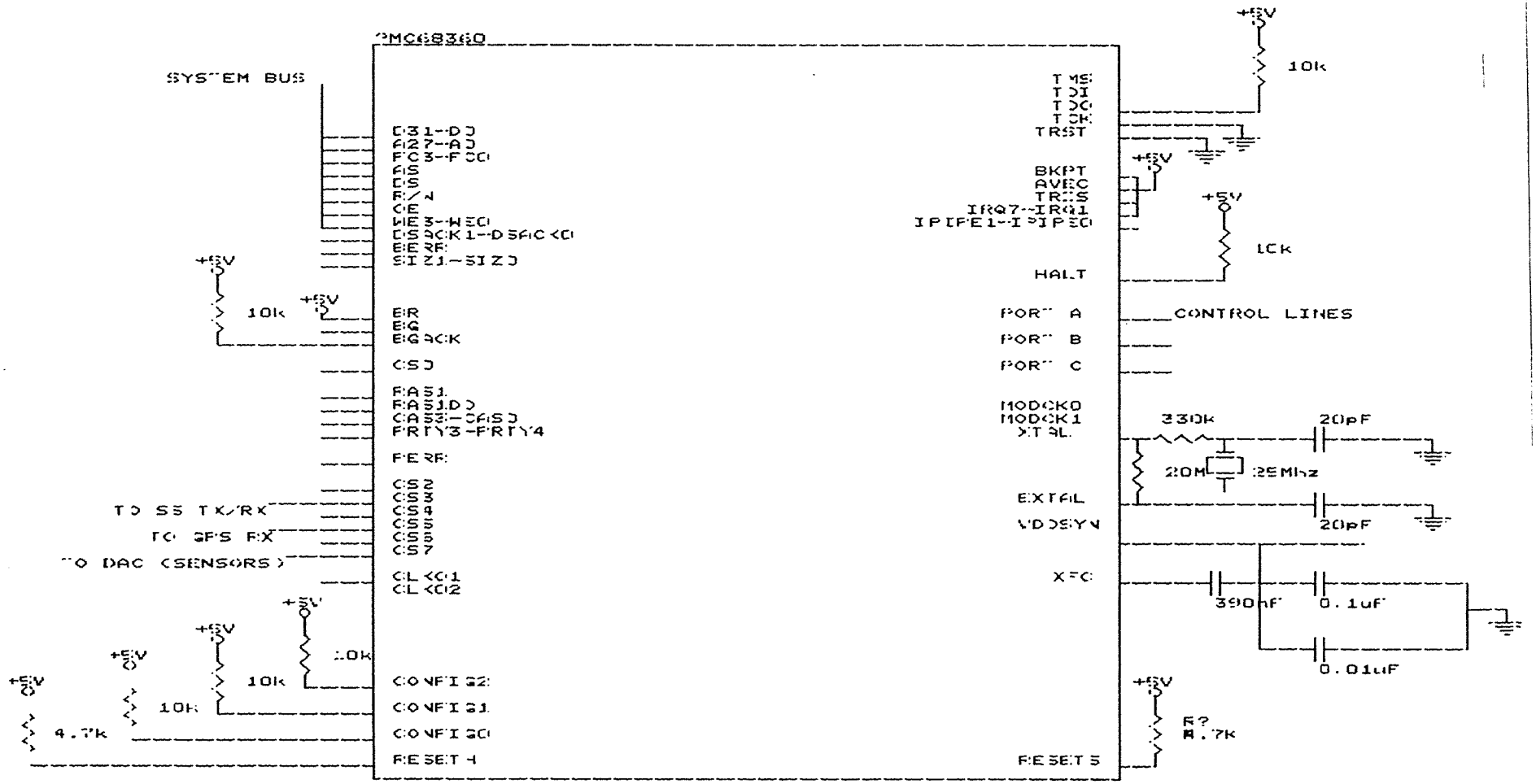

Figure 7.6. MC68306 Pin Connections

7.6 Estimated Cost for the Relative GPS Tracking System

Following is a cost estimate for the proposed Relative GPS Tracking System:

QTY	PART	COST
1	Digital transmitter	$ 1900
1	Digital receiver	$ 1900
2	GPS receivers	$ 4000
1	Microcontroller programmer	$ 300
1	Microcontroller	$ 70
3	Transducers	$ 300
	Various resistors, capacitors, and cables	$ 100
Total Cost Estimate for Relative GPS		$ 8,170

The GPS system is also used to transmit information other than GPS data such as Lead Vehicle speed to Shadow Vehicle and Shadow Vehicle status to the Lead Vehicle driver.

8.0 LONGITUDINAL CONTROL DESIGN & SIMULATION

8.1 Objectives

The objectives of the design are multifaceted. We are primarily interested in a control algorithm that places the shadow vehicle at a safe distance from the lead vehicle. The desired range between the two vehicles could be set as constant or could be selected by a spacing policy that is consistent with the California Department of Transportation regulations. The speed of response and accuracy in estimating the actual range cannot be compromised. Therefore steps were taken to simulate anomalies, such as transmission delay, to insure that the controller would compensate by continuously regulating the range.

The control law selected is nonlinear sliding mode adaptive controller. It accounts for the changing dynamics in the vehicle as a function of air resistance, gear selection and velocity. One of the objects of the design was to integrate the system in a manner where in most cases the range is determined by the throttle. This implies that the shadow vehicle, when approaching the lead vehicle, releases some of the throttle to increase the range between the two vehicles. If the range rate is decreasing rapidly, beyond a certain threshold, the brakes are then applied, the controller adapts to the different braking dynamics and the range is then rapidly increased. After the vehicle reaches the desired value again, the vehicle shifts back into throttle mode. Increasing range is not always controlled by the braking so that brake pads would not be worn prematurely.

In addition to brake/throttle shifting, the controller has limitors on both the brake and throttle torque commands so that the engine is not raced and the braking is not sudden to cause slippage. The jerk is controlled by a first order low pass filter with a time constant of 0.7 seconds. The LPF reduces sudden force inputs and helps keeping the ride smooth.

8.2 Literature Search

Two primary goals were met by the literature search. The first was to find a vehicle dynamics model that was realistic and accounted for the changing dynamics of the velocity response as a function of throttle, air resistance and other external factors. The second was to build on existing control laws in order to design a controller that adapts to the changing dynamics of the vehicle.

Most of the information available could be characterized as a proposed simulation model for a longitudinal control algorithm. None of the models however accounted for the discrepancy between braking and throttle dynamics. The algorithms investigated could be divided into two categories: 1) linear vehicle dynamics and control and 2) nonlinear vehicle dynamics and control. Each control law candidate was simulated and its performance was analyzed. The simulated algorithms were mostly the product of a cumulative study of an author or a set of authors and were developed over time. Our simulations incorporated a whole design path for each series of published papers focusing on a single proposed control law and accounting for the suggested changes. The conclusion of the literature search was the adoption of a vehicle model, proposed by Fenton [61], [62], [63], and [64] that accounted for velocity-dependent engine parameters.

Linear dynamics and control:

Many of the algorithms we analyzed were successfully simulated. The simulation results for some of the successful ones indicated a rising steady-state error in the range that was a function of lead vehicle velocity variations [65]. Others accounted for the delay caused by the transmission of necessary variables from the lead vehicle [66], [67]. The time delay was a realistic control constraint and was therefore included in our design. The adopted model for braking was a first order linear system.

Nonlinear dynamics and control:

The Fenton vehicle model was used in a design by Hauksdottir that was rather complex, in which it was redeveloped for control adaptability [68], [61], [62], and [69]. The Hauksdottir controller was not successfully simulated due to lack of necessary information in the published papers. However, the Hauksdottir vehicle model was used as the basis of our engine model.

8.3 Longitudinal Controller Design

The controller design was based on a nonlinear adaptive sliding surface control law. The sensed range is given as an input and a torque command is delivered as an output. Based on the range and the error, a sliding surface function is formed and parameters converge as functions of the sliding surface. In the simulation, a logical decision determines which of the two dynamic models will be actuated by the controller. Figure 8.1 shows a block diagram of the simulation design.

The system is constructed to receive three inputs and delivers one output. It requires the initial spacing between vehicles, the desired range between the vehicles and the current velocity of the lead vehicle. The controlled variable is the range.

There are two separate "plants" to be controlled. The throttle and the braking of the shadow vehicle. Both are controlled by the same control law. The control law consists of two major blocks. The first receives the sensed range and calculates a sliding surface based on an error estimation algorithm. The second block is the adaptive algorithm; it calculates the two gain parameters to be used in the torque command. The torque output is added to an integrated value of the error, then multiplexed by a logical operand. If torque is positive, throttle is applied, and if torque is negative, brakes are applied. In the simulation only one part operates based on the current variables. When the other plant is actuated, the current variables are sent to it in order to update the state of the system.

The throttle command is derived from the inverse dynamics of a robot actuator. The inverse dynamic parameters are set to be variable, so that the Lyapunov is selected accordingly. The sliding mode control is derived from the sliding surface as follows:

$s = \dot{e} + \lambda e = 0$

The state x $\ni$ $\ddot{x} = f(x) + u$

$u = -f + \ddot{x} - \lambda\dot{e} \Rightarrow \dot{s} = 0$

$s(t_0) \neq 0$ for the initial condition .

$Ksgn(s), K > 0$

Estimate of f ,

$u = \hat{u} - Ksgn(s)$

$u = -\hat{f} + \ddot{x}d - \lambda\dot{e} - Ksgn(s)$

$\dot{s} = f - \hat{f} - Ksgn(s)$, choose K > $\|f - \hat{f}\|$

Terminal attractors ,

$\dot{x} = -x^{\frac{1}{3}}$

$\int_{t_0}^{t_{eq}} \dot{x} \Rightarrow (t_{eq} - t_0) = \frac{3}{2} x_i^{\frac{3}{2}}$, increased local stability .

Most general attractor ,

$\dot{x} + X(x) = 0$, X bounded for bounded x.

$sgn(X) = sgn(x)$ as $\frac{\alpha X}{\alpha x} \rightarrow \infty$, as $x \rightarrow 0$

Attractor used :

$\dot{x} = \alpha x^{\frac{\beta_n}{\beta_d}}, \alpha > 0, \ \beta_n, \beta_d = (2i+1), \ \beta_d > \beta_n$

$\therefore s = \dot{e}_i + \alpha e_i^{\frac{\beta_n}{\beta_d}} = 0.$

For bounded u and e,

$\frac{\beta_n}{\beta_d} > \frac{1}{2} \Rightarrow \beta_n > \frac{1}{2}\beta_d$

$u = \ddot{x}d - \alpha\frac{\beta_n}{\beta_d} e^{\frac{\beta_n}{\beta_d}}\dot{e} - \gamma s^{\frac{\delta_n}{\delta_d}} - \hat{f}(x).$

The dynamic terminal slider converges to s in finite time faster than an exponential response .

This eliminates the need for high gain control switching .

$P = \dot{s} + \gamma s^{\frac{\delta_n}{\delta_d}} = 0$

Given robot motor and load dynamic equation ,

$$\tau_M = M(q_M)(q_M)\ddot{q}_M + C(\dot{q}_M, q_M)\dot{q}_M + G(q_M)$$

$$e \equiv q_M - q_{d_M}, \dot{e} \equiv \dot{q}_M - \dot{q}_{d_M}$$

$$s = \dot{e} + \alpha e^{\frac{\beta_n}{\beta_d}}$$

$$v = \ddot{q}_{d_M} - \alpha \frac{\beta_n}{\beta_d} e^{\left(\frac{\beta_n}{\beta_d} - 1\right)} \dot{e} - \gamma s^{\frac{\delta_n}{\delta_d}}$$

The CONTROL LAW: (Terminal Sliding Control)

$$\underline{\tau_{COM_M} = \hat{M}V + \hat{C}\dot{q}_M + \hat{G}(q_M)}$$

results in $\dot{s} + \gamma s^{\frac{\delta_n}{\delta_d}} = 0$, that is terminally stable .

$$\alpha > 0, \gamma > 0, \beta_n = (2i+1), \beta_d = (2j+1), \beta_n > \frac{1}{2}\beta_d.$$

$$\delta_n = (2k+1), \delta_d = (2l+1),$$

$$0.5 \le \frac{\delta_n}{\delta_d} < 1$$

Adaptive Inverse Dynamics

$$M\ddot{R} + C\dot{R} + G(R) = \hat{M}v + \hat{C}\dot{R} + \hat{G}(R)$$

$$M\ddot{R} - \hat{M}\ddot{R} + \hat{M}\ddot{R} + C\dot{R} + q\theta = \hat{M}v + \hat{C}\dot{R} + \hat{\theta}q$$

$$M(\ddot{R} - v) = (\hat{M} - M)\ddot{R} + (\hat{C} - C)\dot{R} + (\hat{\theta} - \theta)q$$

$$Y \equiv \begin{bmatrix} \ddot{R} & \dot{R} & q \end{bmatrix}, P_e \equiv \hat{P} - P \Rightarrow M(\ddot{R} - v) = Y \begin{bmatrix} (\hat{M} - M) \\ (\hat{C} - C) \\ (\hat{\theta} - \theta) \end{bmatrix}; \dot{P}_e \approx \hat{P}$$

assuming P is constant over a sufficiently long time .

$$\dot{R} - v = M^{-1}YP_e = \Phi P_e, \Phi = M^{-1}Y, \beta = \begin{bmatrix} 0 \\ I \end{bmatrix}$$

$$\dot{\hat{P}} = -\Gamma^{-1}\Phi^{\mathrm{T}}\beta^{\mathrm{T}}PX$$

$$\hat{P} = P + \dot{P}\Delta t.$$

$$\ddot{R} = \frac{s}{\tau_R s + 1}\dot{R}, \text{ if } \tau_R \text{ is small, } \ddot{R} = s\dot{R}$$

$$\tau_R s\ddot{R} + \ddot{R} = s\dot{R}$$

$$\ddot{R} = \left(\frac{1}{\tau_R}\right)\dot{R} - (\ddot{R})\frac{\Delta t}{\tau_R} = w_R\dot{R} - \ddot{R}(w_R\Delta t).$$

Select Lyaponov .

$$w \equiv (\ddot{R} - v); Mw = YP_e$$

$$V = \frac{1}{2} w^T M w + \frac{1}{2} P_e{}^{\mathrm{T}} \Gamma P_e$$

$$\dot{V} = \frac{1}{2} w^T M \dot{w} + \frac{1}{2} \dot{w}^T M w + \frac{1}{2} P_e{}^{\mathrm{T}} \Gamma \dot{P}_e + \frac{1}{2} \dot{P}_e{}^{\mathrm{T}} \Gamma P_e$$

$$w = \frac{YP_e}{M}$$

$$\dot{V} = \frac{1}{2} \frac{YP_e{}^T}{M} M\dot{w} + \frac{1}{2} \dot{w}^T M \frac{YP_e}{M} + P_e{}^{\mathrm{T}} \Gamma \dot{P}_e$$

$$\dot{V} = P^{\mathrm{T}}{}_e \left(Y^{\mathrm{T}} \dot{w} + \Gamma \dot{P}_e \right)$$

For $\dot{V} \le 0 \Rightarrow V \to 0$ since trajectory does not vanish . Hence $w \to 0$.

$\dot{V}$ can be 0 since trajectory cannot vanish until it reaches equilibrium .

$$\therefore Y^{\mathrm{T}} \dot{w} + \Gamma \dot{P}_e = 0 \Rightarrow \dot{V} = 0$$

$$\dot{P}_e = \frac{d(\hat{P} - P_e)}{dt} \approx \dot{\hat{P}}$$

$$\Gamma \dot{\hat{P}} = -Y^{\mathrm{T}} \dot{w}; \dot{\hat{P}} = -\Gamma^{-1} Y^{\mathrm{T}} \dot{w}.$$

$$\begin{bmatrix} \hat{M} \\ \hat{C} \\ \hat{\theta} \end{bmatrix} = \dot{\hat{P}} = - \begin{bmatrix} g_M & 0 & 0 \\ 0 & g_C & 0 \\ 0 & 0 & g_G \end{bmatrix} \begin{bmatrix} \ddot{R} \\ \dot{R} \\ g \end{bmatrix} \dot{w}$$

Where g is acceleration due to gravity .

$$\dot{w} = \frac{\Delta w}{\Delta t}$$

$\therefore$

$$\hat{M} = \hat{M} - g_M \ddot{R} \Delta w$$

$$\hat{C} = \hat{C} - g_c \dot{R} \Delta w$$

$$\hat{\theta} = \hat{\theta} - g_g g \Delta w.$$

Since the Hauksdottir model is a function of the current vehicle velocity, the gravity parameter was neglected. Gravity is a force and its effect, similar to friction and air resistance, will affect the velocity. Therefore the final velocity is a function of the external forces and the throttle command.

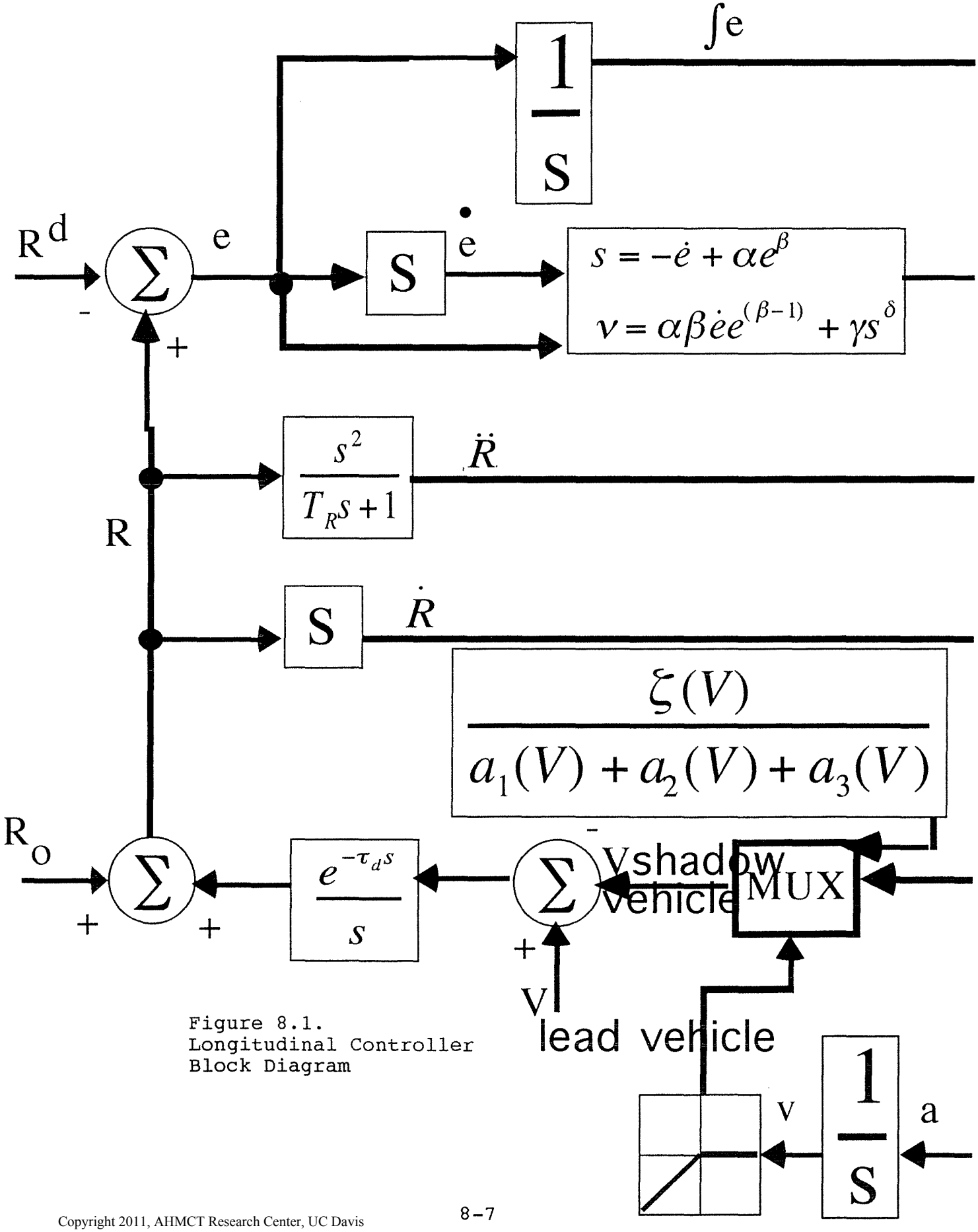

Figure 8.1.
Longitudinal Controller
Block Diagram

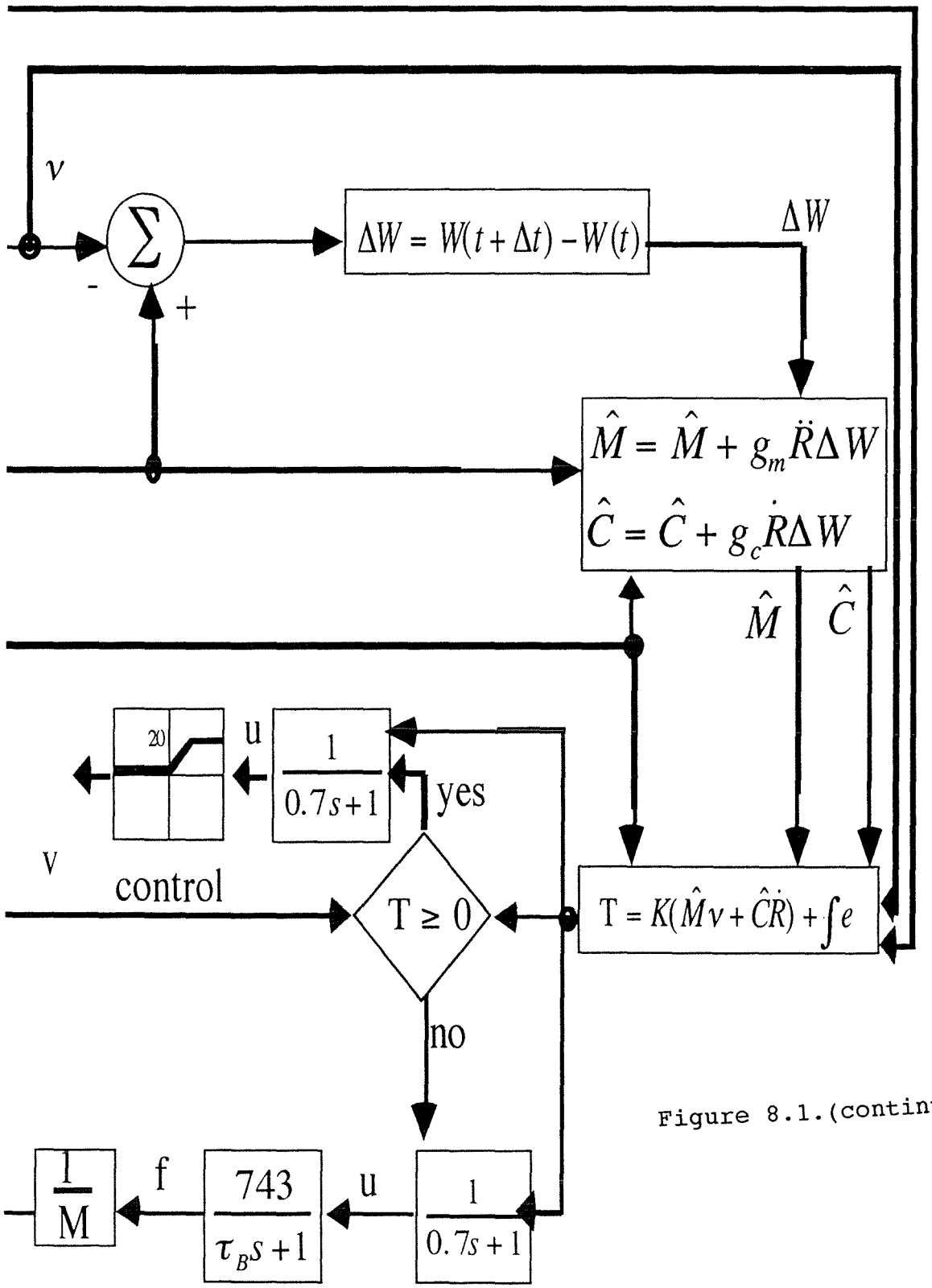

Figure 8.1.(continued)

8.4. Simulation Results

Figures 8.2 - 8.4 show the simulation results of the system. Three cases were simulated. The first was run with initial range equal to the desired range. The second with the initial range greater than the desired range and the third run was with initial range less than the desired range. All three simulations show the step response to the lead vehicle velocity, as well as the step response of the range variable. The control variable step response added to another input step function, push the system to the limits of stability. The system proved to be stable with all the oscillations in the torque command filtered by the low pass filter.

The braking was only actuated when a threshold was exceeded. This was shown in Figures 8.4.1-2. After the system is run, the first stage of the demonstration is the convergence of the control parameters. Then the range reaches a steady value, could be other than that of the desired value. The final tuning of the range is controlled by the steady-state error eliminator, the integral of the error function that was added to the system. The coefficient of the eliminator had to be large enough to cause timely convergence, but small enough to avoid parameter divergence. As is shown, the initial values of the control parameter v is quite large, which also affects the sliding surface. These initial values could be lowered by lowering the steady-state error coefficient, but then the simulation would have taken a long time to run.

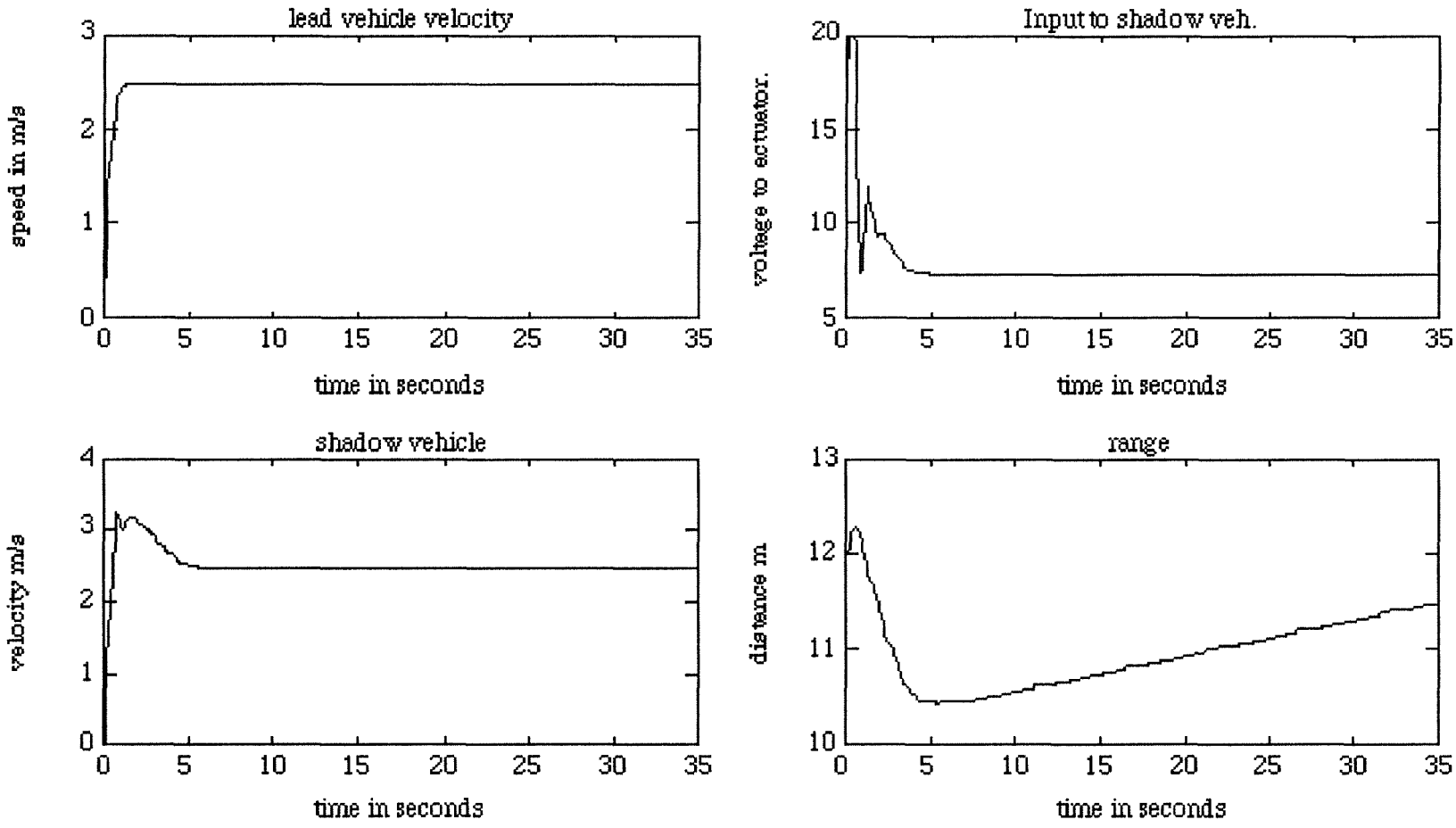

Figure 8.2.1. Velocity Step Response initiating with desired range.

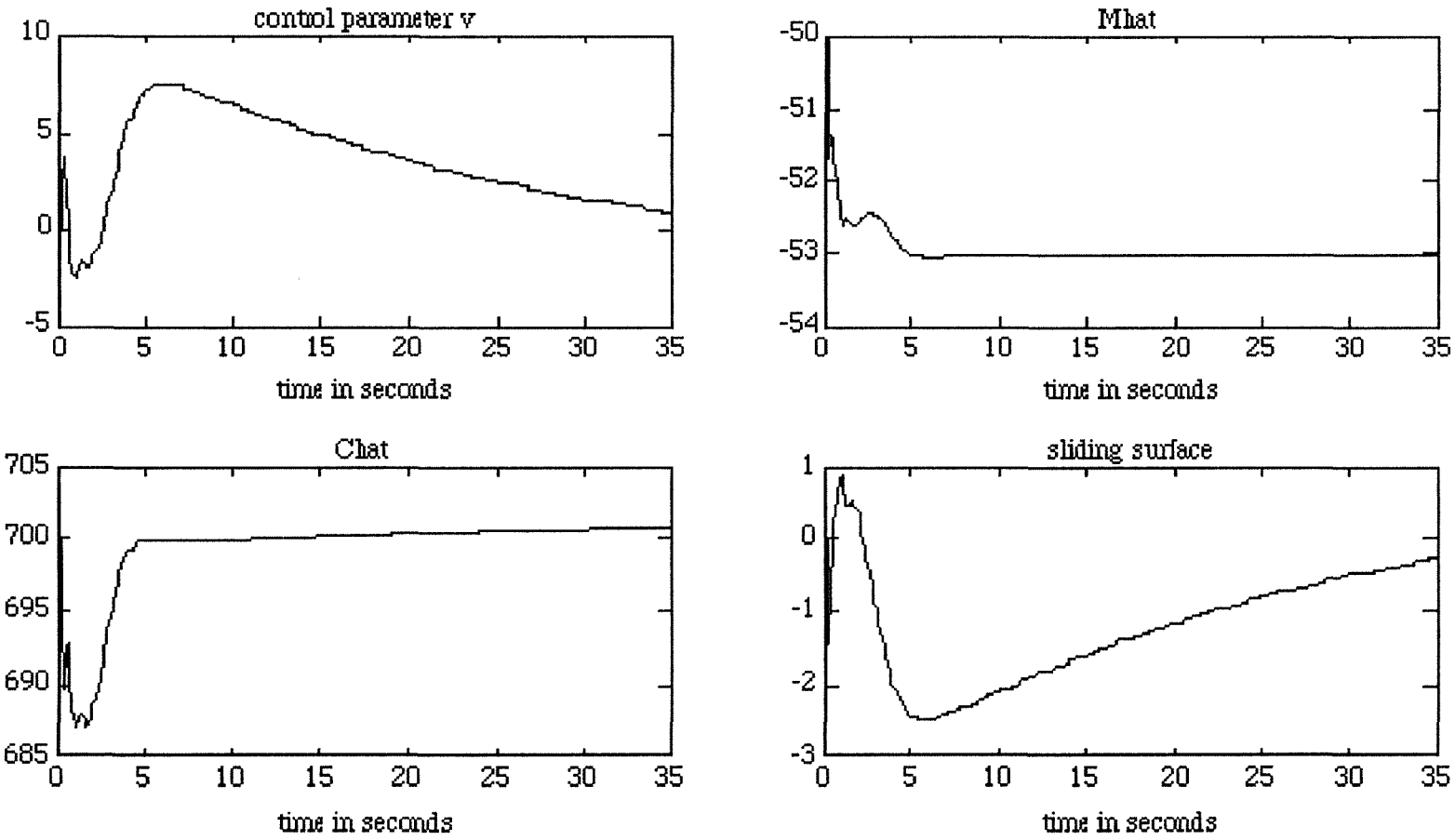

Figure 8.2.2. Control Parameters for velocity step response intitiating with desired range

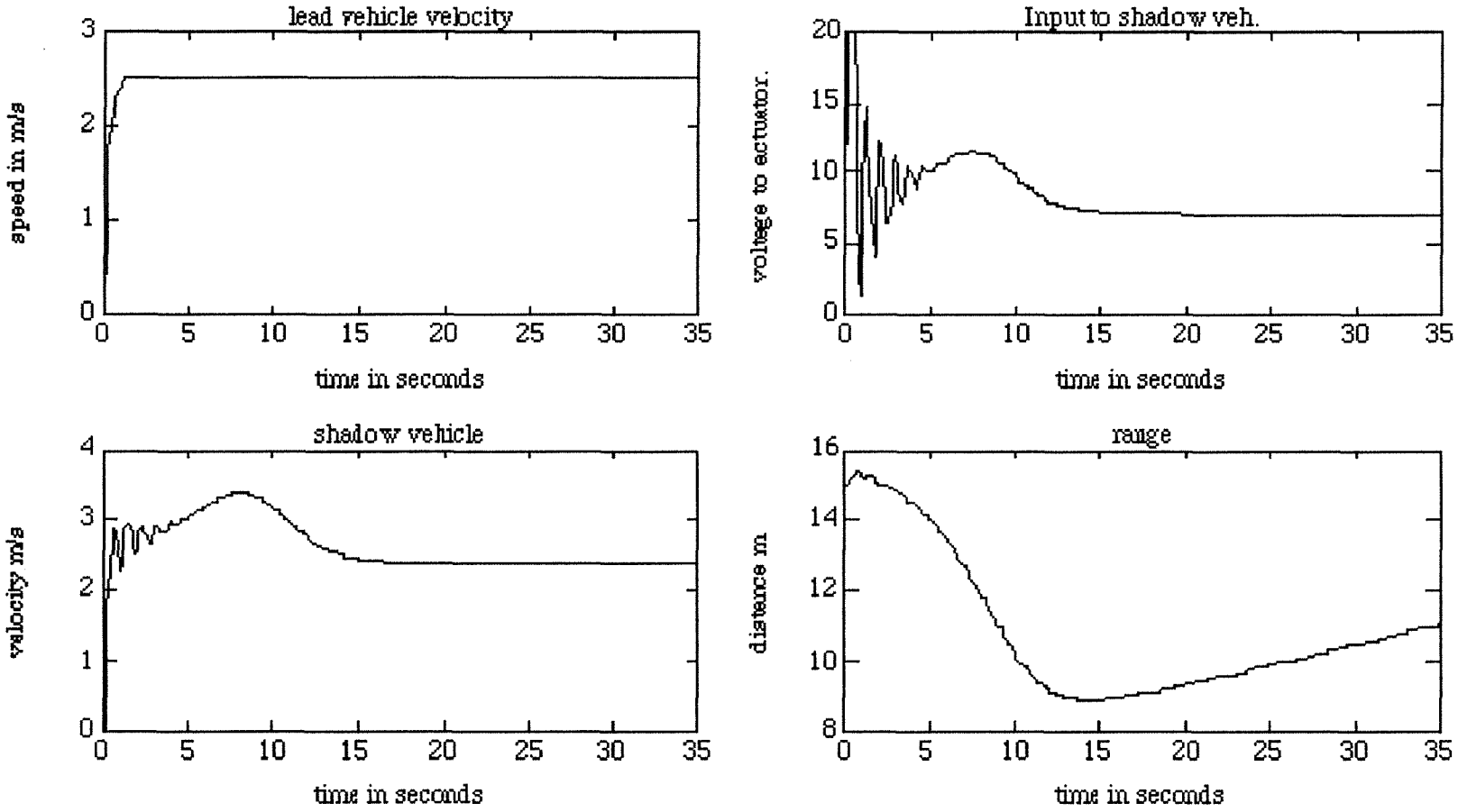

Figure 8.3.1. Velocity step response with initial range greater than the desired range.

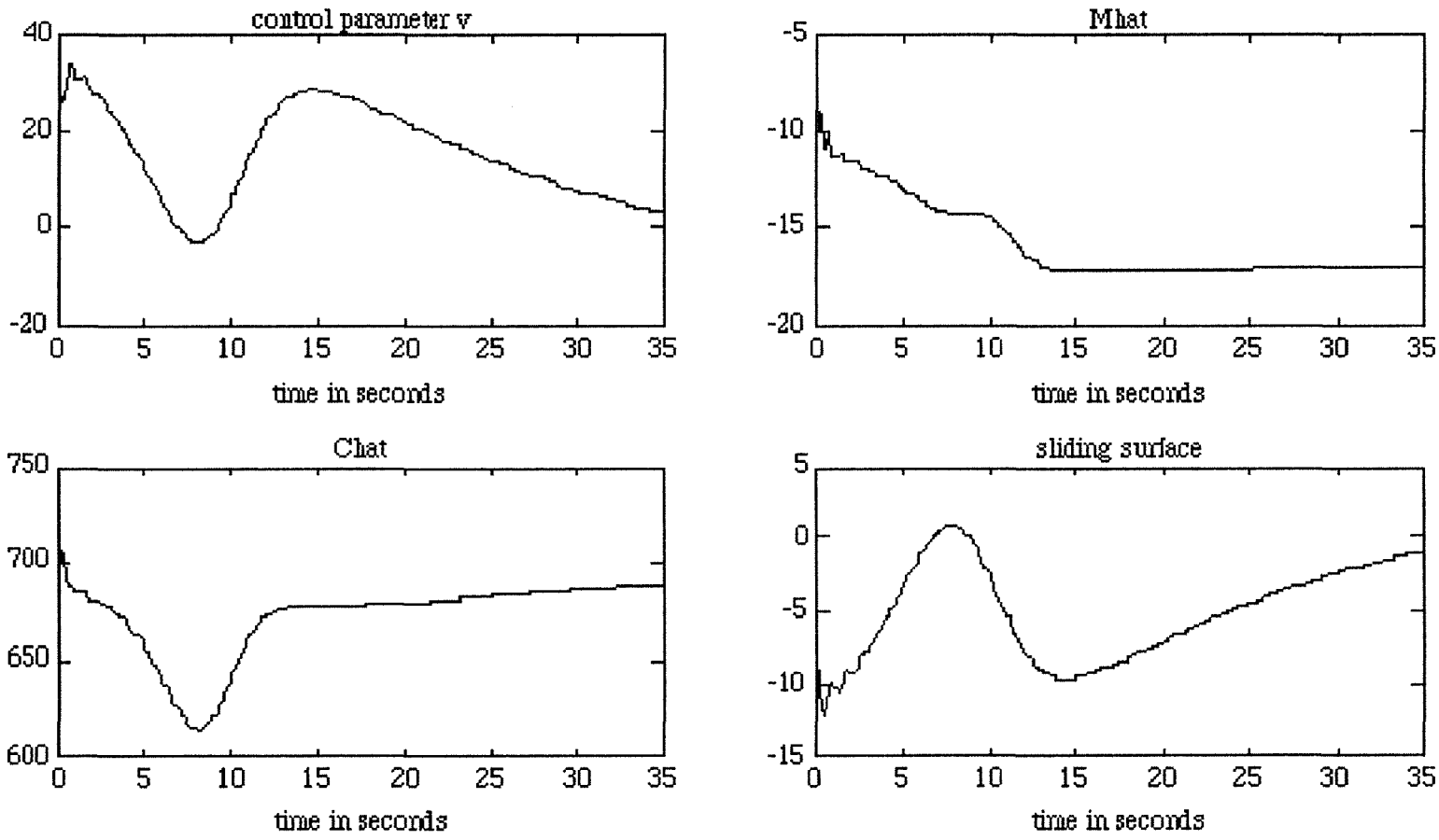

Figure 8.3.2. Control parameters for velocity step response initiating with a range greater than desired range.

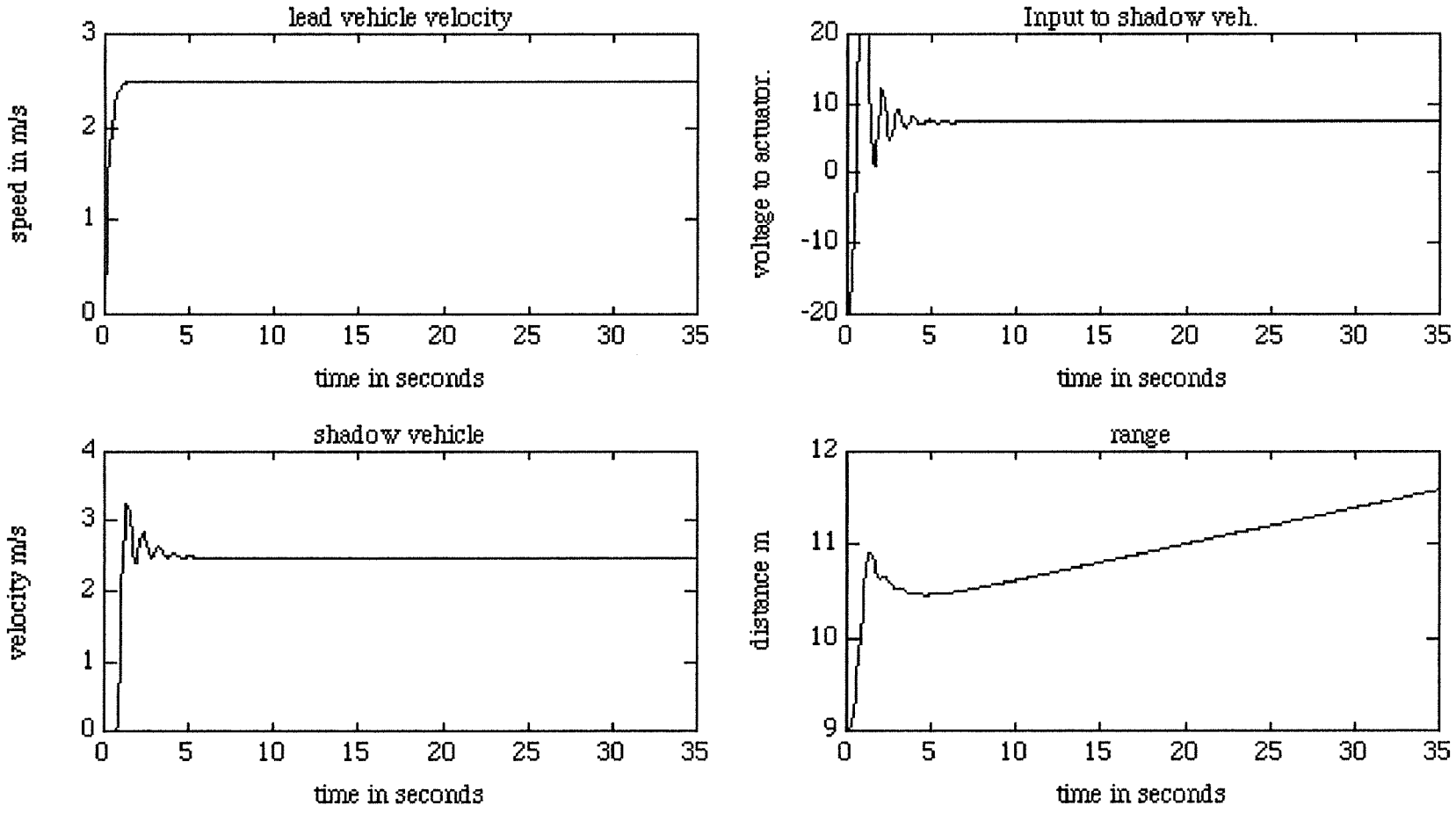

Figure 8.4.1. Velocity step response initiating with a range less than desired range

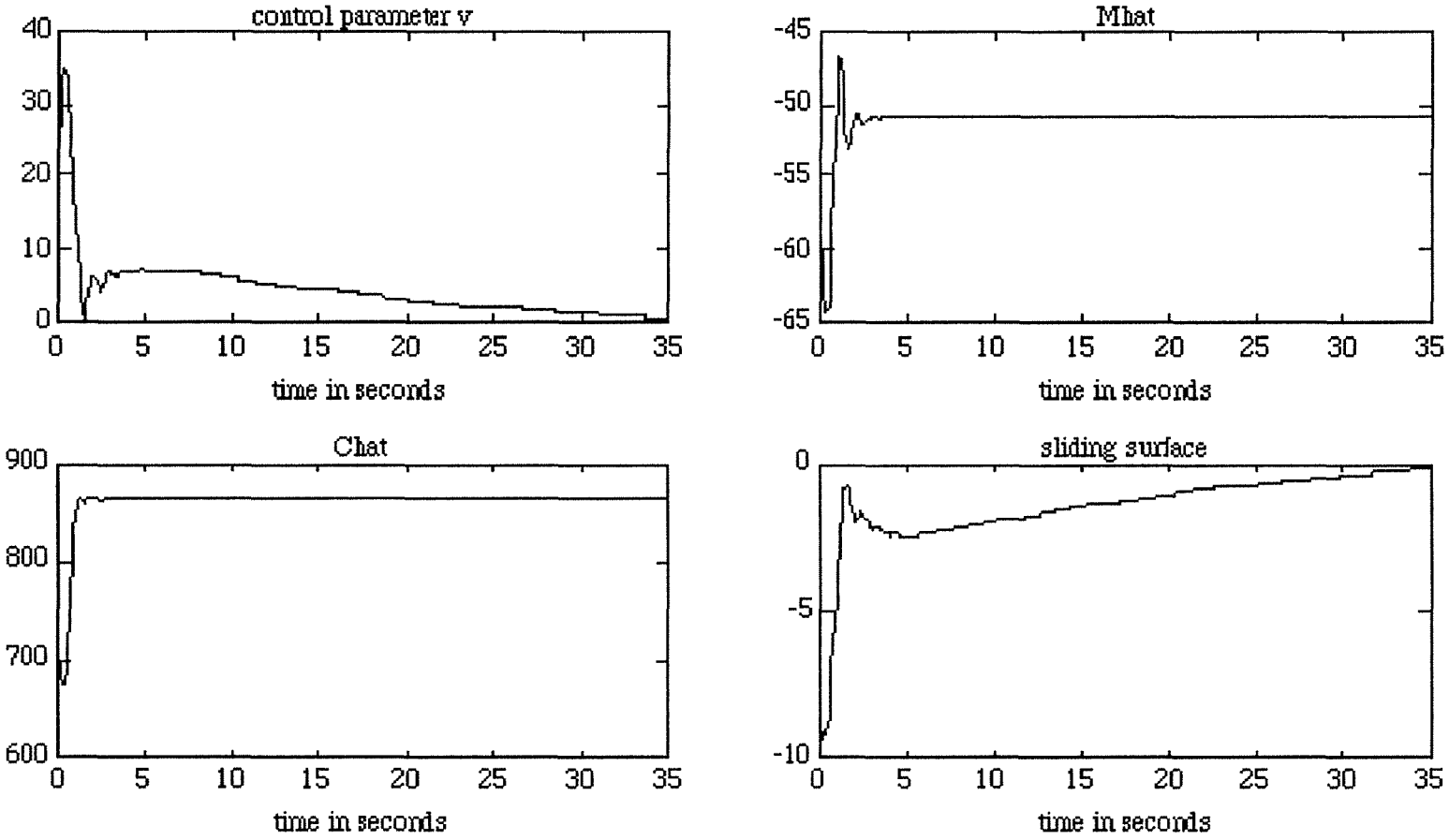

Figure 8.4.2. Control parameters for veloity step response initiating with a range less than desired range

9. LATERAL CONTROL DESIGN & SIMULATION

9.1 Objective

The objective of this research is to design and simulate a digital steering controller that will steer an Autonomous Shadow Vehicle such that it will track the reference of a Lead Vehicle to within ±1 foot for speeds up to 30 mph whether straight or curved.

9.2 Background

The researcher has demonstrated lateral control of a Chevrolet Celebrity Wagon at speeds up to 50 mph on an 1/4 mile track using vision as the reference sensor [102] and [111]. The controller design was based on a "sliding mode" control approach. The standard steering of the Chevrolet Celebrity Wagon was used, hence, backlash with a deadzone in the order of ±0.75 degrees was encountered. Others have reported steering controllers but usually have neglected the effect of steering backlash and sampling interval for implementation as a digital controller.

The approach of this lateral control research is to design a digital adaptive controller with a target sampling rate of 0.1 seconds. We estimate that the tracking systems can provide lateral displacement and yaw angle in 0.1 second.

9.3 Derivation

The approach chosen for this research is to persuade the closed-loop response to approximate that of a desired response by adapting controller parameters. We begin by representing the desired system in block diagram form as

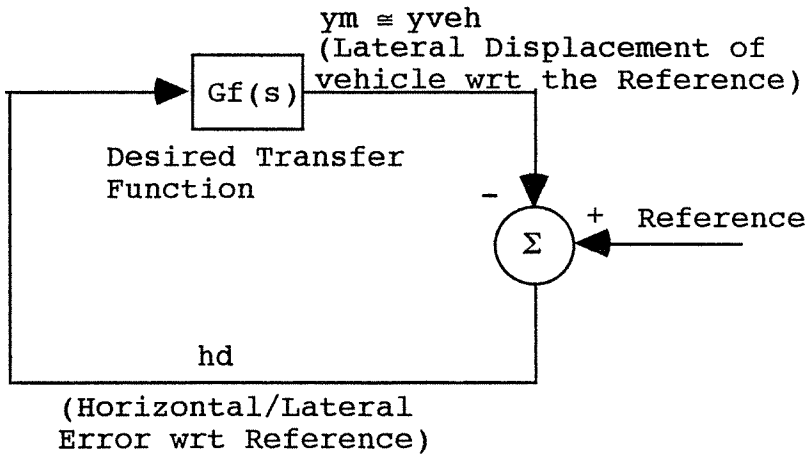

Hence,

$$\frac{ym(s)}{Reference(s)} = \frac{Gf(s)}{1 + Gf(s)} = Gcl(s) \tag{9.1}$$

and

$$ym(s) = Gf(s)*hd(s). \tag{9.2}$$

Since we desire curve tracking, we will require the steady-state error for a parabolic input to be zero. We select the desired transfer function

$$Gf(s) = \frac{Nf(s)}{s^3} \tag{9.3}$$

where Nf(s) is a polynomial in s, the Laplace variable. For convenience we will drop the function in s notation. Furthermore, we require that Gf be strictly proper. This restriction leads us to specify

$$Nf = K(a_2 s^2 + a_1 s + 1). \tag{9.4}$$

The closed-loop transfer function Gcl is then

$$Gcl = \frac{\frac{Nf}{s^3}}{1 + \frac{Nf}{s^3}} \tag{9.5a}$$

$$= \frac{Nf}{s^3 + Nf} \tag{9.5b}$$

$$= \frac{Nf = K(a_2 s^2 + a_1 s + 1)}{s^3 + Ka_2 s^2 + Ka_1 s + K}. \tag{9.5c}$$

Next, we select three negative real poles for Gcl. That is, we desire the denominator to be of the form

$$(s + \omega cl)^3 = s^3 + 3\omega cl\, s^2 + 3\, \omega cl^2\, s + \omega cl^3 \tag{9.6}$$

for three poles at $-\omega c1$. Comparing the coefficients of the denominator of (9.5c) with those of (9.6) we find

$$K = \omega c1^3, \tag{9.7}$$

$$a_2 = \frac{3}{\omega c1^2} \tag{9.10}$$

and

$$a_1 = \frac{3}{\omega c1}. \tag{9.11}$$

The desired closed-loop transfer function is

$$Gcl = \frac{\omega c1^3 \left(\frac{3}{\omega c1^2} s^2 + \frac{3}{\omega c1} s + 1\right)}{s^3 + \frac{3}{\omega c1^2} s^2 + \frac{3}{\omega c1} s + 1} \tag{9.12}$$

and the desired forward path transfer function is

$$Gf = \frac{\omega c1^3 \left(\frac{3}{\omega c1^2} s^2 + \frac{3}{\omega c1} s + 1\right)}{s^3}. \tag{9.13}$$

We approximate the vehicle dynamics as [97]:

$$\dot{X} = Aveh * X + B * U \tag{9.14}$$

where

$$Aveh = \begin{bmatrix} -2\frac{c(L1^2 + L2^2)}{V * I} & 0 & 2\frac{c(L1 - L2)}{V * I} & 0 \\ 1 & 0 & 0 & 0 \\ \left(2\frac{c(L1 - L2)}{V * M} - V\right) & 0 & -4\frac{c}{V * M} & 0 \\ 0 & V & 1 & 0 \end{bmatrix}, \tag{9.15}$$

$$Bveh = \begin{bmatrix} 2\frac{c * L1}{I} & 0 & 0 \\ 0 & 0 & -1 \\ 2\frac{c}{M} & \frac{1}{M} & 0 \\ 0 & 0 & 0 \end{bmatrix}, \tag{9.16}$$

and c is the tire cornering coefficient, V is the vehicle speed, M is the vehicle mass, I is the vehicle yaw inertia, L1 is the front-wheel position relative to the cg of the vehicle, and L2 is the rear-wheel position relative to the cg of the vehicle.

The state variables are

x1 = yaw angle rate of the vehicle
x2 = yaw angle of vehicle between the vehicle & the reference
x3 = lateral acceleration of vehicle
x4 = lateral displacement of vehicle with respect to reference

and the inputs are

u1 = front-wheel steering angle
u2 = lateral wind disturbance
u3 = yaw angle rate between vehicle and road

The output equation is selected to be

$$y = \begin{bmatrix} 0 & 0 & 0 & 1 \\ 0 & 1 & 0 & 0 \end{bmatrix} X \tag{9.17}$$

where

y1 = lateral displacement of vehicle with respect to reference
y2 = yaw angle of vehicle between the vehicle & the reference

Using symbolic manipulation application software, MAPLE, a vehicle transfer function

$$Gveh = \frac{hd}{\delta com}, \tag{9.18}$$

was obtained as

$$Gveh = \frac{(\frac{2c}{M})(s^2 + \frac{a_1}{VI}s + \frac{6cL1}{I})}{s^2(s^2 + (\frac{2cL2^2}{I} + \frac{4c}{M} + \frac{2cL1^2}{I})s + (\frac{2cL1}{I} - \frac{2cL2}{I} + \frac{4c^2L1^2 + 8c^2L1L2 + 4c^2L2^2}{V^2IM}))} . \tag{9.19}$$

Combining constants in (9.19) we define Gveh as

$$Gveh = \frac{kveh(s^2 + \frac{a1veh}{V}s + a0veh)}{s^2(s^2 + (2kveh + \frac{b1veh}{V})s + \frac{b0veh}{V^2})} . \tag{9.20}$$

The poles and zeros of (9.19) were examined as the parameters in (9.19) were varied for vehicles of 10000 to 25000 lbs in weight. Neglecting poles and zeros whose real parts are less than -5(assuming a time constant of 2 sample intervals = 0.2, pole = -1/0.2 = -5) we approximate (9.20) as

$$Gveh \cong \frac{kveh(s + a0veh * V)}{s^2(s + \frac{b0veh}{V^2})} \qquad (9.21)$$

where kveh, a0veh, and b0veh are adapted. It may be more accurate to state that kveh is "gain scheduled" as a function of velocity and vehicle mass.

A block diagram of the proposed lateral guidance digital control system is drawn in Figure 9.1. A high pass/lead transfer function

$$\frac{Steer2}{Steer1} = Gdamp \qquad (9.22a)$$

$$= \frac{kdamp\ s^4}{(s^2 + 4\omega d2s + \omega d2^2)^2} \qquad (9.22b)$$

was added to assist in damping the yaw oscillation of the controlled vehicle at speeds of 20 to 30 mph. The 0.1 second delay introduced by the digital control system is the main cause of the yaw oscillation. Steering backlash was also added. The backlash deadzone is adjustable, however, a ±0.5 degree deadzone was used for all simulation runs.

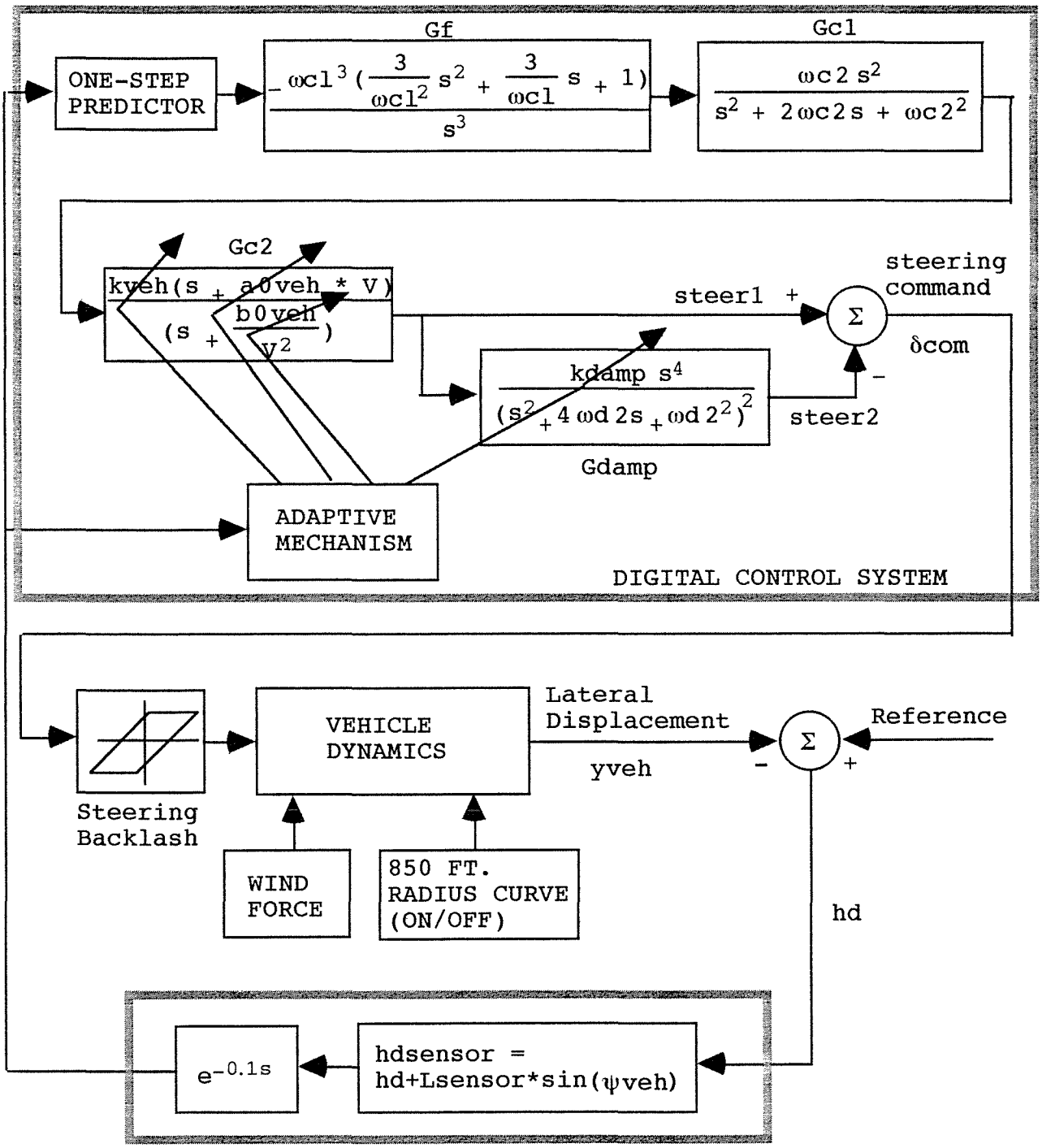

Figure 9.1. Block Diagram of Steering Digital Control System

9.4 Adaptation Rule

Update rules for a0veh and b0veh are presented in this section. The objective is to find update rules that adjust these parameters in a stable manner. The following derivations of the update rules are based on a modified MIT adaptation rule [114].

We begin by defining

$$\text{hd(lateral error wrt reference)} = \text{Reference} - \text{yveh}, \tag{9.23}$$

$$\text{Gc} = \text{Gf}*\text{Gc1}, \tag{9.24}$$

$$\text{Gveh} = \frac{\text{Nveh}}{\text{Dveh}}, \tag{9.25}$$

and

$$\text{Gc2} = \frac{\text{Dveh}}{\text{Nveh}}. \tag{9.26}$$

Gdamp will be ignored in the derivation of the update rules. Also, we assume that the vehicle speed can be considered constant over 0.1 seconds. We use a gradient approach to find an estimate of the change of the parameter of interest. That is, we want to update the parameters such that the lateral error is driven to a minimum. This motivates us to write

$$\frac{\partial \text{hd}}{\partial \text{a0veh}} = \frac{\partial(\text{Reference} - \text{Gc} * \text{Gc2} * \text{Gveh} * \text{hd})}{\partial \text{a0veh}} \tag{9.27a}$$

$$= -\text{Gc}\left(\frac{-2\,\text{kveh} * \text{V} * \text{Dveh}}{\text{Nveh}^2}\right)\left(\frac{\text{Nveh}}{\text{Dveh}}\right)\text{hd} \tag{9.27b}$$

$$= 2\,\text{V}\left(\frac{\text{Gc}}{\text{Nveh}}\right)\text{hd}. \tag{9.27c}$$

The estimated rate of change of a0veh with respect to time such that hd is driven to be minimum is

$$\frac{\text{d(a0veh)}}{\text{dt}} \cong -\text{adaptrate} * \left[\frac{\text{hd}\left(\frac{\partial \text{hd}}{\partial \text{a0veh}}\right)}{\alpha + \left(\frac{\partial \text{hd}}{\partial \text{a0veh}}\right)^2}\right]_{\text{Limited to} \pm \beta} \tag{9.28}$$

where adaptrate, α and β are constants greater than zero. α is used to prevent the denominator of (9.28) from becoming too small.

The update of a0veh is then

$$a0veh(k*T) = a0veh((k-1)*T + \frac{d(a0veh)}{dt} * T \qquad (9.29)$$

where k is an integer that represents the sample number and T is the sample interval.

The derivation of the update rule for b0veh follows the above procedure. We write

$$\frac{\partial hd}{\partial b0veh} = \frac{\partial(Reference - Gc * Gc2 * Gveh * hd)}{\partial b0veh} \qquad (9.30a)$$

$$= -Gc\left(\frac{kveh\left(\frac{1}{V^2}\right)}{Nveh}\right)\left(\frac{Nveh}{Dveh}\right)hd \qquad (9.30b)$$

$$= -Gc\left(\frac{kveh\left(\frac{1}{V^2}\right)}{Dveh}\right)hd \qquad (9.30c)$$

The estimated rate of change of b0veh with respect to time such that hd is driven to be minimum is

$$\frac{d(b0veh)}{dt} \cong -adaptrate * \left[\frac{hd\left(\frac{\partial hd}{\partial b0veh}\right)}{\alpha + \left(\frac{\partial hd}{\partial b0veh}\right)^2}\right] \text{ Limited to } \pm\beta \qquad (9.31)$$

where adaptrate, α and β are constants greater than zero. α is used to prevent the denominator of (9.28) from becoming too small.

The update of b0veh is then

$$b0veh(k*T) = b0veh((k-1)*T + \frac{d(b0veh)}{dt} * T \qquad (9.32)$$

where k is an integer that represents the sample number and T is the sample interval.

The gain kveh is a function of vehicle speed and vehicle mass. kdamp is a function of vehicle mass.

9.5 Continuous Transform to Discrete Transform Mapping & Simulation

Simulations were performed for a 25,000 lb and a 10,000 lb vehicle for vehicle speeds of 0 to 30 mph. An 850 foot radius curve can be applied at a time specified by the user. Following is a screen print out of the simulation options used most frequently:

Vehicle Weight(lbs) = 25000

Initial Vehicle Speed (ft/sec) = 0

Vehicle Accel. (ft/s^2) = 4

Max Vehicle Speed (ft/sec) = 44

Lateral Displacement(feet) = 2

Wind Disturbance(lbs) = 100

Backlash Deadzone(degrees) = 0.5

Time at which to Switch to Curve(sec) = 60

The position of the sensor, Lsensor, was set at 6 feet forward of the cg of the vehicle. Lsensor was not varied since yaw of an Autonomous Shadow Vehicle relative to a Lead Vehicle is known. However, it was noticed that yaw angle is important to the stability of the system and that having the sensor 6 feet forward of the cg contributed to increased stability of the system. Jürgen Ackermann [112] has shown that the vehicle yaw mode can be decoupled from its lateral mode by using yaw rate feedback.

The continuous transfer functions in Figure 9.1 were converted to pulse transfer functions in z using the bilinear transform approach. Discrete equations were then obtained from the pulse transfer functions. Other transformations were used such as the Boxer-Thaler continuous to discrete transform. However, it was

found that the bilinear transform was more stable than the other transforms [113]. The vehicle state equation was integrated using fourth order Runge-Kutta integration with a step size of 0.005 seconds.

9.6 Simulation Results

The simulation results indicate that a sampling rate for the digital control system of 0.1 seconds is adequate for speeds up to 30 mph for 10,000 to 20,000 lb vehicles. The conditions under which a simulation run was made are listed on the plots for that run. Straight freeway road sections are "feathered" into curves. The simulation assumes an abrupt encounter between straight and curved reference sections. Hence, the simulation provides a worst case scenario.

Runs were made using constant vehicle velocities and vehicle velocities that ramped-up at 4 ft/sec^2. Wind loads of 100 and 500 lbs were used. The wind effects were small as expected due to the heavy vehicles simulated. Yaw inertia was also significantly changed, but has little effect and was therefore kept at a constant.

A steering backlash deadzone of ±0.5 degrees results in a continuous oscillation of the steering wheel in the order of 1 cycle/sec. However, the vehicle with backlash follows in an average sense the vehicle path generated using a deadzone of zero degrees(no backlash). The figures, Figures 9.2 through 9.12, were selected as representative. The following table summarizes the conditions selected for the simulation runs:

FIGURE	WEIGHT	SPEED	WIND	BACKLASH DEADZONE
9.2	25,000	1.22 m/s, 0 m/s^2	0	0.5
9.3	25,000	3.66 m/s, 0 m/s^2	0	0.5
9.4	25,000	0-3.66 m/s, 1.22 m/s^2	0	0.5
9.5	25,000	0-6.71 m/s, 1.22 m/s^2	0	0
9.6	10,000	13.41 m/s, 0 m/s^2	0	0.5
9.7	25,000	0-6.71 m/s, 1.22 m/s^2	0	0.5
9.8	25,000	1.22 m/s, 0 m/s^2	0	0.5
9.9	25,000	6.1 m/s, 0 m/s^2	0	0.5
9.10	25,000	0-13.41 m/s, 1.22 m/s^2	0	0.5
9.11	25,000	6.1 m/s, 0 m/s^2	100	0.5
9.12	25,000	6.1 m/s, 0 m/s^2	500	0.5

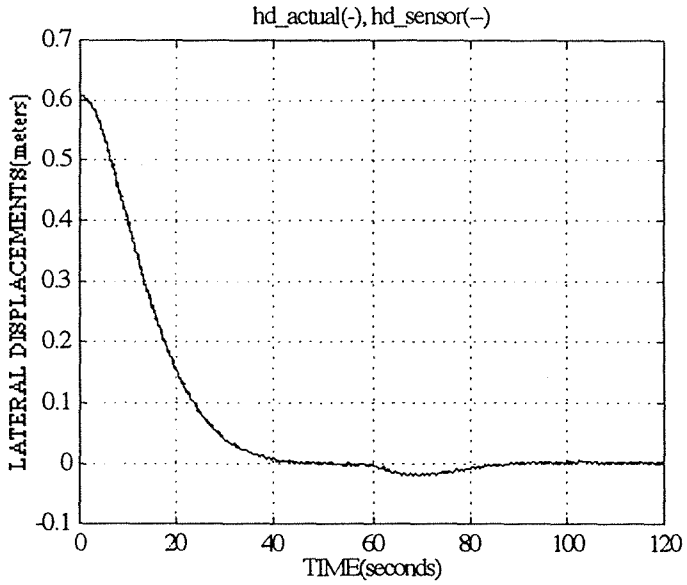

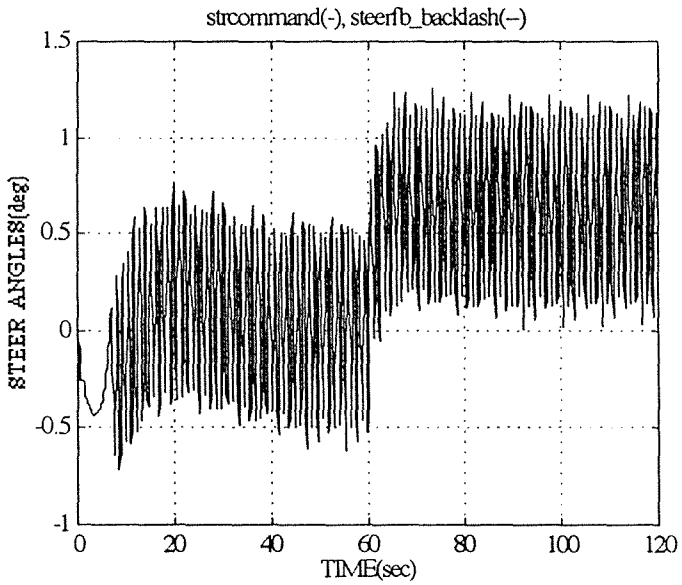

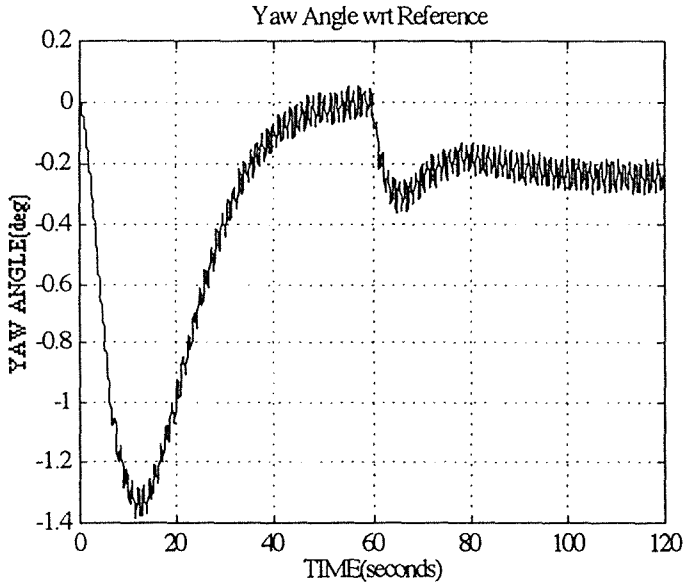

Date(month/day/year): 8/5/1994
Start Curve at 60 sec, radius = 259.1 m
Sample Interval, dt = 0.1 sec
Vehicle Accel.= 0.00 m/sec^2
Speed: start= 1.219 m/sec, end= 1.219 m/sec
Deadzone=+/- 0.5 deg, Wind=0.0 kg
Wt.= 11339.81 kg, Inertia= 69.13 kg-m-sec^2
c=1208 kg/rad, L1=1.448 m, L2=1.448 m
Loc. sensor from CG= 1.829 m
Steer comd. limit= 6 deg, Learn Rate= 0.5
kvehinv: ic= 7, end= 7
a0veh: ic= 0.15, end= 0.1224
b0veh: ic= 6.857, end= 18.1
kdamp= 0.3, wdamp= 0.005 rad, tauc= 5

Fig. 9.2. Simulation Run: Straight to Curved Reference
Weight: 25,000 lb
Speed : 1.22 m/s, 0 m/s^2
Wind : 0 lb
Backlash Deadzone: 0.5 deg

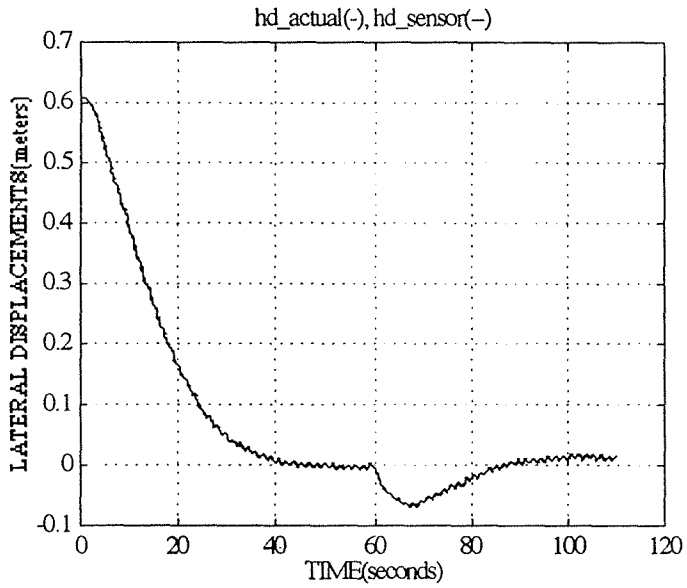

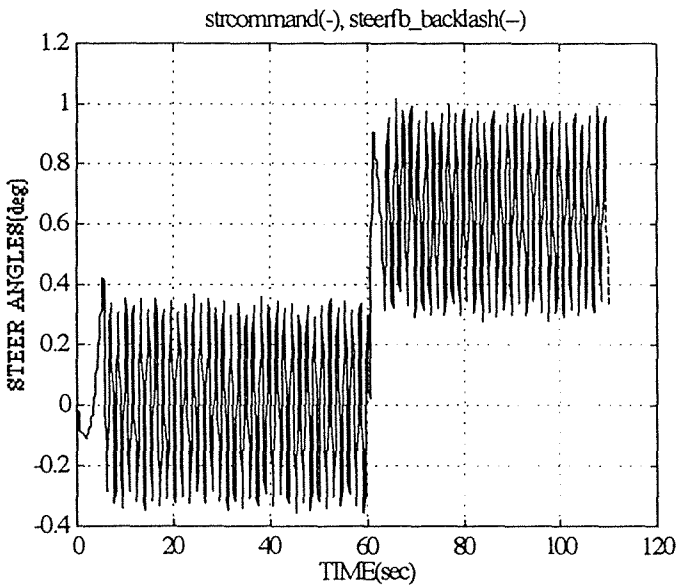

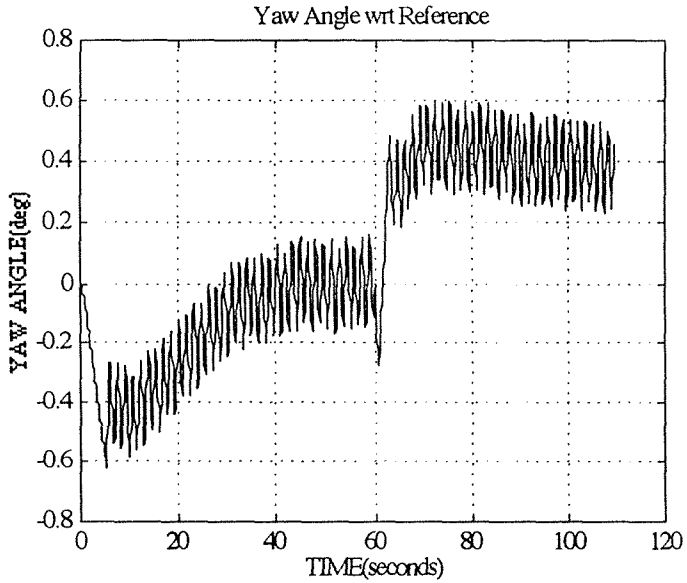

Date(month/day/year): 8/5/1994
Start Curve at 60 sec, radius = 259.1 m
Sample Interval, dt = 0.1 sec
Vehicle Accel.= 0.00 m/sec^2
Speed: start= 3.658 m/sec, end 3.658 m/sec
Deadzone=+/- 0.5 deg, Wind=0.0 kg
Wt.= 11339.81 kg, Inertia= 69.13 kg-m-sec^2
c=1208 kg/rad, L1=1.448 m, L2=1.448 m
Loc. sensor from CG= 1.829 m
Steer comd. limit= 6 deg, Learn Rate= 0.5
kvehinv: ic= 2, end 2
a0veh: ic= 0.15, end 0.1238
b0veh: ic= 6.857, end 18.1
kdamp= 0.3, wdamp= 0.005 rad, tauc= 5

Fig. 9.3. Simulation Run: Straight to Curved Reference
Weight: 25,000 lb
Speed : 3.66 m/s, 0 m/s^2
Wind : 0 lb
Backlash Deadzone: 0.5 deg

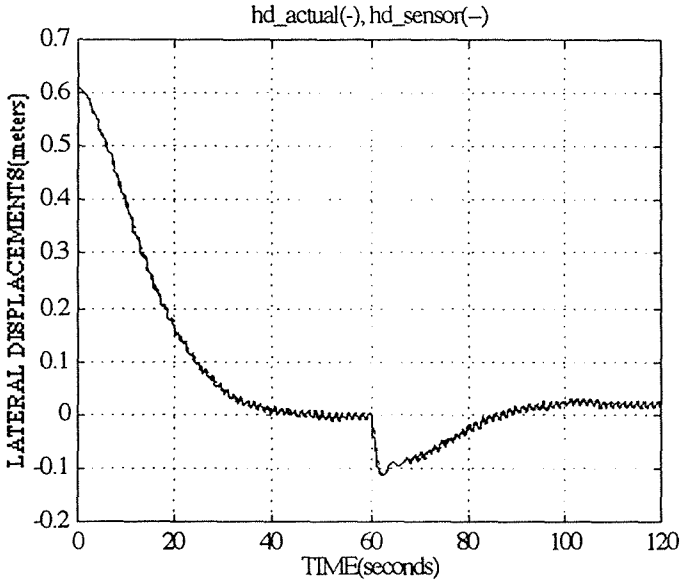

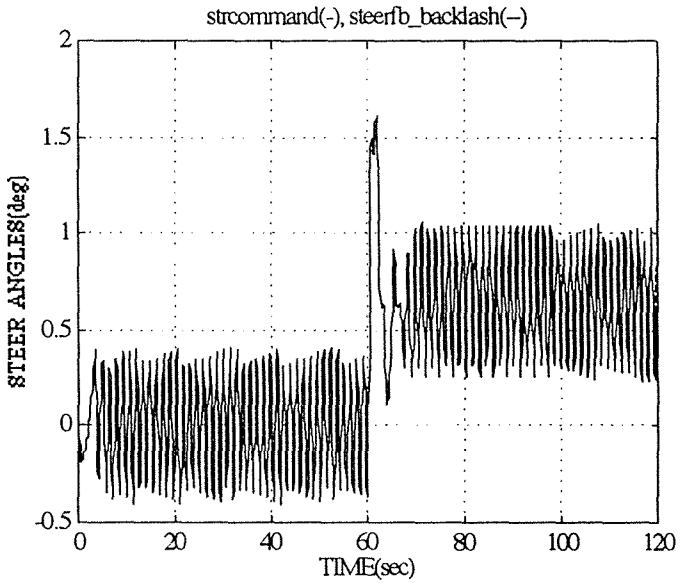

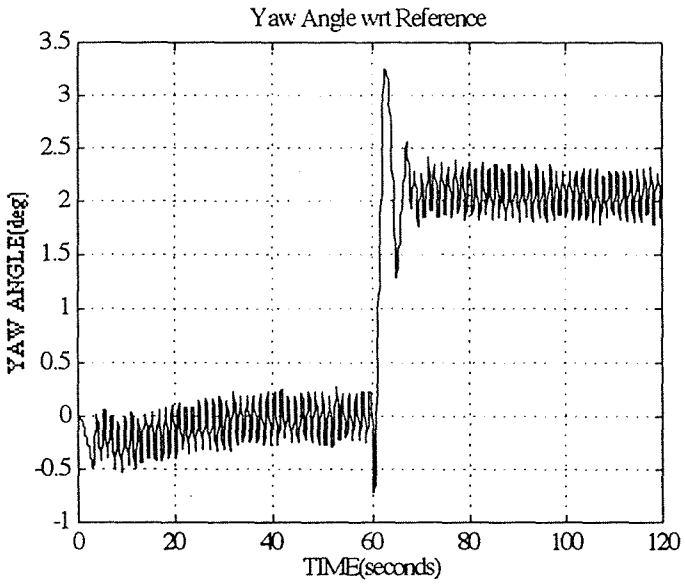

Fig. 9.4. Simulation Run: Straight to Curved Reference
Weight: 25,000 lb
Speed : 0 to 6.71 m/s, 1.22 m/s2
Wind : 0 lb
Backlash Deadzone: 0.5 deg

Date(month/day/year): 8/6/1994
Start Curve at 60 sec, radius = 259.1 m
Sample Interval, dt = 0.1 sec
Vehicle Accel.= 1.22 m/sec^2
Speed: start= 0 m/sec, end 6.706 m/sec
Deadzone=+/- 0.5 deg, Wind=0.0 kg
Wt.= 11339.81 kg, Inertia= 69.13 kg-m-sec^2
c=1208 kg/rad, L1=1.448 m, L2=1.448 m
Loc. sensor from CG= 1.829 m
Steer comd. limit= 6 deg, Learn Rate= 0.5
kvehinv: ic= 10.88, end 1.325
a0veh: ic= 0.15, end 0.1263
b0veh: ic= 6.857, end 18.1
kdamp= 0.3, wdamp= 0.005 rad, tauc= 5

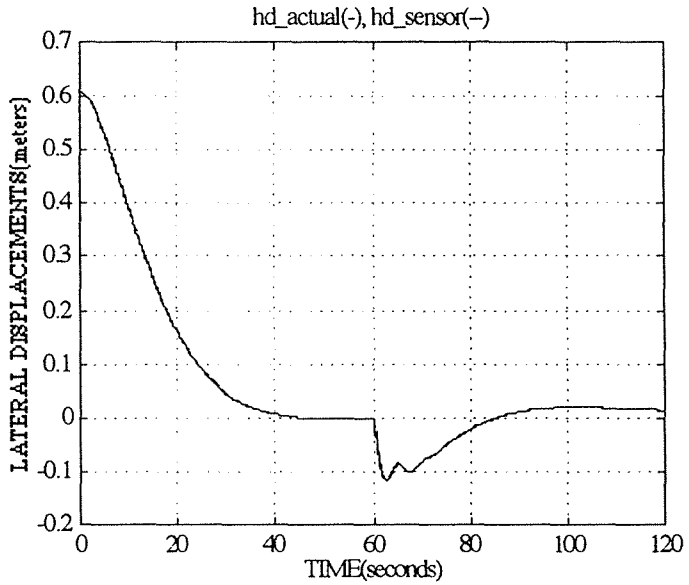

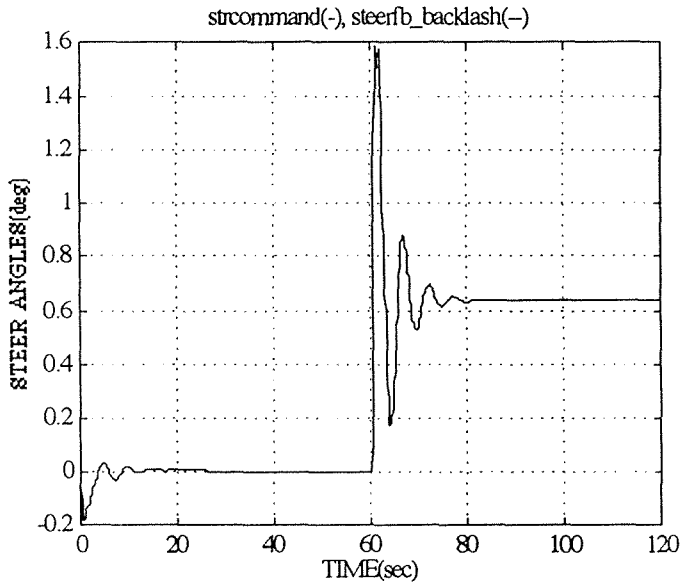

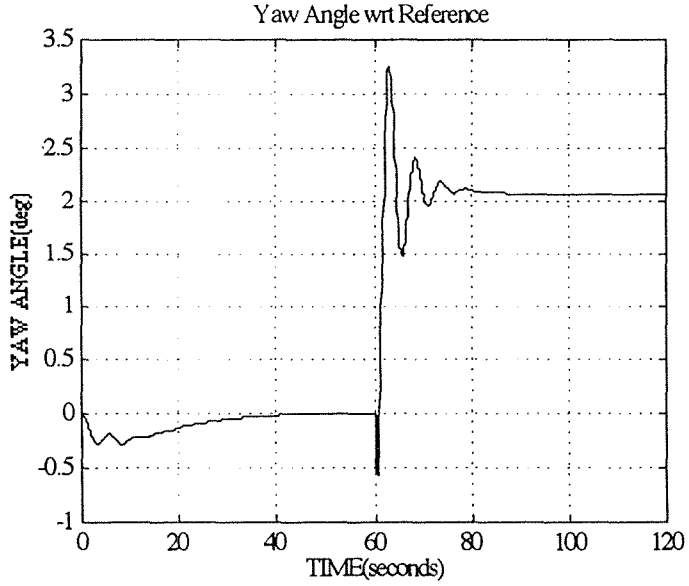

Date(month/day/year): 8/6/1994
Start Curve at 60 sec, radius = 259.1 m
Sample Interval, dt = 0.1 sec
Vehicle Accel.= 1.22 m/sec^2
Speed: start= 0 m/sec, end 6.706 m/sec
Deadzone=+/- 0.0 deg, Wind=0.0 kg
Wt.= 11339.81 kg, Inertia= 69.13 kg-m-sec^2
c=1208 kg/rad, L1=1.448 m, L2=1.448 m
Loc. sensor from CG= 1.829 m
Steer comd. limit= 6 deg, Learn Rate= 0.5
kvehinv: ic= 10.88, end 1.325
a0veh: ic= 0.15, end 0.1174
b0veh: ic= 6.857, end 18.1
kdamp= 0.3, wdamp= 0.005 rad, tauc= 5

Fig. 9.5. Simulation Run: Straight to Curved Reference
Weight: 25,000 lb
Speed : 0 to 6.71 m/s, 1.22 m/s^2
Wind : 0 lb
Backlash Deadzone: 0 deg

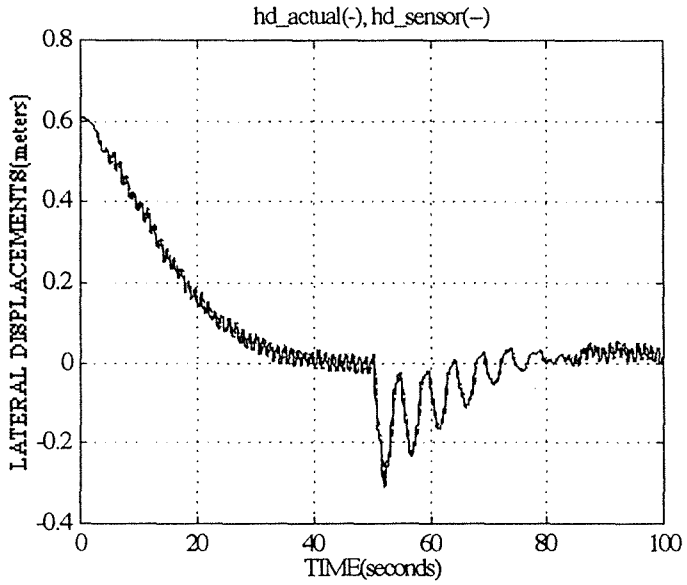

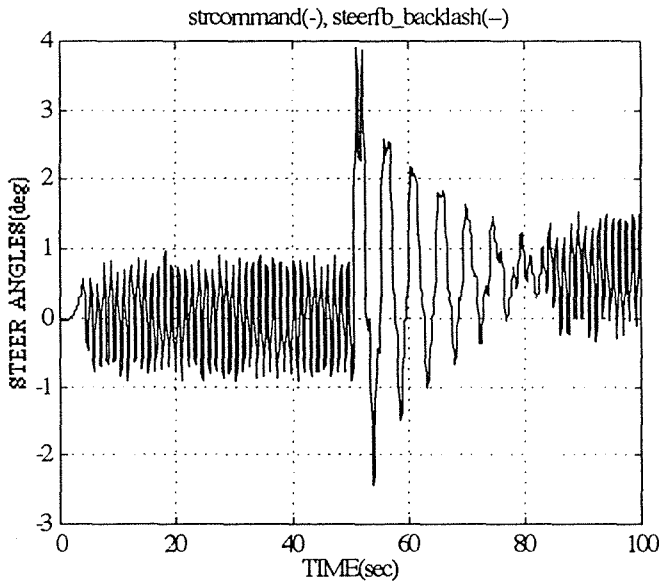

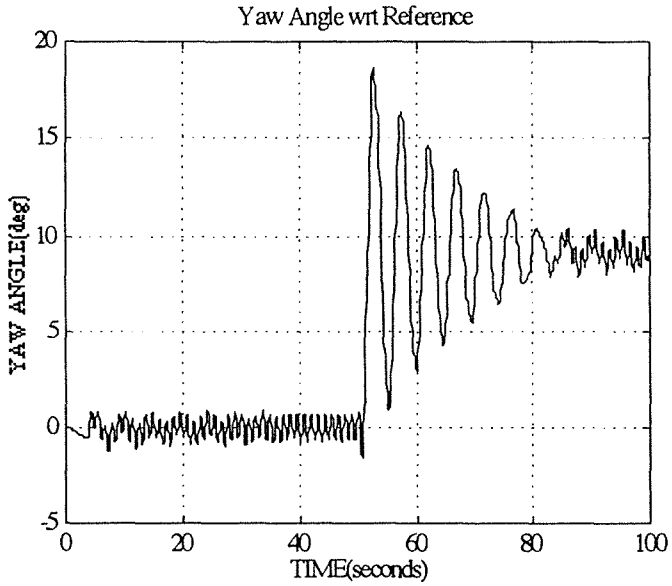

Date(month/day/year): 8/5/1994
Start Curve at 50 sec, radius = 259.1 m
Sample Interval, dt = 0.1 sec
Vehicle Accel.= 0.00 m/sec^2
Speed: start= 13.41 m/sec, end= 13.41 m/sec
Deadzone=+/- 0.5 deg, Wind=0.0 kg
Wt.= 11339.81 kg, Inertia= 69.13 kg-m-sec^2
c=1208 kg/rad, L1=1.448 m, L2=1.448 m
Loc. sensor from CG= 1.829 m
Steer comd. limit= 6 deg, Learn Rate= 0.5
kvehinv: ic= 1, end= 1
a0veh: ic= 0.15, end= 0.1309
b0veh: ic= 6.857, end= 18.1
kdamp= 0.3, wdamp= 0.005 rad, tauc= 5

Fig. 9.6. Simulation Run: Straight to Curved Reference
Weight: 25,000 lb
Speed : 13.41 m/s, 0 m/s^2
Wind : 0 lb
Backlash Deadzone: 0.5 deg

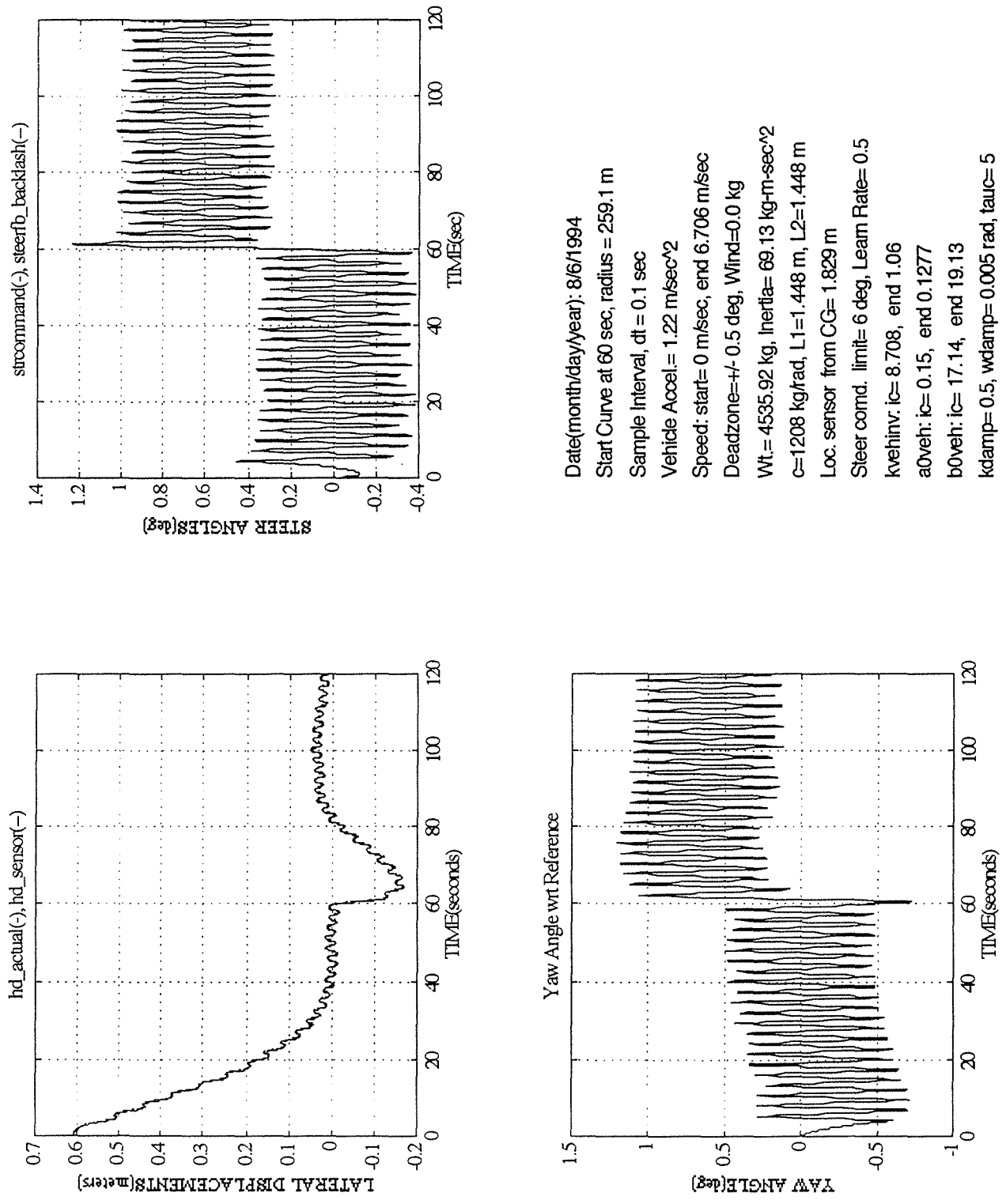

Fig. 9.7. Simulation Run: Straight to Curved Reference
Weight: 10,000 lb
Speed : 0 to 6.71 m/s, 1.22 m/s^2
Wind : 0 lb
Backlash Deadzone: 0.5 deg

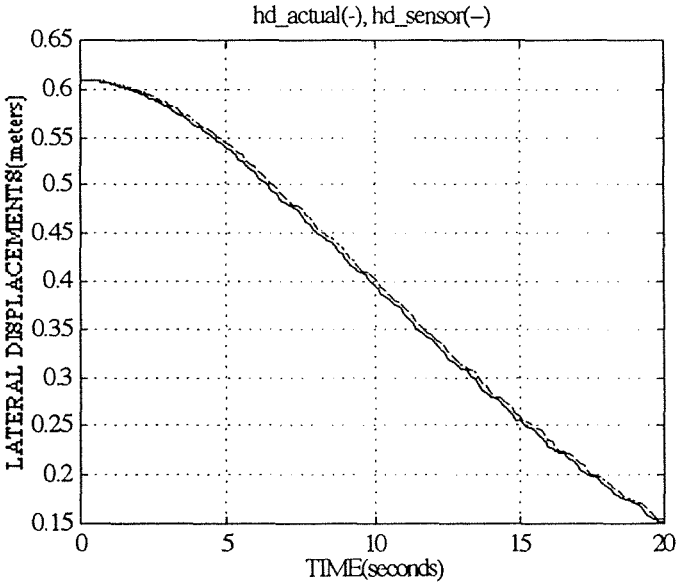

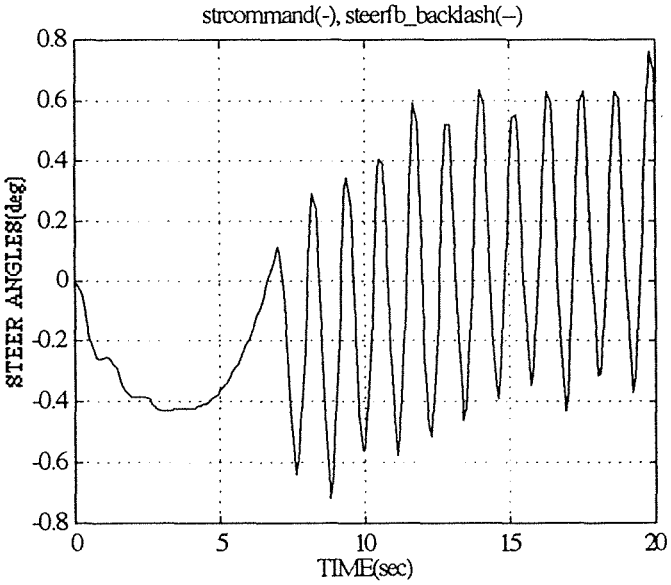

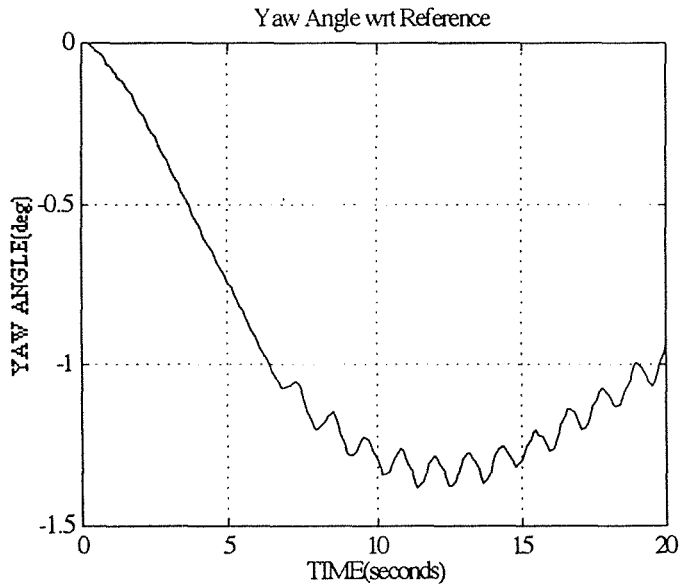

Date(month/day/year): 8/5/1994
No Curve
Sample Interval, dt = 0.1 sec
Vehicle Accel.= 0.00 m/sec^2
Speed: start= 1.219 m/sec, end 1.219 m/sec
Deadzone=+/- 0.5 deg, Wind=0.0 kg
Wt.= 11339.81 kg, Inertia= 69.13 kg-m-sec^2
c=1208 kg/rad, L1=1.448 m, L2=1.448 m
Loc. sensor from CG= 1.829 m
Steer comd. limit= 6 deg, Learn Rate= 0.5
kvehinv: ic= 7, end 7
a0veh: ic= 0.15, end 0.1177
b0veh: ic= 6.857, end 18.1
kdamp= 0.3, wdamp= 0.005 rad, tauc= 5

Fig. 9.8. Simulation Run: Straight Reference
Weight: 25,000 lb
Speed : 1.22 m/s, 0 m/s2
Wind : 0 lb
Backlash Deadzone: 0.5 deg

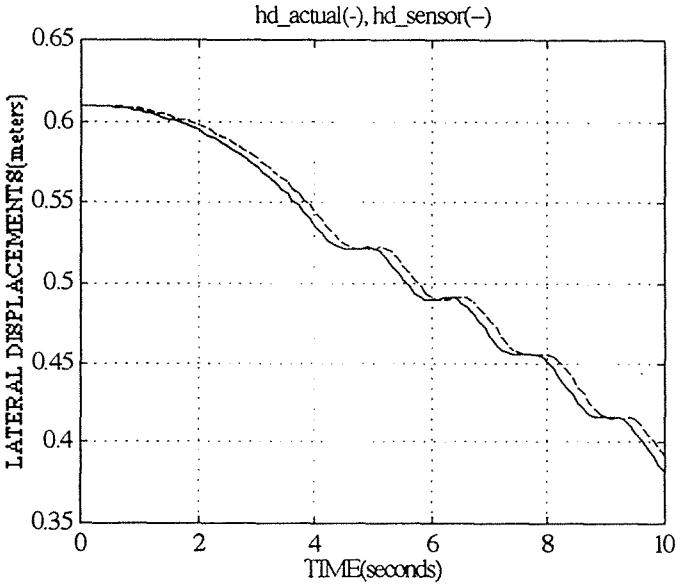

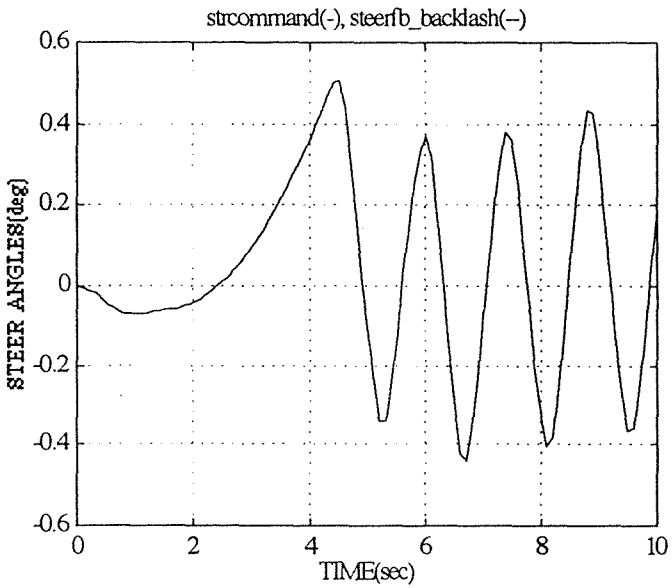

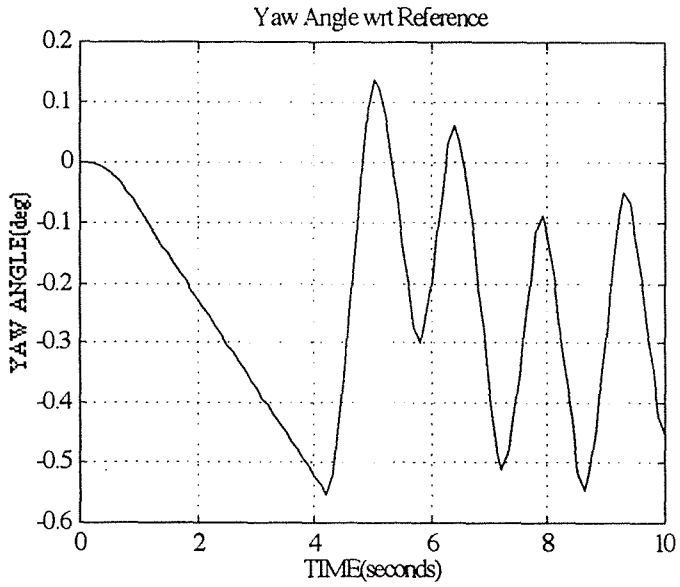

Fig. 9.9. Simulation Run: Straight Reference
Weight: 25,000 lb
Speed : 6.1 m/s, 0 m/s^2
Wind : 0 lb
Backlash Deadzone: 0.5 deg

Date(month/day/year): 8/5/1994
No Curve
Sample Interval, dt = 0.1 sec
Vehicle Accel.= 0.00 m/sec^2
Speed: start= 6.096 m/sec, end 6.096 m/sec
Deadzone=+/- 0.5 deg, Wind=0.0 kg
Wt.= 11339.81 kg, Inertia= 138.3 kg-m-sec^2
c=1208 kg/rad, L1=1.448 m, L2=1.448 m
Loc. sensor from CG= 1.829 m
Steer comd. limit= 6 deg, Learn Rate= 0.5
kvehinv: ic= 1.5, end 1.5
a0veh: ic= 0.15, end 0.1174
b0veh: ic= 6.857, end 18.11
kdamp= 0.3, wdamp= 0.005 rad, tauc= 5

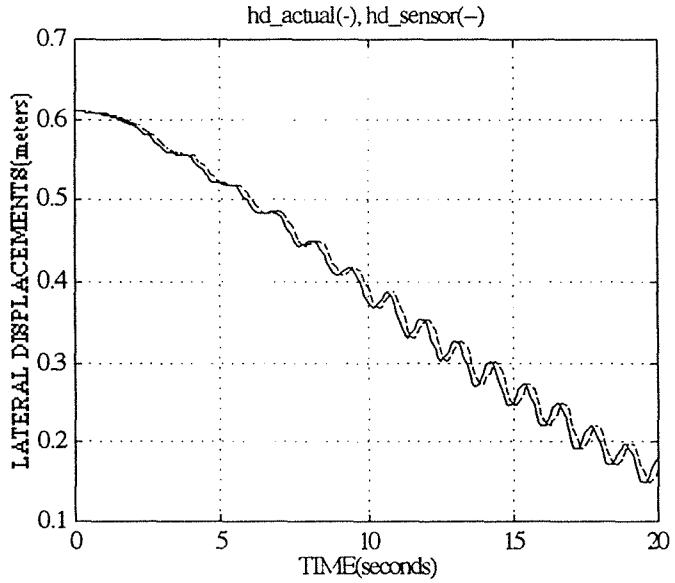

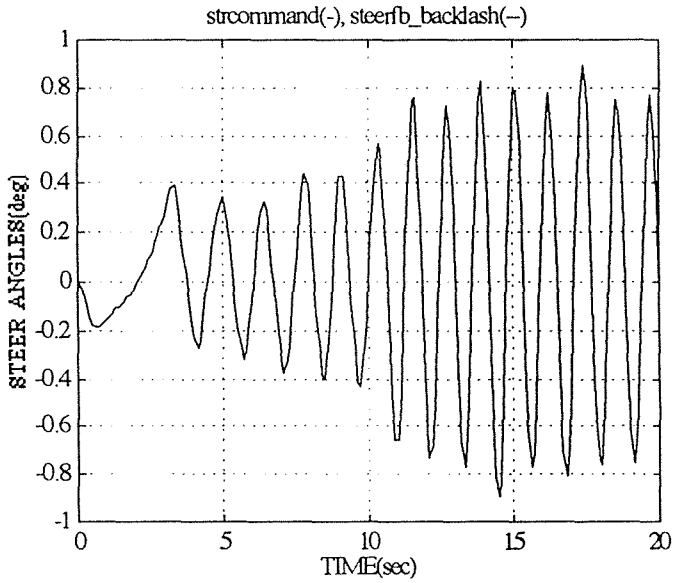

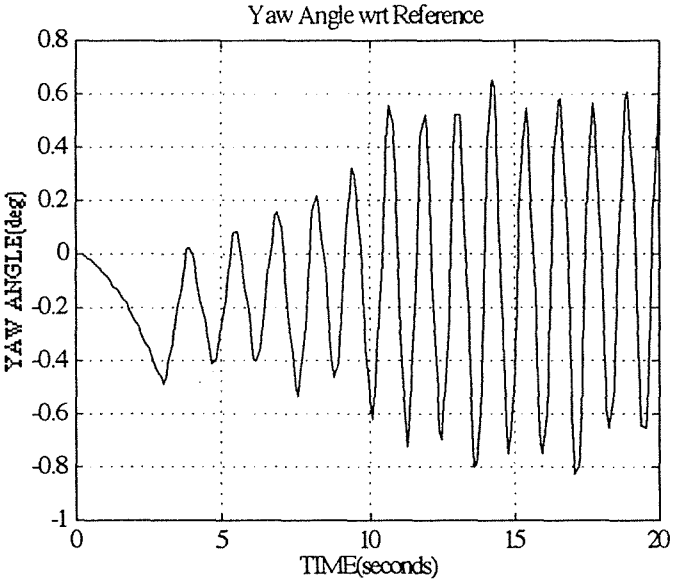

Date(month/day/year): 8/6/1994
No Curve
Sample Interval, dt = 0.1 sec
Vehicle Accel.= 1.22 m/sec^2
Speed: start= 0 m/sec, end 13.41 m/sec
Deadzone=+/- 0.5 deg, Wind=0.0 kg
Wt.= 11339.81 kg, Inertia= 69.13 kg-m-sec^2
c=1208 kg/rad, L1=1.448 m, L2=1.448 m
Loc. sensor from CG= 1.829 m
Steer comd. limit= 6 deg, Learn Rate= 0.5
kvehinv: ic= 10.88, end 1.001
a0veh: ic= 0.15, end 0.1176
b0veh: ic= 6.857, end 18.1
kdamp= 0.3, wdamp= 0.005 rad, tauc= 5

Fig. 9.10. Simulation Run: Straight Reference
Weight: 25,000 lb
Speed : 0 to 13.41 m/s, 1.22 m/s^2
Wind : 0 lb
Backlash Deadzone: 0.5 deg

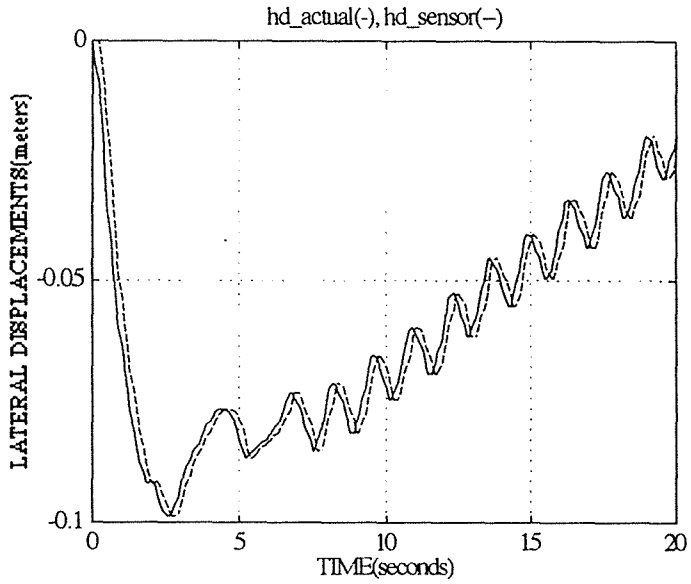

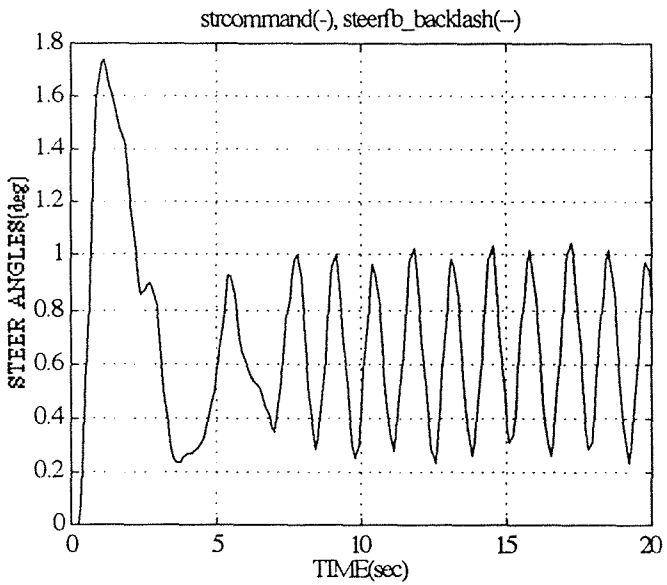

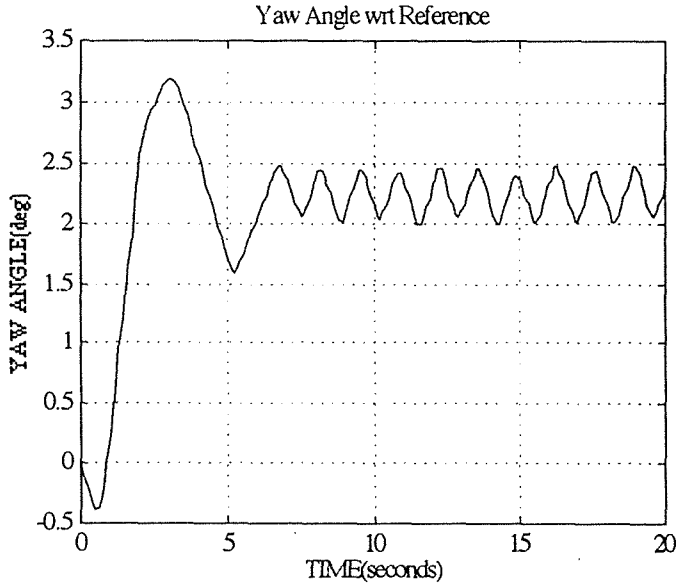

Fig. 9.11. Simulation Run: Straight Reference
Weight: 25,000 lb
Speed : 6.1 m/s, 0 m/s^2
Wind : 100 lb
Backlash Deadzone: 0.5 deg

Date(month/day/year): 8/5/1994
Start Curve at 0 sec, radius = 259.1 m
Sample Interval, dt = 0.1 sec
Vehicle Accel.= 0.00 m/sec^2
Speed: start= 6.096 m/sec, end 6.096 m/sec
Deadzone=+/- 0.5 deg, Wind=-45.4 kg
Wt.= 11339.81 kg, Inertia= 69.13 kg-m-sec^2
c=1208 kg/rad, L1=1.448 m, L2=1.448 m
Loc. sensor from CG= 1.829 m
Steer comd. limit= 6 deg, Learn Rate= 0.5
kvehinv: ic= 1.5, end 1.5
a0veh: ic= 0.15, end 0.1156
b0veh: ic= 6.857, end 18.11
kdamp= 0.3, wdamp= 0.005 rad, tauc= 5

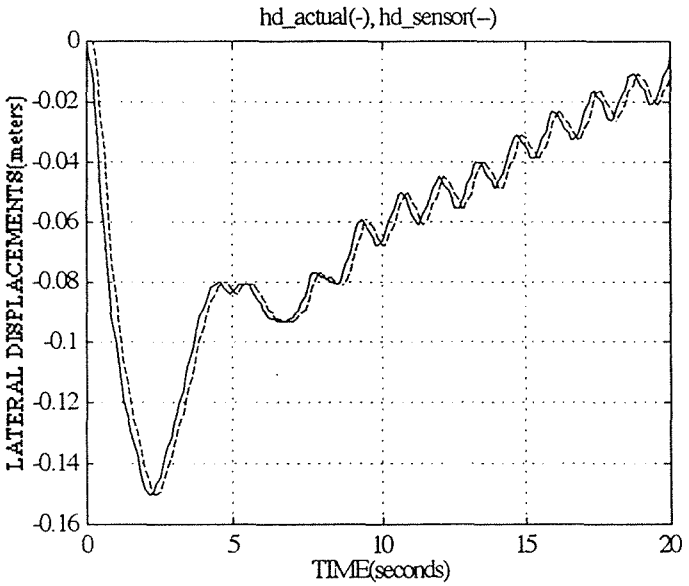

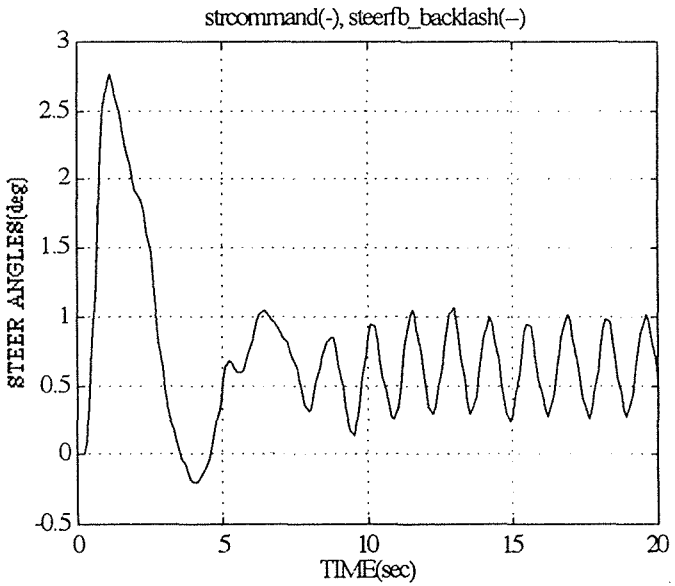

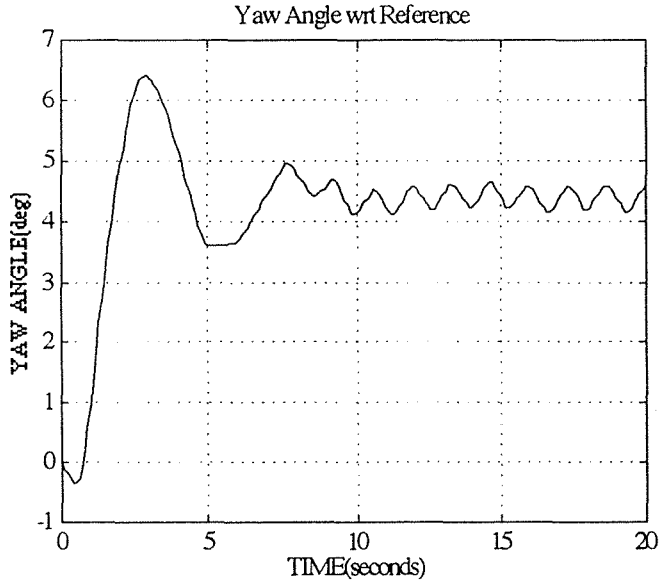

Fig. 9.12. Simulation Run: Straight Reference
Weight: 25,000 lb
Speed : 6.1 m/s, 0 m/s^2
Wind : 500 lb
Backlash Deadzone: 0.5 deg

Date(month/day/year): 8/5/1994
Start Curve at 0 sec, radius = 259.1 m
Sample Interval, dt = 0.1 sec
Vehicle Accel.= 0.00 m/sec^2
Speed: start= 6.096 m/sec, end 6.096 m/sec
Deadzone=+/- 0.5 deg, Wind=-226.8 kg
Wt.= 11339.81 kg, Inertia= 69.13 kg-m-sec^2
c=1208 kg/rad, L1=1.448 m, L2=1.448 m
Loc. sensor from CG= 1.829 m
Steer comd. limit= 6 deg, Learn Rate= 0.5
kvehinv: ic= 1.5, end 1.5
a0veh: ic= 0.15, end 0.1154
b0veh: ic= 6.857, end 18.11
kdamp= 0.3, wdamp= 0.005 rad, tauc= 5

10. CONCLUSION & RECOMMENDATIONS

The objectives of Phase I have been met. Following are recommendations and comments for implementation in subsequent phases of this research project:

1) Proceed with Phase II using the proposed Antenna, Vision, and Relative GPS Tracking Systems. The execution speed of the current 33 MHz 486 PC that was used for previous lateral guidance research may not be sufficient to handle vehicle speeds of 20 to 30 mph. Hence, feasibility tests of the proposed tracking systems may have to be run at lower vehicle speeds. Our target will be 15 mph with the current computing power available.

2) Early in Phase II, a weight for the Autonomous Shadow Vehicle needs to be determined. If it desired to tow the Autonomous Shadow Vehicle, the Autonomous Shadow Vehicle must be lighter than the vehicle towing it. Furthermore, the weight of the Autonomous Shadow Vehicle determines the tracking range required.

3) Accelerate the Autonomous Shadow Vehicle so that it maintains a line-of-sight range(40 feet for an 850 ft. radius curve) when the Lead Vehicle proceeds into a curve.

4) Integrate curve preview into the lateral guidance control system and add yaw rate damping using a rate gyro. It will be easy to change lateral guidance control software to include curve preview. Curve preview will be obtained from the tracking sensor systems. Using curve preview will permit lowering the control system loop gain, hence, reducing the frequency of the steering backlash oscillation. Lateral displacement will still be updated every 0.1 seconds, however, the rate gyro will permit us to update the steering command every 0.02 seconds to facilitate damping yaw oscillations.

5) Reduce steering backlash as much as possible. This can be accomplished by: 1) modifying the Autonomous Shadow Vehicle's steering mechanism and/or 2) attaching a wheel angle sensor on one of the front wheels of the Autonomous Shadow Vehicle for use by the control program.

REFERENCES

[1] Leonard j. Bond and Chih-Hung Chiang, "Absorption of Ultrasonic Waves in Air at High Frequencies," *J. Acoust. Soc. Am.*, Oct. 1992.

[2] L. Goldman, "Laser Hazards: Current And Future Concerns," *Optics and Laser Technology*, Feb. 1974.

[3] A. D. Olver, "Millimetrewave Systems-Past, Present And Future," *IEE Proceedings*, Vol. 136, No. 1, Feb. 1989.

[4] GARMIN Communication & Navigation, "Now GARMIN Puts 100 Miles In Your Pocket," *GPS World*, Feb. 1993.

[5] Merrill I. Skolnik, *The Nature Of Radar: Introduction To Radar Systems*, copyright. New York, NY: McGraw-Hill, 1962.

[6] K. L. Fuller, "To See and Not Be Seen," *IEE Proceedings*, Vol. 137, No. 1, February, 1990.

[7] Michael Schmidt, "Taking GPS to the Top of Canada," *GPS World*, February 1993.

[8] Trimble Navigation Limited Survey and Mapping Division, "Common GPS Pathfinder Questions And Answers," *Trimble Navigation*, February 1990.

[9] Jeff Hurn, "GPS a Guide to the Next Utility," *Trimble Navigation*, 1989.

[10] Jean-Pierre R. Bayard, "Target Identification using Optimization Techniques," IEEE Trans. Antenna & Propagation, vol. 38, No. 4, April 1990.

[11] Nasser Kehtarnvaz, Norman C. Griswold, and Juck S. Lee, "Visual Control of an Autonomous Vehicle: [BART]--The Vehicle-Following Problem," *IEEE Trans. Veh. Technol.*, vol. 40, No. 3, Aug. 1991.

[12] N. Kehtarnavaz, N.C. Griswold, and J.K. Eem, "Real-Time Visual Control for an Intelligent Vehicle-The Convoy Problem," *SPIE Real-Time Image Processing II*, vol. 1295,

[13] N.C Griswold and N.Kehtarnavaz, "Experiments In Real-Time Visual Control," *SPIE Mobile Robots V*, Vol.1398,

[14] Yitong Zhou, "Artificial Neural Network Algorithms for Some Computer Vision Problems," Dissertation, 1988.

[15] C. Ray Smith and Paul M. Goggan, "Radar Target Identification," *IEEE Antennas and Propagation Magazine*, Vol. 35, No. 2, April 1993.

[16] W. S. McCormick and B. Y. Tsui, "Suboptimal Real-Time Frequency/Incident-Angle Estimator for Multiple Radar Pulses," *IEE Proceedings*, Vol. 138, Pt. F, No. 3, June 1991.

[17] F. R. Castella and S. A. Rudie, "Detection Performance of Phase-Coded Radar Waveforms with Various Types of Limiting," *IEE Proceedings*, Vol. 136, Pt. F, No. 3, June 1989.

[18] D. J. Wilkin, I. Harrison, and M. S. Woolfson, "Target Tracking Algorithms for Phased Array Radar," *IEE Proceedings*, Vol. 138, Pt. F, No. 3, June 1991.

[19] Ping Tcheng, Thomas Jordan, John Franke, and Kenneth Cate, "Scanning Light Sheet would Measure Deflection of Beam," *NASA Tech Brief*, LAR-14218.

[20] Y. R. Shayan and T. Le-Ngoc, "All Digital Phase-Locked Loop: Concepts, Design and Applications," IEE Proceedings, Vol. 136, Pt. F, No. 1, Feb. 1989.

[21] Kerim Demirbas, "Manoeuvering-Target Tracking with the Viterbi Algorithm in the Presence Of Interference," *IEE Proceedings*, Vol. 136, Pt. F, No. 6, Dec. 1989.

[22] J. A. Roecker and C. D. McGillem"Target Tracking in Maneuver-Centered Coordinates," *IEEE Trans. Aerospace and Elect. Sys.*, Vol. 25, No. 6, Nov. 1989

[23] B. Z. Kobb, "Personal Wireless," *IEEE Spectrum*, June 1993.

[24] M. Leonard, "Improved SAW Technology Benefits Remote Control," *Electronic Design*, Feb. 1993.

[25] C. L. Lichtenberg, P. W. Shores, and H. S. Kobayashi, "Transponder System for High-Frequency Ranging," *NASA Tech Briefs*, Sept./Oct. 1986.

[26] W. J. Mills, "Pulse Modulation Scheme for Voice and Telemetry," NASA Tech Briefs, July 1993.

[27] "Spread Spectrum Generator: Model MCS-T," *LNR Communications Inc.*, Oct. 1992.

[28] C. E. Cook and H. S. Marsh, "An Introduction to Spread Spectrum," *IEEE Communications Magazine*, March 1993.

[29] "FCC News: FCC Adopts New Rules For 220-222 MHz Band," IEEE Vehicular Society, Vol. 38, No. 2, May 1991.

[30] L. J. Duchnowski, "Vehicle and Driver Analysis with Real-Time Precision Location Techniques," Sensors, May 1990.

[31] A. Christman, "Phased Driven Arrays For The Low Bands," *QST*, May 1992.

[32] R. T. Hoctor, "High Resolution Coherent Source Location using Transmit/Receive Arrays," *IEEE Transactions on Image Processing*, Vol. 1, No. 1, Jan. 1992.

[33] B. W. Henderson, "Ground Forces Rely on GPS to Navigate Desert Terrain," *Aviation Week & Space Technology*, Feb. 1991.

[34] E. H. Phillips, "GPS/IRU Data Guides New Autoland System," *Aviation Week & Space Technology*, Jan. 1991.

[35] M. Cross, "Japanese Cars Learn to Navigate by Satellite," *New Scientist*, May 1990.

[36] B. Flemming, "GPS Antennas and a Look Back at Automotive Electronics," IEEE Vehicular Technology Society Newsletter,August "92

[37] B. Hossfeld, "GPS For Vehicle Tracking," *GPS World*, Oct. 1991

[38] F. Dufour and M. Mariton, "Tracking a 3D Maneuvering Target with Passive Sensors," *IEEE Transactions On Aerospace And Electronic Systems*, Vol. 27, No. 4, July 1991.

[39] R. D. Horton, "Target Cueing and Tracking System for Smart Video Processing," *IEEE AES Systems Magazine*, March 1991.

[40] Milt Leonard, "Wireless Symposium Looks At Communications Issues," *Electronic Design*, Jan. 1993.

[41] Rebecca D. Horton, "Target Cueing and Tracking System [TCATS] for Smart Video Processing," *IEEE AES Systems Magazine*, March 1991.

[42] A. Y. Lee, "A Preview Steering Autopilot Control Algorithm for Four-Wheel-Steering Passenger Vehicles," Journal Of Dynamic Systems, Measurement, and Control, vol. 113, Sept. 1992.

[43] Edward N. MacLeod and Marianne Chiarella, "Automated Vehicle for Enhanced Work Crew Safety," *Strategic Highway Research Program*, SHRP-H-676, Washington, D.C., 1994.

[44] H. C. Okean, "Spread Spectrum Transceivers For Array Antenna Experiments [Informational Notes]," *LNR Communications Inc.*, Jan. 1994.

[45] Martin McKinney aaaand Garnet Brace, "Build A Micro TV Transmitter," *Electronics Now*, Dec. 1993.

[46] Yitong Zhou, "Artificial Neural Network Algorithms For Some Computer Vision Problems," Dissertation, 1988.

[47] T. Yamamoto, "Two-dimensional Vehicle Tracking Using Video Image Processing," *3rd Vehicle Navigation and Information Systems Conference*, Oslo, Norway, 1992.

[48] S. J. Dickinson and L. S. Davis, "An Expert Vision System for Autonomous Land Vehicle Road Following," *U.S. Army Corps of Engineers*, Engineer Topographic Laboratories, 1988.

[49] Jaekwon Eem, "A Real-Time Vision Guided Vehicle-Following System," Dissertation, 1991.

[50] *California Department of Transportation Maintenance Manual*. Caltrans, July 1993.

[51] *California State Department of Transportation Highway design Manual.* Caltrans.

[52] Garber and Hoel, *Traffic and Highway Engineering.*

[53] Said M. Easa, "Exact Minimum Sight Distance on Sag Curves with centered Overpass," *ASCE Journal of Transportation Engineering*, Technical Note, Aug. 1992.

[54] M. D. Heller, *Basics of Machine Vision*, CSUS Electrical Engineering Dept., Sacramento, CA, 1991.

[55] M. C.Fairhurst, *Computer Vision for Robotic Systems*, Prentice Hall, 1988.

[56] R. C. Gonzalez and R. E. Woods, *Digital Image Processing.* Reading, Mass.: Addison-Wesley, 1992.

[57] R. J.Schalkoff, *Digital Image Processing and Computer Vision*, Wiley, 1989.

[58] M. James, *Pattern Recognition*, Wiley, 1988.

[59] J. S.Dods, "The ARRB Lateral Position Indicator," *Technical Manual ATM No. 15*, Australian Road Research Board, Victoria, Australia, 1982.

[60] M. Heller, R. Trahms, S. Chatusripitak, "Vehicle Lateral Guidance Using a DSP Based Vision System," *Applications of Advanced Technologies in Transportation Engineering: Proceedings Of The Second International Conference*, Minneapolis, Minnesota, August 18-21, 438-442, 1991.

[61] A.S. Hauksdottir, R.E. Fenton, "On Vehicle Longitudinal Controller Design", *IEEE Workshop on Automotive Applications of Electronics*,1988.

[62] A.S. Hauksdottir, R.E. Fenton, "On the Design of a Vehicle Longitudinal Controller", *IEEE Transactions on Vehicular Technology*, V. vt-34.4, November 1985.

[63] R.E. Fenton, P.M. Chu," On Vehicle Automatic Longitudinal Control", *Transportaion Science*, V.II, No. 1, pp.73-91. Feb. 1977.

[64] G.M. Takasaki, R.E. Fenton, "On the Identification of Vehicle Longitudinal Dynamics", *IEEE Transactions on Automatic Control*, V. AC-22.4, Aug. 1977.

[65] S. Sheikholeslam, C. Desoer, "Longitudinal Control of a Platoon of Vehicles I: Linear Model", Program on Advanced Technology for the Highway, Institue of Transportation Studies, University of California, Berkeley, Aug., 18, 1989.

[66] S. Liu, A. Frank, "Simulation of a Vehicle Platoon Control System for Automatic Highway Using The Fuzzy Control Concept", Vehicle Highway Automation.

[67] A.A. Frank, S.C. Liang, "Longitudinal Control Concepts for Automated Automobiles and Trucks Operating on a Cooperative Highway", *SAE Conference*, Toronto, Canada, 1989.

[68] A.S. Hauksdottir, G Siguroardottir," On the Use of Robust Design Methods in Vehicle Controller Design", *Proceedings of the American Control Conference*, 1991, V.3 pp.3113-18.

[69] A.S. Hauksdottir, G Sigroardottir," On the Use of Robust Design Methods in Vehicle Controller Design", *Transactions of the ASME, Journal of Dynamic Systems Measurements and Control*, V.115, pp.166-172, Mar. 1993.

[70] J.K. Hedricck, D. McMahon, V. Narendran, D. Swaroop, "Longitudinal Vehicle Controller Design for IVHS Systems",*Proceedings of the American Control Conference*, 1991, V.3 pp.3107-12.

[71] J.K. Hedricck, D. McMahon, V. Narendran, D. Swaroop, "Longitudinal Vehicle Controller Design for IVHS Systems",*Proceedings of the American Control Conference*, 1992, pp.1753-57.

[72] R.J. Rouse, L.L. Hoberock, "Emergency Control of Vehicle Platoons: Control of Following-Law Vehicles", *ASME Journal of Dynamic Systems, Measuremant, and Control*, pp. 239-243, Sept. 1976.

[73] R.J. Rouse, L.L. Hoberock, "Emergency Control of Vehicle Platoons: System Operation and Platoon Leader Control", *ASME Journal of Dynamic Systems, Measuremant, and Control*, pp. 245-251, Sept. 1976.

[74] L.L. Hoberock, "A Survey of Longitudinal Acceleration Comfort Studies in Ground Transportation Vehicles", *ASME Journal of Dynamic Systems, Measuremant, and Control*, pp. 76-84, June. 1977.

[75] S. Sheikholeslam, C. Desoer, "Longitudinal Control of a Platoon of Vehicles III: Noninear Model", Institue of Transportation Studies, Program on Advanced Technology for the Highway, University of California, Berkeley, April, 1990.

[76] S. Sheikholeslam, C. Desoer, "Longitudinal Control of a Platoon of Vehicles: A system-level study", Institue of Transportation Studies, Program on Advanced Technology for the Highway, University of California, Berkeley, Sept. 16, 1991.

[77] S. Sheikholeslam, C. Desoer, J.K. Hedrick, M. Tomizuka, J. Warlrand, W.B. Zhang, D.H. McMahon, H. Peng, S. Shladover, N. Mckeown, "Automatic Vehicle Control Developments in the PATH Program", *IEEE Transactions on Vehicular Technology*, V. 40.1, Feb, 1991.

[78] S. Sheikholeslam, C. Desoer, "Longitudinal Control of a Platoon of Vehicles with no communication of Lead Vehicle Information", *Proceedings of the American Control Conference*, 1991, V.3 pp.3102-06.

[7]. S. Sheikholeslam, C. Desoer, "Combined Longitudinal and Lateral Control of a Platoon of Vehicles III", *Proceedings of the American Control Conference*, 1992, pp.1763-67.

[80] S.E. Shladover,"Longitudinal Control of Automotive Vehicles in Close-Formation Platoons", *ASME Journal of Dynamic Systems, Measurements, and Control*, V.113 pp. 231-241, June, 1991.

[81] S.E. Shladover, "Operation of Automated Guideway Transit Vehicles in Dynamically Reconfigured Trains and Platoons", *ISBN UMTA-MA-06-0085-79-1*,April, 1979.

[82] R.J. Caudill and W.L. Garrard, "Vehicle Follower Longitudinal Control for Automated Guideway Transit Vehicles", U.S. Dept. of Transportation, *UMTA-MN-11-0002-77-1*, Feb. 1977.

[83] C.C. Chien and P. Ioannou," Automatic Vehicle-Following", *Proceedings of the American Control Conference*, 1992, pp.1748-52.

[84] P.G. Smith, "Discrete-Time Longitudinal Control of Dual Mode Automobiles", *Intersociety Conference on Transportation*, 1973.

[85] H.Y. Chiu, G.B. Stupp, S.J. Brown, "Vehicle-Follower Control with Variable-Gains for Short Headway Automated Guideway Transit Systems", *ASME Journal of Dynamic Systems Measurements and Control*, Sept. 1977, pp.183-189.

[86] K.H. Chang, CN. Georgiades, "A Position Estimation Algorithm for Vehicle Following", *Proceedings of the American Control Conference*, 1992, pp.1758-62.

[87] B.M. Bobrotin, G.R. Hansen, T.K.C. Peng, D.A. Rennels, "Fully Automated Urban Traffic System", U.S Department of Transportation, *DOT-TST-78-3*, 1977.

[88] S.Tsugawa, S. Murata, "Velocity Control for Vehicle Following Through Vehicle/Vehicle Communication", *22nd International Symposium on Automotive Technology & Automation*, Florence Italy, May 1990, V.1, pp.343-350

[89] K.C. Kapur, "Development of Vehicle-Following Behavior for Automated Vehicle Systems", *Vehicle System Dynamics*, V.1.1, 1972, pp.1-16.

[90] X. Zhang, "Intelligent Driving, Prometheus Approaches to Longitudinal Traffic Flow Control", *Vehicle Nvigation & Information Systems Conference Proceedings, Part II, SAE*, OCT. 1991, pp.999-1010.

[91] J. Glimm, "On Safe Longitudinal Control of Ground Transportation Vehicles", *International Federation of Automatic Control*, No.3, 1984, pp. 357-364.

[92] I.J. Ha, A.K. Tugcu, N.M. Boustany, "Feedback Linearizing Control of Vehicle Longitudinal Acceleration", *IEEE Transactions on Automatic Control*, V.34.7, July 1989, pp.689-698.

[93] R. Limpert, Brake Design and Safety, 1992, Society of Automotive Engineers.

[94] H.Y. Chiu, D.L. Kershner, P.J. McEvaddy, "A Network Management Simulation of Automated Guideway Rapid Transit Systems Under Vehicle-Follower Control", *Dept. of Transportation, UMTA-MD-06-0047-84-1*, Oct. 1984.

[95] A.J. Pue, H.Y. Chiu, S.J. Brown, "Operation Concepts and Implementation Techniques for Vehicle-Follower Control of AGT Systems", *Dept. of Transportation, UMTA-MD-06-0038-79-1*, Aug. 1979.

[96] T.B. Cribbs, M.S. Thesis, "Studies in the Control of Automated Highway Vehicle Propulsion", Ohio State University, 1979.

[97] Sijiu M. Liu and Andrew A. Frank, "On Lateral Control of Highway Vehicles Guided by a Forward Looking Sensor." First International Conference on Applications of Advanced Technologies in Transportation Engineering, San Diego, Calif, 1989.

[99] Terence S.Abbott and Charles Knox, "Capturing and Tracking Performance of the Horizontal Guidance and Control Systems of the Terminal Configured Vehicle," *National Aeronautics and Space Administration, Scientific and Technical Information Office*, NASA technical memorandum 80069, Washington, D.C. 1979.

[100] N. Kehtarnavaz and W. Sohn, "Steering Control of Autonomous Vehicles by Neural Networks," *Proceedings of the 10th American Control Conference*, Boston, Mass., 1991.

[101] Alain L. Kornhauser,"Neural Network Approaches for Lateral Control of Autonomous Highway Vehicles," *Conference proceedings 2nd Vehicle Navigation and Information Systems Conference*, Dearborn, Mich., Vol. 2, 1991.

[102] M. D. Heller and M. Huie, "Lateral Vehicle Guidance using Vision, Passive Wire, and Radar Sensors," *Vehicle Navigation & Information Systems Conference*, Ottawa, Canada, 1993.

[103] C. Kelley, "Vehicle Lateral Guidance Using Vision," *Master of Science Project*, California State University, Sacramento, CA., 1992.

[104] J. Zhuang, "Design and Development of a Vehicle Lateral Steering Control System." *Master of Science Project*, California State University, Sacramento, CA., 1991.

[105] J. Z. Zhou, "A Steering Control System With a Vehicle Lateral Guidance Adaptive Control Law." *Master of Science Project*, California State University, Sacramento, CA., 1991.

[106] S. Shaldover, C. Desoer, J. Hedrick, M. Tomizuka, J. Walrand, W. Zhang, D. McMahon, H. Peng, S. Skeikoleslam, and N. McKeown, "Automated vehicle control developments in the PATH program," *IEEE Trans. Vehicular Tech.*, vol. 40, pp. 114-130, Feb., 1991.

[107] Ichiro Masaki, Editor, *Vision-based Vehicle Guidance*. Springer-Verlag New York, Inc., New York, 1992.

[108] R. G. Trahms III, "Vehicular Relative Position Information Techniques Using an Image Input Neural Network." *Master of Science Thesis*, California State University, Sacramento, CA., 1992.

[109] M. W. Spong and M. Vidyasagar, *Robot Dynamics and Control*. John Wiley & Sons, Inc., New York, 1989.

[110] J-J. E. Slotine and Weiping Li, *Applied Nonlinear Control*. Prentice Hall, New Jersey, 1989.

[111] M. Heller, "Lateral Electronic Guidance System for Vehicles," *Caltrans and Federal Highway Administration, Report No. FHWA-CA/Tl-93-16, Study No. 65n154*, June 1993.

[112] J. Ackermann, "Robust Car Steering by Yaw Rate Control," Proc. IEEE Conf. Decision Contr., Honolulu, HI, Dec. 1990, pp. 2033-2034.

[113] T. T. Hartley, G. O. Beale, and S. P. Chicatelli, *Digital Simulation of Dynamic Systems: A Control Theory Approach*. Prentice Hall, New Jersey, 1994.

[114] K. J. Astom and B. Wittenmark, *Adaptive Control*. Addison Wesley, Reading, Mass., 1989.